ngineering

RR

Journal of Research

of the

National Bureau of Standards

AUGUST 1934

VOLUME 33 NUMBER 2

U. S. DEPARTMENT OF COMMERCE
Herbert Hoover, Secretary
NATIONAL BUREAU OF STANDARDS
A. V. Astin, Director

AUGUST • 1934
VOLUME • 13
NUMBER • 2

JOURNAL OF RESEARCH

of the

NATIONAL BUREAU OF STANDARDS

PERIODICALS OF THE NATIONAL BUREAU OF STANDARDS

The National Bureau of Standards is engaged in fundamental and applied research in physics, chemistry, mathematics, and engineering. Projects are conducted in eleven fields: chemistry, optics and metrology, heat and power, atomic and radiation physics, chemistry, mechanics, organic and fibrous materials, metallurgy, mineral products, building technology, applied mathematics, electricity, and radio propagation. The Bureau has custody of the national standards of measurement and provides means leading to the improvement of scientific and engineering standards and of techniques and methods of measurement. Testing methods and instruments are developed; properties of materials are determined; and composition and structure are investigated.

JOURNAL OF RESEARCH

The Journal of Research publishes papers by authors in the above-mentioned fields of physics, mathematics, chemistry, and engineering. Complete details of the [illegible], including [illegible] data, supplemental proofs, and bibliographical and mathematical [illegible]. Annual subscription: Domestic, $4.50; foreign, $5.50.

TECHNICAL NEWS BULLETIN

Publication of [illegible] at the National Bureau of Standards [illegible] The articles are [illegible] on the [illegible] Research Papers, [illegible] Miscellaneous Publications [illegible] Annual subscription: [illegible]

BASIC RADIO [illegible]

[illegible] information [illegible] world at any [illegible] communications [illegible] to its investigators [illegible] three months [illegible] Annual subscription: [illegible]

All publications [illegible] Government [illegible] has been appointed [illegible]

Journal of Research of the National Bureau of Standards Vol. 53, No. 2, August 1954 Research Paper 2517

Delta Ferrite-Austenite Reactions and the Formation of Carbide, Sigma, and Chi Phases in 18 Chromium-8 Nickel-3.5 Molybdenum Steels

H. C. Vacher and C. J. Bechtoldt

Three 18 Cr-8 Ni-3.5 Mo steels of slightly different compositions were given "solution treatments" at 2,500°, 2,000°, and 1,800° F, and samples of each were reheated at 1,700°, 1,500°, and 1,200° F. Ferrite residues, remaining after dissolving the austenite in the solution-treated steels were analyzed chemically and given the reheat treatments, along with the parent steels. A metallographic study of the effect of chemical composition of the delta ferrite and austenite phases, and of the amount of delta ferrite, on the formation of carbide, sigma, and chi phases, was made. It was found that the products formed at a certain reheating temperature were influenced by the amount and composition of the delta ferrite phase present in the solution-treated steels, the amount and composition of the delta ferrite being determined by the solution-treatment temperature. Distribution ratios for Cr, Ni, Mo, and Mn in the delta ferrite and austenite phases of the solution-treated steels were 1.2, 0.5, 1.7, and 0.9, respectively.

1. Introduction

Commercial austenitic stainless steels are available ordinarily in the "solution-treated" condition, that is, as rapidly cooled from temperatures above 1,900° F. In this condition, AISI 316 and 317 steels frequently contain delta ferrite (δ) in a matrix of austenite (γ). During fabrication and in service the solution-treated steels are sometimes reheated in the range of 1,200° to 1,800° F. In this temperature range, reactions occur in or between the δ and γ phases that result in the formation of the microconstituents, carbide ($M_{23}C_6$), σ, and χ [1].[1] At the lower temperatures in this range the diffusion rates are extremely low, so that true chemical equilibrium is rarely, if ever, attained. Consequently, after exposure at temperatures near 1,200° F. for an arbitrarily chosen heating period, examination of the microstructure will always show an incompleted δ-γ reaction. The sequence of formation and the amounts formed of the carbide, σ, and χ phases will be influenced by the chemical composition, relative amount, and distribution of the δ and γ phases. Bowen and Hoar [2] have shown that when the reaction takes place within the δ phase, σ is formed first and γ later. This γ presumably differs from the γ initially present in the solution-treated condition only in composition [3] and would lose its identity after diffusion had equalized the elemental concentrations. For convenience in this paper, the γ formed during a solution treatment will be referred to as γ_S, and that formed in reheating to lower temperatures as γ_R. A metallographic study of the effect of chemical composition of the δ and γ phases, and of the amount of δ, on the formation of carbide, σ, and χ phases has been made and is reported in this paper.

2. Material and Heat Treatments

Three 18:8 Mo types of steel rods, ¾ in. diameter by 4 in. long, differing slightly in chemical composition, table 1, were used in this investigation. The "as received" condition of steel 1 was not known, but the microstructure indicated that it had been worked in the temperature range in which δ was stable. Steels 2 and 3 were obtained through the courtesy of Mason Clogg, Armco Steel Corp., Baltimore, Md. They were from the same stock material used in the investigation, "The Development of Metallographic Methods for the Identification of the Sigma Phase in Iron-Chromium-Nickel Stainless Steels," sponsored by Sub-Committee VI, Committee A–10 American Society for Testing Materials [4]. As received, steels 2 and 3 had been heated at 2,000° F for ½ hour and water quenched.

In order to obtain δ and γ phases of different compositions and δ in different amounts, the three steel rods were given three solution treatments, table 2. This procedure takes advantage of the fact that for a certain steel the chemical composition of the reacting phases at equilibrium varies with temperature and that equilibrium concentrations are approximated in the solution treatment. It is not possible to vary the relative amounts of δ and γ and maintain their composition constant by heat treatment because, like composition, the relative amounts vary with temperature. The δ-γ reaction was studied both in the presence and in the absence of the γ_S phase. This was done by separating the δ phase from the solution-treated steels and reheating it in the range 1,200° to 1,700° F, along with the solution-treated steels. Table 2 lists the reheating treatments. The constitution of the reheated ferrites and solution-treated steels was then determined by a metallographic study.

TABLE 1. *Chemical composition of chromium-nickel-molybdenum austenitic alloys*

Steel	C	Cr	Ni	Mo	Mn	Si
1	0.05	17.6	7.9	3.2	0.71	0.48
2	.08	17.8	9.4	3.6	1.65	.49
3	.07	18.4	13.5	3.6	1.58	.68

[1] Figures in brackets indicate the literature references at the end of this paper.

TABLE 2. *Heat treatments given steels 1, 2, and 3* [1]

Solution treatment			Reheat treatment		
Identification	Temperature	Period	Identification	Temperature	Period
	°F	hr		°F	hr
A	2,500	½	K	1,700	340
B	2,000	½	L	1,500	500
C	1,800	18	M	1,200	500
D [2]	2,250	18			
E [2]	1,900	2			

[1] All specimens were water quenched from all temperatures.
[2] Steels 2 and 3 only.

3. Procedures

3.1. Microscopic Examination of the Specimens

Sections of the specimens were mounted, ground, and polished by conventional procedures. The specimens were electropolished for a short period before polishing with fine alumina. The electrolyte for the electropolishing consisted of 3 parts of phosphoric acid, 3 parts of glycerol, and 4 parts of ethyl alcohol.

Among the etchants tried were weak and strong alkaline ferricyanide, sodium cyanide, and several acid reagents. It was found that aqua regia and a 10-percent sodium cyanide solution, the latter used electrolytically, were the most satisfactory for this work. Steels that contained only δ and γ_s were etched with aqua regia, and those that contained carbide, σ, and χ were etched with the sodium cyanide reagent. In examining the reheated steels a preliminary examination was made by a series of successive etchings. Usually 5 to 15 seconds was sufficient to reveal the carbide phase, and an additional etch for 30 seconds brought out σ. At this stage χ, if present, usually could be seen faintly in the background because of relief polishing. Further etching developed χ but overetched the σ and carbide phases. After this preliminary examination, the specimen was repolished and the surface etched to reveal the complete structure. In this condition the carbide and σ were usually overetched. It was not always possible to distinguish with certainty between σ, χ, and δ when they were present as minute particles or as particles of the same size. In such steels a chemical separation of the microconstituents as an insoluble residue and a qualitative analysis of the separated residue by X-ray diffraction greatly aided the interpretation of the microstructure.

3.2. Chemical Separation of Microconstituents from Austenite

In work done in cooperation with Subcommittee VI of ASTM Committee A–10, it was found that the microconstituents in the AISI 317 steels were relatively insoluble, with respect to the γ_s matrix, in solutions that contained the chlorine ion. This gave a means of concentrating the microconstituents in a manner convenient for their identification by X-ray diffraction.

The reagents that were tried included ferric chloride used electrolytically, cupric-ammonium chloride, and aqua regia. It was found that, in general, δ was relatively insoluble in the ferric chloride reagent but soluble in aqua regia. On this basis one of two reagents was used for the work reported in this paper: ferric chloride for steels containing δ, and aqua regia for those containing one or more of the microconstituents—carbide, σ, and χ.

In the aqua regia dissoltuon procedure the bulk sample was placed in approximately 100 ml of the solution and allowed to stand overnight at room temperature. In the ferric chloride procedure as used in the collection of large amounts of residue, the electrolyte consisted of 350 g of $FeCl_3 \cdot 6H_2O$ dissolved in 1 liter of water. The cell consisted of a 2-liter beaker containing 1 liter of electrolyte, with the specimen as the anode and a stainless-steel strip, 0.050 in. thick by 2 in. wide, as the cathode. The length of the specimen rod in contact with the electrolyte was approximately 3 in. The potential across the cell was controlled so as to pass a current of 1.5 amp, or about 0.03 amp/cm^2; this required about 3.5 v. The voltage was not allowed to exceed 6 v. A 150-ml beaker was placed directly under the suspended specimen to catch loosened insoluble matter, although most of the residue adhered to the specimen. Small specimens were placed in a basket formed from platinum wire, and a small dish was placed beneath the basket. The electrolyte was replaced with a fresh solution after approximately 25 g of steel had been dissolved.

The residues from the aqua regia and ferric chloride treatments were separated from the solutions by centrifuging and decanting. The residues then were washed with a 50-percent nitric acid solution and then with water. When free from acid, the residues were washed from the centrifuge tubes with acetone and dried.

The ferric chloride procedure was used to separte δ from the solution-treated steels in quantities sufficient for chemical analyses of the Cr, Ni, and Mn contents. The completeness of the separation was ascertained by X-ray diffraction. These examinations indicated that the amount of γ_s in the residues was less than 3 percent. This was judged from diffractometer charts by the difference in heights of the 111-peak for γ and the 110-peak for δ, as compared with differences obtained from known mixtures of δ and γ.

In steels suspected of containing traces of δ, the residues were examined with a stereomicroscope for movement when a magnetized needle was passed over them. Residues that contained small amounts of δ, as shown by X-ray diffraction, were weakly attracted by the needle, but the attraction was uniformly distributed, that is, all particles were slightly magnetic. Apparently the particles were clusters of microconstituents, some of which were ferromagnetic. In some residues there were occasional particles that were strongly attracted to the needle, and the residue as a whole showed little or no attraction. A separation was made of the strongly magnetic particles in a ferric chloride residue obtained from steel 2 after solution treatment at 2,500° F. and reheating to 1,200° F. An X-ray diffraction chart of the separated magnetic particles showed peaks corresponding to two types of oxides, Fe_3O_4, $NiFe_2O_4$, and $Cr_2O_3Fe_2O_3$. The peaks for the latter were weak.

3. Qualitative Analysis of Residues by X-ray Diffraction

The X-ray diffraction analysis of the residues were made with a Geiger-counter diffractometer and were confined to a 2θ range of 40° to 65° for diffractions of the cobalt Kα radiation. The peaks in the diffractometer charts nearly always could be identified as being from one or more of the γ, δ, σ, χ, and carbide phases. The identification was made by comparing the 2θ angles for the observed peaks with the identified 2θ angles in table 3. The 2θ values are numbered in the order of their occurrence in the charts and are the averages of observed values rather than the specific values that had been reported in the literature. The corresponding d/n values were computed and listed with reported relative intensities obtained from the literature for the pure constituent. The sensitivity of detection with respect to σ is about 5 percent; to γ, δ, and χ, probably about 3 percent. Phases reported as "not detected" may be considered as present in less than these amounts.

The presence of δ and γ in residues separated by the ferric chloride procedure can be verified by treating the residue with aqua regia and comparing diffractometer charts obtained from the residues before and after the treatment. The treatment with aqua regia reduces the δ and γ contents of the residues by dissolution. If the relative heights of peaks 7 and 9 are lowered, the presence of δ and γ is indicated. This is shown in the 1AM and 1BM charts, figure 2.

4. Results and Discussion

4.1. Interpretation of Microstructure with Aid of Qualitative Analysis of Residues by X-ray Diffraction

Examples of the aid that X-ray diffraction analysis of residues gave in interpreting typical microstructures in this investigation are as follows: The small black spots in the microstructure of steel 2 after a solution treatment at 1,800° F (2C), figure 1, are unquestionably the carbide phase, and the large shaded areas are σ. However, the smaller unshaded areas might be χ or δ. A diffraction chart, figure 2, of the residue obtained from 2C by the aqua regia procedure showed easily identifiable peaks for the carbide, σ, and χ phases. It is unlikely that the unshaded areas in the grain boundaries are δ because the δ in the steel before the solution treatment was in the form of stringers. The 2C microstructure therefore was interpreted as showing σ in stringers, χ as outlined areas, and carbide as black spots.

The microstructure of steel 1 after solution treatment at 2,500° F and reheating to 1,200° F (1AM, fig. 3) could not be interpreted with complete satisfaction even with the aid of an X-ray diffraction analysis of the residue. The 1AM diffraction chart (fig. 2), obtained from the residue extracted by the ferric chloride procedure, showed peaks that could be identified easily as those of the carbide and σ phases. The absence of χ is indicated by the absence of peak 6, and the presence of δ is indicated by the relative height of peak 9 not being proportional to the heights of peaks 10 and 11, such as in the 1BM ferric chloride chart. Diffraction maxima from both σ and δ coincide at peak 9, table 3. From the X-ray results it can be concluded that the 1AM microstructure definitely contains carbide and σ, but it is possible that this 1AM microstructure also includes δ that was not recovered in the ferric chloride extraction. In extracting δ from steel 1 after the 2,500° F solution treatment, a very low yield of δ was obtained. This indicated a relatively high solubility of δ in the ferric chloride reagent and would account for the absence of δ in the 1AM residue. On the basis of the foregoing results, the 1AM microstructure was interpreted as showing that the reactions were within the initial δ sites and resulted in the formation of carbide at the δ-γ_S boundary and possibly within the initial δ. These former δ sites contained σ, and probably γ_R and undecomposed δ. The two latter constituents, however, could not be identified.

The 2AL diffractometer chart, figure 2, obtained from the residue from steel 2 after a solution treat-

TABLE 3. *X-ray diffraction data for the identification of γ, δ, carbide, σ, and χ in steels 1, 2, and 3*

Peak No.	Cobalt Kα lines Degrees 2θ	γ		δ		Carbide ($M_{23}C_6$)		σ		χ	
		d/n	Intensity [1]	d/n	Intensity [1]	d/n	Intensity [1]	d/n	Intensity [1]	d/n	Intensity [1]
1	44.4	------	------	------	------	2.37	MS	------	------	2.37	M
2	46.1	------	------	------	------	------	------	2.28	VW	------	------
3	47.7	------	------	------	------	------	------	------	------	2.21	M
4	48.7	------	------	------	------	2.17	M	------	------	------	------
5	49.7	------	------	------	------	------	------	2.13	S	------	------
6	50.8	------	------	------	------	------	------	------	------	2.09	VS
7	51.3	2.07	S	------	------	------	------	2.07	W	------	------
8	51.8	------	------	------	------	2.05	S	------	------	------	------
9	52.5	------	------	2.03	S	------	------	2.02	W	------	------
10	53.7	------	------	------	------	------	------	1.98	M	------	------
11	55.1	------	------	------	------	------	------	1.93	S	------	------
12	56.6	------	------	------	------	1.89	M	1.89	M	1.89	S
13	58.0	------	------	------	------	------	------	1.84	VW	------	------
14	59.6	1.80	M	------	------	1.80	M	------	------	1.80	MS
15	60.4	------	------	------	------	1.78	W	------	------	------	------
16	61.9	------	------	------	------	------	------	------	------	1.74	M

[1] S, MS, M, W, and VW denote decreasing degrees in the relative heights of diffraction peaks in the diffractometer charts. No attempt was made to have these designations correspond to those recommended for the ASTM card index system.

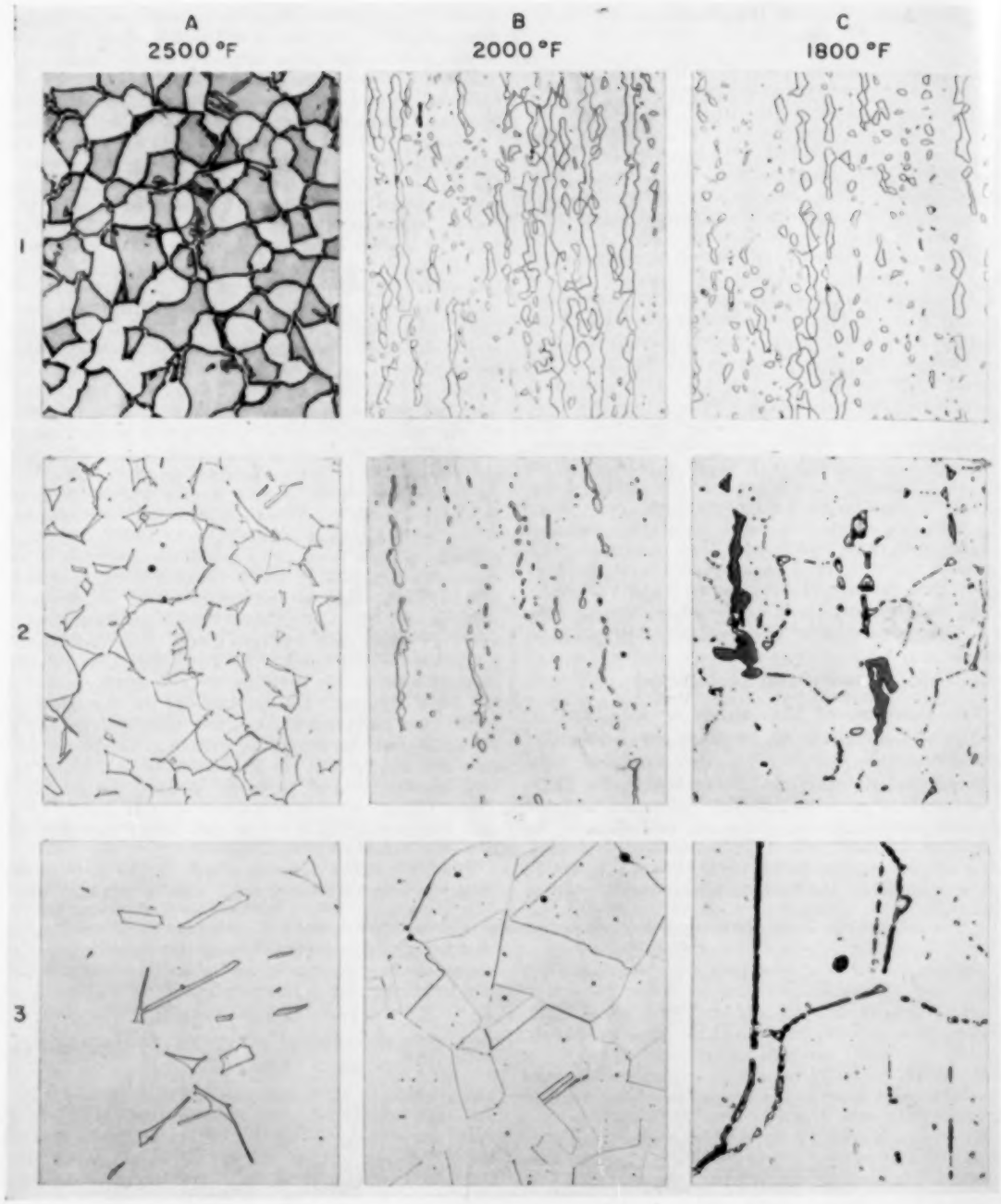

FIGURE 1. *Microstructures of steels 1, 2, and 3 after solution treatments.*

Numbers on the rows identify the steels; letters and temperatures on the columns identify the heat treatments. Identified constituents (matrix in all photomicrographs is γ): 1A, δ (shaded grains); 1B, 1C, 2A, 2B, and 3A, δ (clear, outlined areas); 2C, carbide (dotted, chain-like constituent, mostly at grain boundaries), σ (massive, darkened areas), χ (lighter areas, sometimes heavily attacked at outlines); 3B, none; 3C, carbide and σ. Magnifications: 2C, ×500; 3C, ×1000; all others ×250. 2C and 3C were etched electrolytically with 10-percent NaCN, 1A with dilute alkaline ferricyanide, all others with aqua regia. Reduced slightly in reproduction.

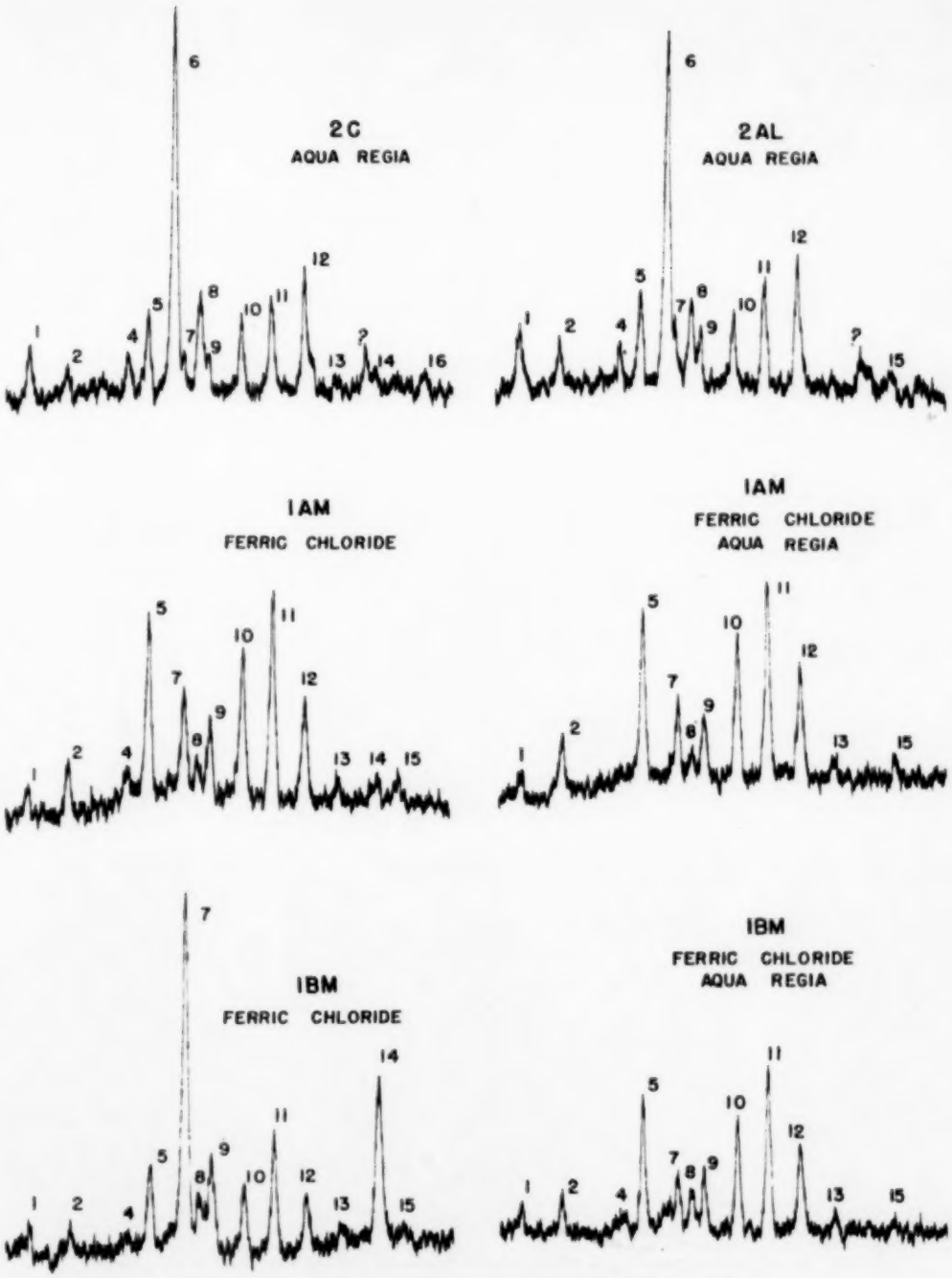

FIGURE 2. *Typical X-ray diffractometer charts obtained from residues.*

Charts 2C, 2AL, 1AM, and 1BM were obtained from residues separated with the ferric chloride and aqua regia reagents from steel 2 after solution treatment at 1,800° F; steel 2 after solution treatment at 2,500° F and reheating to 1,500° F; steel 1 after solution treatments at 2,500° and 2,000° F and reheating to 1,300° F, respectively. Cobalt Kα radiation.

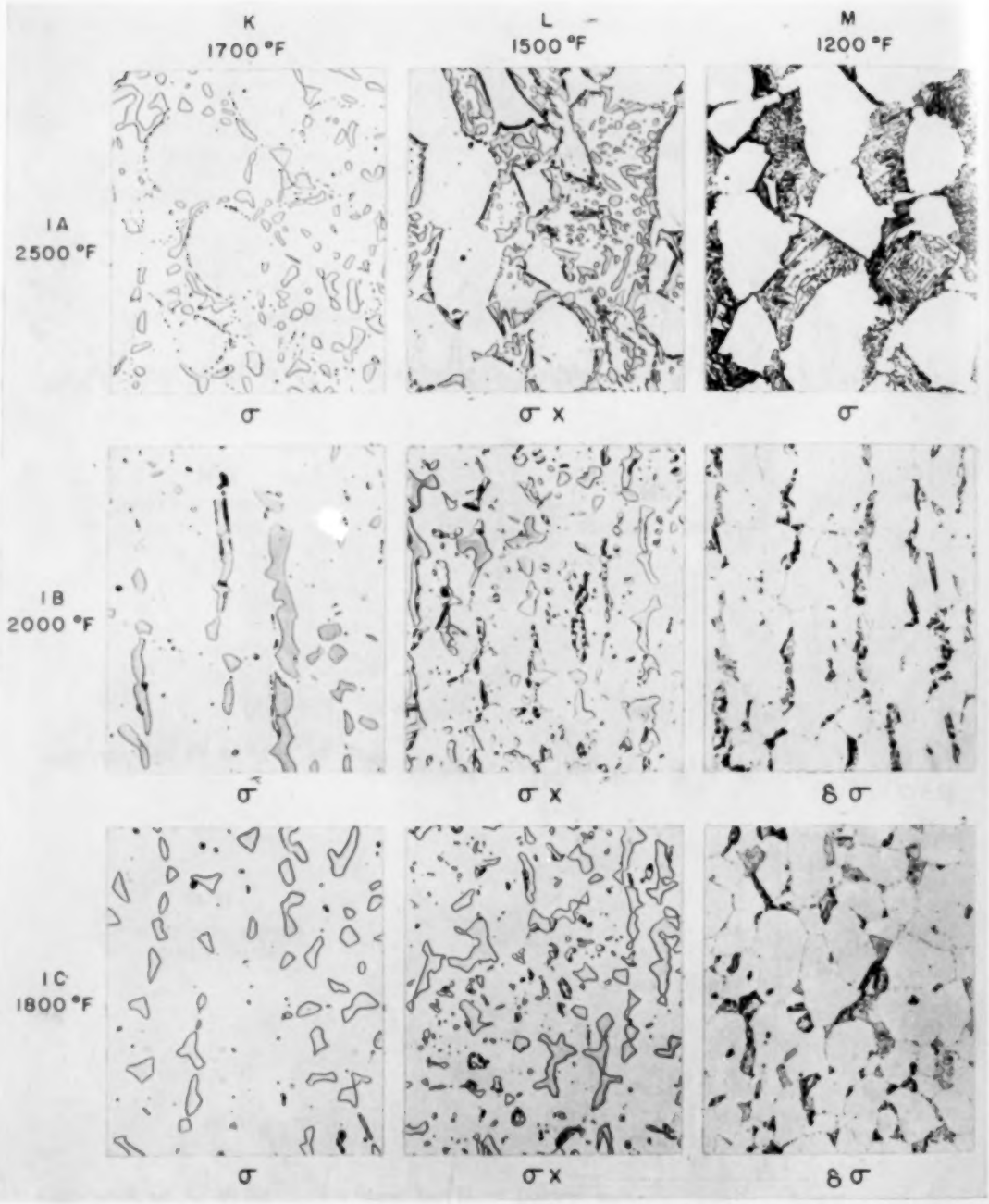

FIGURE 3. *Microstructures of steel 1 after solution treatments and reheating to lower temperatures.*

Numbered letters and temperatures on the rows identify the solution-treated steels; letters and temperatures on the columns identify the reheat treatments. Carbide was possibly absent in 1CK but present in the other microstructures. Identified constituents in corresponding residues are listed below each photomicrograph. Etched electrolytically in 10 percent NaCN; magnification, × 500. Reduced slightly in reproduction.

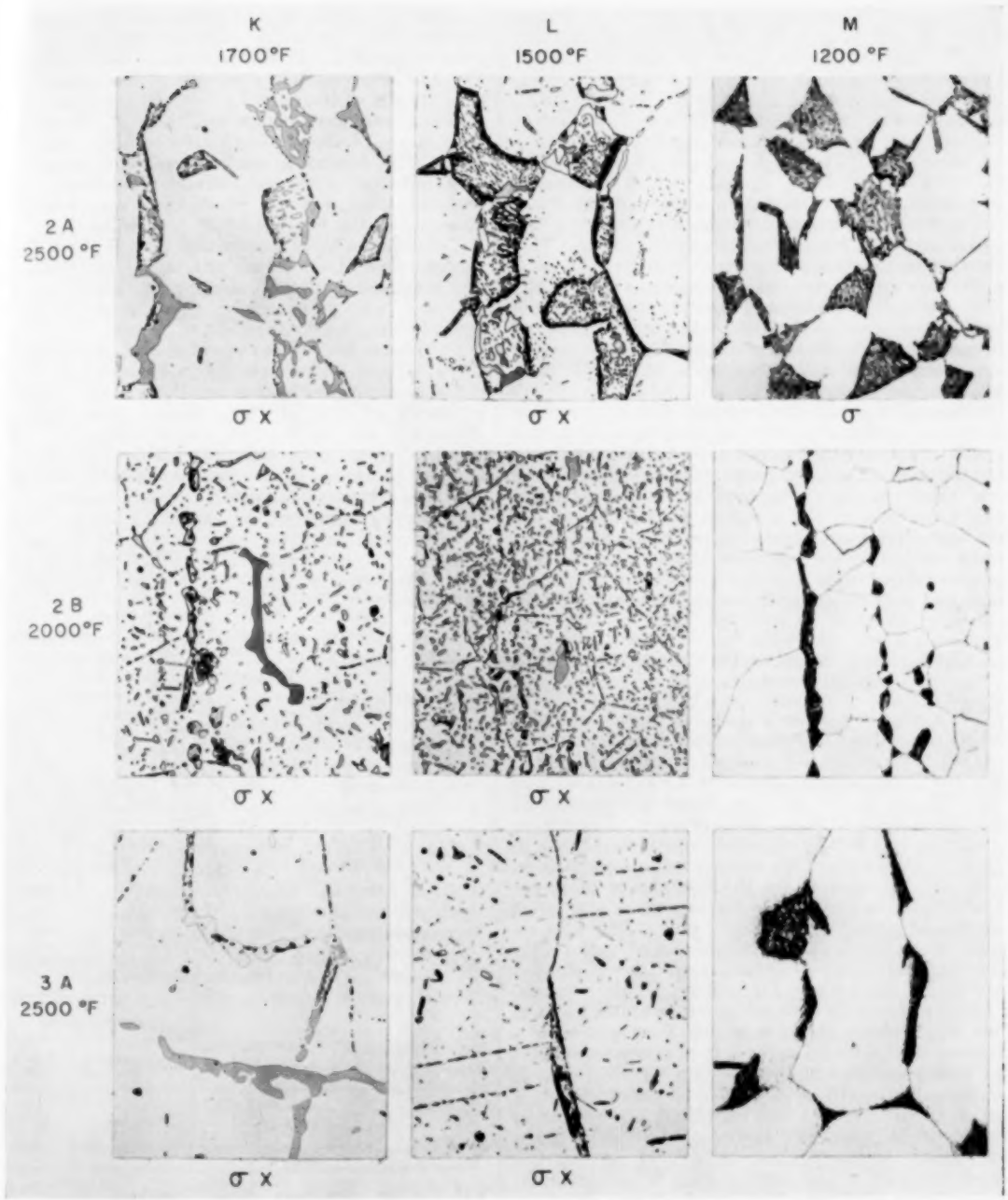

FIGURE 4. *Microstructures of steels 2 and 3 after solution treatments and reheating to lower temperatures.*

Numbered letters and temperatures on the rows identify the solution-treated steels; letters and temperatures on the columns identify the reheat treatments. Carbide was present in all microstructures. Identified constituents in corresponding residues are listed below each photo micrograph. Etched electrolytically in 10 percent NaCN; magnification, × 500. Reduced slightly in reproduction.

ment at 2,500° F and reheating to 1,500° F, indicated carbide, σ, and χ. On the basis of this information the 2AL microstructure, figure 4, was interpreted as showing carbides at the former δ-γ_S grain boundary, σ as large shaded areas, and χ as small intergranular areas, not shaded. It was not always possible to distinguish between small particles of σ and those of χ. The heights of peak 7 in the 1AM and 1BM charts, ferric chloride, figure 2, indicate the presence of γ. Diffraction maxima from σ and γ coincide at peak 7 and in the absence of γ, the heights of peaks 7 and 9 are about the same. This is shown in the other charts of figure 2. There is no obvious explanation for the presence of γ in the 1AM and 1BM residues extracted by the ferric chloride procedure. Experience has shown that the presence of γ is more probable in residues separated from steels that were reheated to 1,200° F than from solution-treated steels.

A successful application of the X-ray diffraction procedure described in the foregoing paragraphs depended upon having small-sized crystals, randomly oriented and intimately mixed. The experience has been that chemically separated residues satisfied these conditions. The relative solubilities of the microconstituents is dependent on the composition of the extracting reagent and of the steel, so that the procedures used for the 18:8 Mo type steels may apply only to austenitic steels containing molybdenum.

4.2. Steels after Solution Treatments at 2,500°, 2,000°, and 1,800° F

It is stated in section 2 that in order to obtain δ and γ_S phases of different compositions so that the δ-γ_S reactions could be studied, steels 1, 2, and 3 were given solution treatments at 2,500°, 2,000°, and 1,800° F. It was found that δ was not present in all of these steels at these temperatures. The microstructures and identified constituents are shown in figure 1. The results are summarized graphically in figure 5. In order to fix the boundaries more accurately, steels 2 and 3 were examined also after solution treatments at 1,900° and 2,250° F, respectively. Microscopic examination of steel 3 after solution treatments at 2,000° and 2,250° F showed only γ_S. A similar range in which only the γ_S phase is stable apparently does not exist for steels 1 and 2. This single-phase range probably increases with a decrease in the Cr/Ni ratio. It is noteworthy that the ferrite content increases with (a) increase in temperature, or (b) with the Cr-Ni ratio. Steels 2 and 3 apparently did not contain δ after solution treatment at 1,800° F; however, they did contain the carbide and σ phases. The χ phase was detected in steel 2 but not in steel 3 at 1,800° F. Examination of the steels after reheat treatments at 1,700° and 1,500° F, figures 3 and 4, indicated that there were fields in which the χ phase was not stable.

In order to determine the compositions of the δ and γ_S phases in the solution-treated steels it was necessary to determine the relative amounts of δ and γ_S. This was done microscopically by lineal analysis according to the procedure developed by Howard and Cohen [5]. The percentages of δ are given in figure 5. With these values, along with the Cr, Ni, Mo, and Mn contents of the separated δ residues and of the parent steels, the compositions of the γ_S phase were computed, table 4. Values for the δ and γ_S phases in steel 1 after solution treatment at 2,500° F are not given because the residues were contaminated with nonmetallic inclusions. This contamination was the result of a very low yield obtained in the ferric chloride separation.

The data in table 4 indicates that the δ/γ_S distribution ratios of the chromium, nickel, molybdenum, and manganese contents are approximately 1.2, 0.5, 1.7, and 0.9, respectively, over these ranges of temperature and composition.

In order to know the approximate compositions of the σ, χ, and carbide phases, residues whose X-ray diffraction analysis had shown them to be composed primarily of one of these phases were analysed chemically for Cr, Ni, Mo, and Mn contents. The small amount of residue available for chemical analysis precluded determinations of the carbon and silicon contents. The results, table 5, show that the manganese contents of the carbide, σ, and χ phases are approximately the same as that of the parent steels. The chromium and nickel contents of σ are about the same as that of χ, but the molybdenum content is appreciably less.

TABLE 4. *Chemical composition of δ and γ_S after solution treatments*

Steel	Solution treatment	Phase	Composition			
			Cr	Ni	Mo	Mn
	° F					
1	2,000 (B)	δ	20.7	5.0	4.9	0.7
		γ_S	17.0	8.4	2.9	.7
	1,800 (C)	δ	21.3	4.5	5.3	.7
		γ_S	17.0	8.4	2.9	.7
2	2,300 (A)	δ	19.1	5.6	5.3	1.3
		γ_S	17.5	10.4	3.2	1.7
	2,000 (B)	δ	18.4	4.9	5.8	1.3
		γ_S	17.8	9.5	3.6	1.6
3	2,300 (A)	δ	21.8	8.0	6.3	1.4
		γ_S	18.3	13.6	3.5	1.6

[1] Composition computed.

TABLE 5. *Chemical composition of residues approximating sigma, chi, and carbide ($M_{23}C_6$) phases*

Phase	Cr	Ni	Mo	Mn	Source of residue		
					Steel	Solution treatment	Reheat treatment
						° F	° F
σ	27.6	3.6	11.9	0.8	1	2,000 (B)	1,700 (K)
χ	27.9	3.0	19.4	1.3	2	2,000 (B)	1,500 (L)
$M_{23}C_6$	52.9	1.9	12.5	1.3	2	2,000 (B)	1,200 (M)

4.3. Ferrite Residues after Heating at 1,700°, 1,500°, and 1,200° F

Samples of the δ residues that were separated from the solution-treated steels were sealed in vacuum in fused-silica tubes and, simultaneously with pieces of parent steels, were given the low-temperature heat treatments listed in table 2. Both the sealed residues

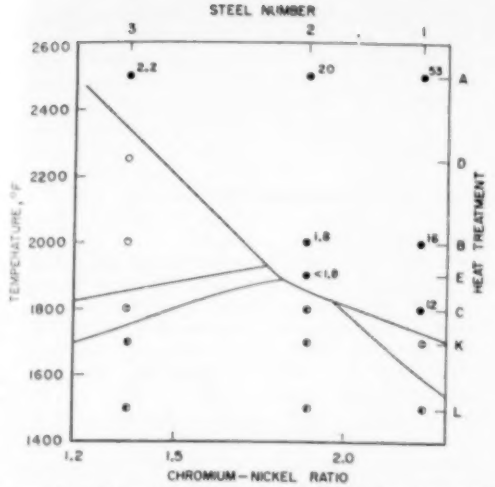

FIGURE 5. *Phases in steels 1, 2, and 3 after heat treatments.*

Phases identified after each heat treatment are indicated as ● for δ and γ; ○ for γ only; ◑ for γ, carbide, and σ; ◐ for γ, carbide, σ, and χ. Numbers adjacent to symbols are percentages of δ as determined by lineal analysis.

and steels were quenched in water. Two of the residues were oxidized because the fused-silica tubes cracked in quenching. The residues so treated were examined for magnetic particles and then analyzed qualitatively by X-ray diffraction. The treated residues undoubtedly contained carbides in addition to the phases reported as present.

The results, table 6, show that δ in the residues from steel 1 did not decompose completely, whereas those from steel 3 did. Excepting the residue from steel 1 after the 2,500° F solution treatment, σ and γ_R were the decomposition products. It is probable that equilibrium was attained in the 1,700° and 1,500° F reheat treatments. This means that the compositions of these residues from steel 1 were such that δ and σ were mutually stable at 1,700° and 1,500° F whereas this was not the case for the residues from steel 3. This difference in stability of δ apparently was caused by differences in composition of approximately 3 percent Ni and 1 percent Mo, see table 4. The decomposition of δ in the residues from steel 2 apparently is more sensitive to composition. Here a decrease of 0.7 percent of Cr, 0.7 percent of Ni, and an increase of 0.5 percent of Mo in the composition of the residue after the 2,500° F solution treatment, appeared to be sufficient to affect the stability of δ and the kind of decomposition products.

4.4. Solution-Treated Steels after Reheating to 1,700°, 1,500°, and 1,200° F

Samples of steels 1, 2, and 3 that contained the δ phase after solution treatments at 2,500°, 2,000°, and 1,800° F, and that were reheated to 1,700°, 1,500°, and 1,200° F, were examined microscopically and their residues analysed by X-ray diffraction. The results with respect to the constituents identified in the microstructures are summarized in figures 3 and 4. In making these identifications it was assumed that the constituents in the residues were present in the microstructures, even though they could not be distinguished by etching. No attempt was made to identify or distinguish oxide inclusions. Inspection shows that the microconstituents found in the reheated steels were not always independent of the previous solution treatments. In steel 1 (fig. 3), after reheating to 1,700° F for 340 hours, the presence of the carbide phase in the sample that had been solution treated at 1,800° F (1CK) was doubtful, whereas its presence was definitely established in samples that had been solution treated at 2,500° and 2,000° F (1AK and 1BK). A similar tendency for less carbide phase after the low-temperature solution treatment also was noted in the microstructures of samples that had been reheated to 1,500° F for 500 hours, figure 3. The 1CL microstructure shows less carbide phase than the 1BL and 1AL microstructures. There is no obvious explanation for the foregoing tendency. Apparently it is affected by the amount of ferrite initially present. When the amount of the initial ferrite is but slightly greater than the σ that is formed, the solubility of carbon appears to be higher than when the initial ferrite is in greater excess. The work of Rosenberg and Irish [6] on high-purity alloys indicates that the solubility of carbide in γ at 1,700° F is of the order of 0.03 to 0.05 percent of carbon, which is slightly less than the 0.05-percent-carbon content of steel 1. In the range of 0.03 to 0.05 percent of carbon, the presence of carbides was questionable at

TABLE 6. *Qualitative analysis by X-ray diffraction of ferrite residues after low temperature heat-treatments*

P, Present; ?, doubtful; and ND, not detected

Steel	Solution-treatment	Heat-treatments											
		1,700° F, 340 hours				1,500° F, 500 hours				1,200° F, 500 hours			
		Undecomposed δ	Decomposition products			Undecomposed δ	Decomposition products			Undecomposed δ	Decomposition products		
			γ_R	σ	χ		γ_R	σ	χ		γ_R	σ	χ
	° F												
1	2,500	P	P	?	ND	P	P	ND	ND	P	P	ND	ND
	2,000	P	P	P	ND	P	P	P	ND	P	P	P	ND
	1,800	P	P	P	ND	(*)	(*)	(*)	(*)	P	P	P	ND
2	2,500	ND	P	P	P	P	P	P	P	P	P	P	ND
	2,000	P	P	ND	P	(*)	*	(*)	(*)	P	P	ND	ND
3	2,500	ND	P	P	ND	ND	P	P	ND	ND	P	P	ND

* Specimen damaged.

1,700° F. On the basis of their results, therefore, the presence of carbides may be expected.

Similar results in figure 4 show that for steel 2, solution treated at 2,000° F, σ was present as a trace after reheating to 1,200° F (2BM); however, the presence of σ was easily detected after solution treatment at 2,500° F and reheat treatment at 1,500° and 1,200° F (2AL and 2AM). Here again the influence of solution treatment can be traced to the amount of ferrite initially present. In addition to the effect on σ the 2AL and 2BL microstructures strikingly show that the amount and distribution of the reaction products have been affected by the amount of initial ferrite. The photomicrographs in figure 3 also show that δ was not detected in steel 1 as reheated to 1,200° F after solution treatment at 2,500° F (1AM), but was present after solution treatment at 2,000° and 1,800° F (1BM and 1CM). It is probable that δ was present in the reheated, 2,500° F solution-treated sample but could not be detected because of the solubility of undecomposed δ in the ferric-chloride reagent. This was discussed in section 4.2.

Inspection of the microstructures of the reheated steels (figs. 3 and 4) shows that if a large amount of δ was present initially, the reactions tended to be wholly within the δ phase. When this is not the case the microconstituents are formed in the γ matrix. This tendency for the reactions to nucleate and continue within the δ phase is illustrated by the photomicrographs in figure 4 obtained for steel 2 as reheated to 1,200° F after solution treatments at 2,500° and 2,000° F (2AM and 2BM). These microstructures show that, except for the formation of carbide in the grain boundaries, the reaction was within the δ phase. No undecomposed δ was identified, indicating that δ had decomposed completely. The results in table 4 showed that the δ in these steels did not decompose in the absence of γ_B; therefore the complete decomposition of δ in the 2AM and 2BM microstructures could not have happened without diffusion of the reacting elements from adjacent γ_B.

The 2BM microstructure, figure 4, is particularly interesting because of the dense mottled structure of the former ferrite, but only carbide was detected in this structure. The mottled structure probably is not entirely the result of carbide precipitation but more probably results from the etching characteristics of a transition phase [7] in the decomposition of δ and formation of σ and γ_R. This conclusion is supported by σ being present in the 2AM microstructure, which shows that σ was stable at 1,200° F; therefore, σ would tend to precipitate in the 2BM microstructure. These comments also apply to the 3AM microstructure.

5. Summary

Three austenitic stainless steels, 18:8 Mo type, of slightly different compositions, were given three solution treatments (2,500° F, ½ hour; 2,000° F, ½ hour; and 1,800° F, 18 hours; all quenched in water), followed by reheating at three lower temperatures (1,700° F, 340 hours, 1,500° F, 500 hours; and 1,200° F, 500 hours) and quenching in water. The steels were examined microscopically, and the electrolytically separated residues were examined by X-ray diffraction methods.

Examination of the heat-treated specimens showed four fields of stability: a region in which γ was the only phase; a region in which γ and δ were stable; a region in which γ, carbide ($M_{23}C_6$) and σ were stable; and a region in which γ, carbide ($M_{23}C_6$), σ, and χ were stable.

The δ was separated from the γ and heated at the lower temperatures along with samples of the parent steels. The chemical analyses of δ and the computed analyses of γ indicated that the distribution ratios for Cr, Ni, Mo, and Mn in the δ/γ phases were approximately 1.2, 0.5, 1.7, and 0.9, respectively, in the range 1,800° to 2,500° F.

Results showed that the decomposition of δ and the kind of products that were formed were influenced by small differences in the Cr, Ni, and Mo contents.

Examination of the reheated steels showed that the amount of δ formed in the solution treatment affected the decomposition of δ and the kind of products formed at certain reheating temperatures. It appeared that there was a tendency for the reactions to nucleate in the δ sites and to continue by diffusion of elements from the matrix. When the volume of decomposition products exceeded the volume of the initial δ, the products tended to be distributed intragranularly.

The authors gratefully acknowledge the assistance of E. A. Buzzard and R. Liss in the earlier work done in cooperation with the American Society for Testing Materials. They also gratefully acknowledge the work done by J. I. Shultz in the chemical analyses of the residues.

6. References

[1] K. W. Andrews and P. E. Brookes, Chi phase in alloy steels, its relationship to sigma phase, Metal Treatment and Drop Forging **18,** 301 (1951).

[2] K. W. J. Bowen and T. P. Hoar, Phase changes associated with sigma formation in 18–8–3–1 chromium-nickel-molybdenum-titanium steel, Am. Soc. Metals (Proc. First World Metallurgical Congress, Cleveland, Ohio, 1951).

[3] T. P. Hoar and K. W. J. Bowen, The electrolytic separation and some properties of austenite and sigma in 18-8-3-1 chromium-nickel-molybdenum-titanium steel, Trans. Am. Soc. Metals **45,** 443 (1953) and discussion.

[4] The sigma phase investigation program of Sub-Committee VI of Committee A–10, Annual Committee Reports, Proc. Am. Soc. Testing Materials **53,** 143 (1953).

[5] R. T. Howard and Morris Cohen, Quantitative metallography by point-counting and lineal analysis, Trans. Am. Soc. Min. and Met. Engr. **172,** 413 (1947).

[6] Samuel J. Rosenberg and Carolyn R. Irish, Solubility of carbon in 18-percent-chromium–10-percent-nickel austenite, J. Research NBC **48,** 40 (1952) RP2281.

[7] A. H. Geisler, Precipitation from solid solutions of metals, Phase transformations in solids, p. 426. (John Wiley & Sons, New York, N. Y., 1951).

WASHINGTON, January 20, 1954.

Determination of Hydrogen by Slow Combustion Over Platinum in Excess Oxygen

Shuford Schuhmann and Martin Shepherd [1]

The accuracy and reproducibility of the determination of hydrogen by combustion with excess oxygen over a hot platinum helix (slow combustion) have been experimentally measured. The combustion of a pure hydrogen gave the observed stoichiometric relationship, $H_2+0.4996\ O_2 \rightarrow 1.4996$ contraction. The ideal relationship, corrected for the deviations of hydrogen and oxygen, is $H_2+0.4994\ O_2 \rightarrow 1.4994$ contraction. Uncorrected, the method gave these results: Hydrogen calculated from the contraction, 99.98 ±0.03 percent; hydrogen from oxygen consumed, 99.91 ±0.13. Corrected, these results became 100.02 ±0.03 and 100.03 ±0.13, respectively.

1. Introduction

This is one of a series of papers [1 to 10] [2] reporting experimental measurements of the accuracy and reproducibility of existing methods of gas analysis, by the analysis of gases of critically known purity or standard gas mixtures. This paper deals with the determination of hydrogen by slow combustion. In work of this kind, the greatest single burden usually is the preparation of the gas of known purity and the determination of its purity to a significance greater than the capability of the analytical method under investigation. All too often, the behavior of a method is reported in terms of the analysis of a "pure" substance or "synthetic mixture," and the results accepted as fact, even when no conclusive evidence of purity or known composition has been presented. This is unfortunate, for no more direct means exists to verify an analytical method than to make repeated analyses of a substance or substances of known composition. If the analyses can be made by many analysts using an identical procedure during a considerable time, so much the better. The accuracy and reproducibility to be expected with such a diffuse effort, which gives the picture of what generally may be expected, are never so favorable as those obtained in a single laboratory by one careful worker. The work reported here, however, is of this more restricted nature.

2. Hydrogen Used for Analysis

The hydrogen for this work was obtained from the electrolytic battery generating the hydrogen used for liquefaction at the Bureau. When this battery has been operating for some time, all air is displaced, and the only impurity occurring in the hydrogen is oxygen, which is removed by passage over hot platinum. The purity of the hydrogen was checked at the plant by a special thermal-conductivity apparatus sensitive to less than 0.01 percent oxygen. Hydrogen so prepared was passed at atmospheric pressure through a previously evacuated in-seal condenser equipped with a glass-wool filter and immersed in liquid hydrogen. The saturation pressure of any higher-boiling impurities is negligible at this temperature. (For oxygen it is of the order of 10^{-15} mm Hg, and the filter removes any fine crystals from the incoming stream of gas.) If helium is not an impurity, this is an effective way of preparing pure hydrogen. Hydrogen so prepared should contain less than 0.00001 percent by volume of higher-boiling impurities. Thus the total impurity of the hydrogen used in this work was several orders of magnitude less than the occasion demanded.

The oxygen used for combustion was obtained from rectification of liquid air. The inert impurity was determined as the residue after absorption in alkaline pyrogallol. The nitrogen in the buret at the beginning of each analysis was prepared initially from air by five complete passages of the gas into the pipet containing alkaline pyrogallol and thereafter by removal of oxygen from the products of combustion.

3. Analytical Procedure

The apparatus described by Shepherd [11] was used for the analysis. The procedure was as follows:

1. Nitrogen (about 60 ml) was prepared, measured, and stored in the pipet containing the solution of alkaline pyrogallol (pyro pipet).
2. Oxygen (about 60 ml) of known composition was measured and transferred to the slow-combustion pipet.
3. Hydrogen (about 60 ml) was measured and slowly (not more than 10 ml/min) passed into the combustion pipet with platinum spiral heated to a cherry-red color. Gas from the arm of the manometer connecting to the distributor was displaced to the buret and transferred to the combustion pipet. Four complete passages between the buret and combustion pipet were made.
4. The residue from the combustion was measured and the contraction computed.
5. Nitrogen from the pyrogallol pipet was transferred to the buret, and the oxygen was removed from the combined nitrogen and residue from the combustion by five complete passages into the pyro-

[1] Deceased, September 17, 1953.
[2] Figures in brackets indicate the literature references at the end of this paper.

gallol solution. The residual nitrogen was measured, and from this the excess oxygen and the oxygen consumed were computed.

4. Stoichiometry and Discussion of Errors

If the reaction involves only hydrogen and oxygen, and is complete; if the gases are all ideal gases; if there are no gains or losses through solution or otherwise except the quantitative absorption of oxygen in the pyrogallol solution, and the contraction caused by condensation of the water formed; and if there are no errors of manipulation or observation during the analysis, the observed values for the analysis would correspond to the ideal stoichiometric equation

$$H_2+0.5\ O_2 \rightarrow H_2O+1.5 \text{ (volume) contraction.} \quad (1)$$

Actually, the observed values did not correspond to this equation. Instead, the average values of 20 analyses are expressed by the volume equation

$$H_2+0.4996\ O_2 \rightarrow 1.4996 \text{ contraction.} \quad (2)$$

An explanation of the observed values involves the discussion of various errors. In this discussion, reference will be made to the stoichiometric data given in table 1. Columns 1 and 2 of this table give the data for observed contraction per sample and oxygen consumed per sample, from which eq (2) was derived.

TABLE 1. *Observed stoichiometric ratios*

Analysis No.	1 Contraction per sample	2 Oxygen consumed per sample	3 N_2 balance	4 Corrected oxygen consumed per sample
			ml	
1	1.4993	0.4989	−0.02	0.4993
2	1.5000	.5004	+.02	.5000
3	1.5000	.4990	−.06	.5000
4	1.4995	.4990	−.03	.4995
5	1.4967	.5002	+.06	.4962
6	1.4990	.4987	−.02	.4990
7	1.5001	.4996	−.03	.5001
8	1.4997	.4992	−.03	.4997
9	1.4988	.5011	+.08	.4988
10	1.4999	.4996	−.02	.4999
11	1.4994	.5002	+.05	.4994
12	1.4993	.4995	+.01	.4993
13	1.4999	.5002	+.02	.4999
14	1.4986	.4982	−.02	.4986
15	1.4999	.4989	−.06	.4969
16	1.4980	.5010	+.11	.4990
17	1.4997	.4994	−.02	.4997
18	1.5006	.5001	+.01	.4999
19	1.4991	.4986	−.03	.4991
20	1.5003	.4993	−.06	.5003
Average	1.49964	0.49956		0.49958
Average deviation	±0.00039	±0.00064		±0.00034

5. Deviation of the Gases from Ideality

The usual chemical volumetric gas analysis involves the measurement of various mixtures of gases. The sample is ordinarily a mixture which is progressively simplified by the removal of one or more constituents at a time. The products of combustion are mixtures. Thus, correction for deviation from ideality is quite difficult, for while deviations for many of the separate gases have been measured, there is no law to predict their behavior in mixtures, and the deviations significant to the analysis must be measured. The present analysis is an exception. Every gas measured throughout is an approximately pure one. Thus, the gases measured at each step of the analysis are (in order) nitrogen, oxygen, hydrogen, oxygen, and nitrogen. A stoichiometric equation accounting for the deviations from ideality at 1 atm and 25° C (for H_2, $PV/nRT=Z=1.0006$ [14]; for O_2, $Z=0.9994$ [15]) may accordingly be written: $1.0006\ H_2+0.5\ (0.9994)O_2 \rightarrow 1.5003$ contraction or,

$$H_2+0.4994\ O_2 \rightarrow 1.4994 \text{ contraction.} \quad (3)$$

This correction alone brings the ideal eq (1) into better agreement with eq (2), for the observed values.

6. Other Considerations

By comparison of eq (2) and (3) it becomes evident that eq (2) would have been identical with eq (3) if the 0.0002 volume less oxygen had been consumed; for then the contraction would also have been 0.0002 volume less. If this correlation is significant, it indicates that the only appreciable error sustained in the combustion was the reduction of slightly more oxygen than commensurate with the amount of hydrogen burned. Several possible fates of this oxygen deserve consideration.

The oxidation of nitrogen is hardly possible in this analysis. Even when air (with high partial pressure of nitrogen) was burned with hydrogen, NO_2 was not found to have been formed during the procedure used for combustion. The only nitrogen present during this combustion was at very low partial pressure, occurring to the extent of 0.09 percent in the oxygen used (in actuality, most of this "nitrogen" was probably argon). Nitrogen dioxide when formed reacts almost completely with the wet mercury and is accordingly observed as part of the contraction. Such an error seems not to have occurred in this instance.

The formation of a small amount of mercuric oxide might have accounted for the slightly high oxygen consumption and an equal increase in contraction. Perhaps a small amount of hydrogen peroxide may have been formed at the hot platinum spiral, then removed from the gas phase by reduction with lubricant in the stopcocks between the combustion pipet and the buret; or a small amount of ozone may have formed at the hot wire, then formed addition products with stopcock lubricant. Loss of oxygen by solution in water formed during combustion was calculated to be insignificant.

Under the conditions of the analysis, an average of less than 0.01 ml of carbon monoxide may have been generated during the absorption of excess oxygen, [12]. This carbon monoxide would not have entered into the next combustion with reuse of the residual nitrogen; but if it occurred, it would have appeared as nitrogen at the last step in the procedure.

this would have made the excess oxygen appear too small and the oxygen consumed correspondingly too large. Indeed, a comparison of eq (2) with eq (3) does show observed oxygen consumed to be high; but this explanation does not fit the case because when oxygen consumed is corrected for nitrogen off-balance the value is insignificantly changed, in the wrong direction. This correction eliminates the error in oxygen consumed caused by the generation of carbon monoxide.

The nitrogen balance, or total loss or gain of gas during each complete analysis, is determined by comparing the nitrogen originally measured with the residual nitrogen. These data are given in column 3 of table 1. While the sum of the gains and losses is algebraically almost zero for the series of analyses (the observed cumulative loss was 0.04 ml, or an average of 0.0002 ml per analysis), and while many of them are near the expected error of volume measurement (± 0.02 ml), nevertheless, there are more losses than gains, and the losses are somewhat more systematic. Every time a loss of nitrogen occurred, the oxygen consumed was found to be low; whereas with every gain of nitrogen the consumed oxygen was high (with a single exception, analysis 12). If the analyses are corrected individually for this off-balance of nitrogen to adjust the oxygen consumed, 15 of the 20 show improved values for oxygen consumed (column 4, table 1). Of these, 15, 12 occur when the nitrogen balance shows a loss. This seems significant, and indicates complete absorption of excess oxygen, complete combustion of the sample, and no significant production of carbon monoxide. Since the solution of alkaline pyrogallol was in equilibrium with nitrogen before and after each absorption, and is one of the best reagents with respect to exchange of inerts by sorption and desorption [13], what seems to be a slight apparent loss of nitrogen could hardly have been caused by physical solution of nitrogen.

When the oxygen consumed is corrected for nitrogen balance on the assumption that the latter was a measure of the error made in the measurement of excess oxygen, the observed stoichiometric eq (2) is not changed significantly, but the reproducibility of the oxygen value is considerably improved. The previous discussion may therefore seem partly gratuitous; but the errors considered may affect individual analyses rather than the average of a large group—and usually only a few analyses of a single sample are made, so that the possibility of such errors should always be kept in mind.

The application of this correction renders the value for oxygen consumed independent of the inert content of the oxygen. Since it does not appreciably change the average oxygen value, assurance is afforded that the analysis of the oxygen was accurate; or that generation of carbon monoxide by pyrogallol, if it occurred, compensated for the error in the analysis of the oxygen.

7. Analytical Data

The results of computing the analyses from the observed and corrected stoichiometric relations just discussed are given in table 2. The percentages of hydrogen calculated from the observed contraction and oxygen consumed (columns 1 and 2) average 99.975 ± 0.027 and 99.912 ± 0.126, respectively. The observed contraction yielded more satisfactory results with respect to both accuracy and reproducibility than oxygen consumed; but this is to be expected, since there are more chances for errors in this measurement, and the arithmetic involved penalizes this measurement while favoring the measurement by contraction. The net error in oxygen consumed is multiplied by 2 in calculating hydrogen, but divided by 1.5 in calculating hydrogen from the contraction. The measurement of contraction involves the measurement of 3 gas volumes (oxygen, hydrogen, and residual oxygen) and a simple catalytic combustion in which the possibilities of side reactions and errors of sorptions are probably limited to those discussed under "other considerations." The measurement of oxygen consumed involves the measurement of 4 gas volumes (oxygen, residual oxygen, original nitrogen, and residual nitrogen), and an absorption which might include a side reaction and errors of solubility. In addition, another analysis—that made to determine the purity of the oxygen used—is also involved. Altogether, the measurement of oxygen consumed is relatively handicapped, and its analytical use as a check on the contraction is of doubtful value. If the measurement is made, it is probably advisable to correct it for nitrogen off-balance; for while this correction does not

TABLE 2. *Apparent percentages of hydrogen*

Analysis No.	1 Contraction per 1.5 sample	2 $2\ O_2$ per sample	3 $2\ O_2'$ per sample	4 Contraction per 1.4994 sample	5 2.0024 O_2 per sample	6 2.0024 O_2' per sample
1	99.95	99.79	99.86	99.99	99.90	99.96
2	100.00	100.07	100.00	100.04	100.20	100.12
3	100.00	99.79	100.00	100.04	99.92	100.12
4	99.97	99.80	99.90	100.01	99.92	100.04
5	99.98	100.03	99.84	100.02	100.16	100.04
6	99.93	99.73	99.80	99.97	99.86	99.92
7	100.00	99.92	100.02	100.04	100.04	100.12
8	99.98	99.83	99.94	100.02	99.96	100.04
9	99.98	100.21	99.96	100.02	100.34	100.04
10	100.00	99.91	99.98	100.04	100.04	100.10
11	99.97	100.05	99.88	100.01	100.16	100.00
12	99.95	99.90	99.86	99.99	100.02	100.00
13	100.00	100.05	99.98	100.04	100.16	100.10
14	99.90	99.65	99.72	99.94	99.76	99.84
15	100.00	99.78	99.98	100.04	99.90	100.10
16	99.93	100.19	99.80	99.97	100.32	99.92
17	99.98	99.88	99.94	100.02	100.00	100.04
18	100.03	100.02	99.98	100.07	100.14	100.10
19	99.93	99.72	99.82	99.97	99.84	99.94
20	100.02	99.87	100.06	100.06	99.98	100.18
Average	99.975	99.912	99.916	100.016	100.032	100.036
Avg. deviation	±0.027	±0.126	±0.092	±0.027	±0.128	±0.068

greatly change the average value (compare the 99.916 average of column 3 with 99.912 of column 2), the reproducibility is improved (± 0.092 compared with ± 0.126), and the chance for a good individual analysis is better. Correction for nitrogen off-balance really amounts to eliminating 2 of the 4 measurements involved in determining oxygen consumed; and these 2 are more subject to error than the 2 actually used, i. e., the original measurement of oxygen taken for the combustion, and the measurement of the residual oxygen. The average deviations shown in table 1 are in order of increasing deviation: 0.60034 for corrected oxygen consumed per sample, 0.00039 for contraction per sample, and 0.00064 for oxygen consumed per sample. Correspondingly, corrected oxygen consumed per sample, contraction per sample, and oxygen consumed per sample, were obtained by the combination of 2, 3, and 4 independent gas-volume measurements, respectively.

If the percentages of hydrogen are corrected for deviations from ideality, the values given in columns 4, 5, and 6 are obtained. Hydrogen from corrected contraction gives the average 100.016 ± 0.027 percent; from corrected oxygen consumed, 100.032 ± 0.128; and from corrected oxygen consumed adjusted for nitrogen off-balance, 100.036 ± 0.068 percent. Although adjustment for nitrogen unbalance throws the average corrected value from oxygen consumed still further above the theoretically correct result, it may be desirable because of the improved reproducibility it affords. Thus, when only one or two analyses are available, such correction may yield the more accurate result. The fact that making this adjustment changed so little the average apparent hydrogen content is evidence that a substantial portion of the observed unbalance was not from a systematic effect but represented instead nearly random distribution of the errors in the measurement of the two additional gas volumes involved when the adjustment was not made.

In attempting to decide whether or not to correct the contraction, one is tempted by the relative amounts of the differences from the known purity, disregarding sign, to make the corrections. From a practical point of view, uncorrected contraction is probably the better choice, because a reported purity of less than 100 percent is infinitely more believable than a value greater than 100. This consideration applies equally to values from uncorrected oxygen consumed. Adjustment for nitrogen off-balance is applicable and results not only in improved reproducibility but also in a nearer approach of the computed value to the known.

The application of the ideality corrections was helpful in unmasking a slightly excessive consumption of oxygen as probably the effect that compensated the observed results for the deviations from ideality. The verification of this is a subject for future study.

8. References

[1] M. Shepherd and J. R. Branham, BS J. Research **11,** 783 (1933) RP625.
[2] J. R. Branham and M. Shepherd, J. Research NBS **13,** 377 (1934) RP715.
[3] J. R. Branham, M. Shepherd, and S. Schuhmann, J. Research NBS **26,** 571 (1941) RP1396.
[4] M. Shepherd, J. Research NBS **36,** 313 (1946) RP1704.
[5] M. Shepherd, J. Research NBS **38,** 19 (1947) RP1759.
[6] M. Shepherd, J. Research NBS **38,** 491 (1947) RP1789.
[7] M. Shepherd, J. Research NBS **44,** 509 (1950) RP2098.
[8] M. Shepherd, Anal. Chem. **19,** 635 (1947).
[9] M. Shepherd, Anal. Chem. **22,** 881 (1950).
[10] M. Shepherd, Anal. Chem. **22,** 885 (1950).
[11] M. Shepherd, BS J. Research **6,** 121 (1931) RP266.
[12] M. V. Kilday, J. Research NBS **45,** 43 (1950) RP2112.
[13] J. R. Branham and M. Sucher, J. Research NBS **21,** 63 (1938) RP1113.
[14] H. W. Woolley, R. B. Scott, and F. G. Brickwedde, J. Research NBS **41,** 379 (1948) RP1932.
[15] C. Cragoe (private communication).

Washington, March 9, 1954.

Anhydrous Sodium Hydroxide: The Heat Content From 0° to 700° C, the Transition Temperature, and the Melting Point*

Thomas B. Douglas and James L. Dever

Samples of sodium hydroxide, whose purity as indicated by analyses was approximately 99.3 percent, were sealed in pure silver. Cryoscopic measurements indicated a transition temperature of 293° C. Using a "drop" method and a Bunsen ice calorimeter, the enthalpy[1] change between 0° and each of 11 temperatures up to 700° C was measured. With reasonable simplifying assumptions, the thermal measurements near the freezing point were used to correct for the impurity, giving for pure sodium hydroxide a melting point of 319° C and the same value, 159 absolute joules per gram, for the heat of fusion and the heat of transition. The heat capacity derived for the liquid is estimated to be correct within 2 percent, whereas the derived heats of fusion and transition may be in error by as much as 5 percent. Values of heat capacity, entropy, relative enthalpy, and relative free energy are tabulated at regular intervals from 298° to 1,000° K.

1. Sample and Containers

As a container material for the sodium hydroxide, oxygen-free silver was selected, as tests made elsewhere [2] indicate that this material is attacked only slightly by molten sodium hydroxide at the high temperatures to be used. Any disintegration of the silver surface, which is thought to be the only interaction that would occur, was not expected to affect the total enthalpy of such a sample. An examination of two of the silver containers after exposure to molten sodium hydroxide at 700° and 800° C is described in section 3.

Silver of 999.5 fineness that had been cast in an inert atmosphere to remove the oxygen was obtained from the American Platinum Works, of Newark, N. J., in the form of tubing 0.015 in. thick and of ¾-in. diameter. Each container was fabricated from a length of this tubing by drawing down one end by dies to a neck of 2 in. in length and ¼-in. diameter. After turning down the neck to an average wall thickness of 0.012 in. (to decrease heat conduction and so facilitate the subsequent sealing off), the larger open end was closed by welding to it a silver cap of 0.02-in. thickness.

Four such containers were loaded with solid sodium hydroxide (about 4 g each) in a dry box continuously swept out with argon dried by activated alumina. They were then promptly evacuated to a pressure of 1 mm or less. Under an internal pressure of 25 mm of helium (added for good heat transfer during the subsequent measurements), their necks were then flattened and sealed off in a gas-oxygen flame. That the samples to be used were gas-tight was confirmed by evacuating the surrounding space and then surrounding them by helium. If they had not been tight, the air that had consequently leaked in (several milligrams) would have been replaced by helium. However, there was no detectable decrease in weight. The part of the final mass of each sample due to silver and the part due to sodium hydroxide were easily obtained using the masses of the empty silver vessel and of the silver removed on sealing. Preliminary tests had shown that consistently about 1 mg of silver was lost during such a sealing process.

The stock of sodium hydroxide used had been obtained from the Oak Ridge National Laboratory, which gave as its analysis "100.0 percent (±0.05%) alkalinity, calculated as NaOH; 0.05 percent Na_2CO_3." Simultaneously with filling the silver vessels, three additional samples were taken in the dry box, and were sealed and stored in a desiccator over solid potassium hydroxide. Two of these samples were titrated at the Bureau, using both phenolphthalein and methyl orange as indicators, in the presence of barium chloride and using standardized normal hydrochloric acid. These analyses gave the following results.

Sample	NaOH	Na_2CO_3
	%	%
1	99.2	0.33
2	99.4	.27

It seems likely that the remaining approximately 0.4 percent was largely water. A considerable portion of the impurities may have entered during handling in the dry box.

2. Cryoscopic Measurements

Careful measurements of the temperatures of halt during cooling were undertaken in order to determine the freezing and transition points of the two samples on which nearly all of the enthalpy measurements were made. Measuring the equilibrium temperatures during freezing provided also an estimate of the amount of impurity in the samples. The general

*This work was supported by the United States Air Force, Wright Air Development Center, Wright-Patterson Air Force Base, Ohio.

[1] The terms *enthalpy* and *heat content* are used interchangeably to designate the same thermodynamic property, which is symbolized by *H*.

[2] L. G. Overholser, Oak Ridge National Laboratory, private communication.

method and type of apparatus used have been described in detail elsewhere[1].[2] Because higher temperatures are involved here, it was necessary to construct a new apparatus held together by silver solder instead of tin.

The apparatus used is shown in figure 1. The sample container was surrounded by a close-fitting gold-plated copper cylinder suspended in the silver surrounded furnace core that was later used with a Bunsen ice calorimeter for the enthalpy measurements. A single-junction thermocouple (chromel P versus constantan) measured the difference in temperature between the furnace wall and the sample, whereas a platinum resistance thermometer accurately measured the furnace temperature. The method used was entirely similar to the conventional cooling-curve technique, except that after a desired amount of cooling (usually 1 deg), the environing furnace was then held constant at a temperature sufficiently close to that of the sample to halt most of the cooling and so to permit a dependable evaluation of the sample temperature. (Because the thermal conductivity of sodium hydroxide is so much smaller than that of metals, it was found in preliminary trials that the conventional dynamic cooling-curve method led to such large thermal lags as to be entirely useless here.)

[2] Numbers in brackets refer to literature references at the end of this paper.

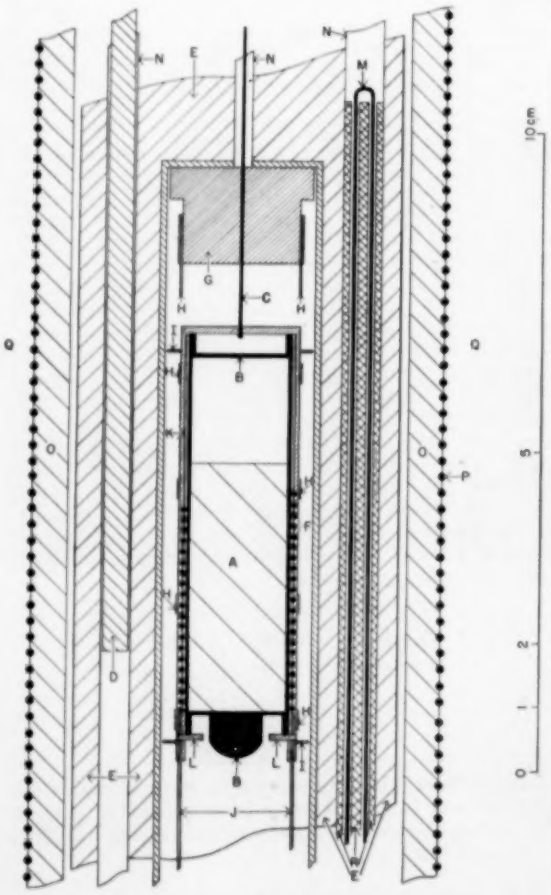

FIGURE 1. *Cryoscopic apparatus.*

A, Sample of sodium hydroxide; B, sealed container for sample (silver) (shown slightly different in shape from that actually used); C, suspension wire (nichrome V); D, platinum resistance thermometer; E, isothermal jacket (silver); F, heater for sample (glass-covered constantan); G, thermocouple reference block (gold-plated copper); H, thermocouple junctions (silver bands); I, spacers (nichrome-V wire); J, heater leads (copper); K, jacket for sample container, and heater cover (gold-plated copper); L, pins for supporting sample container; M, auxiliary heater for silver jacket (nichrome); N, Inconel tubing; O, Alundum tube; P, main furnace heater (platinum); Q, furnace insulation (silica powder); R, porcelain tube.

The technique adopted consisted in melting all the sample and then cooling it in stages by lowering the furnace temperature 1 deg at a time. After a small amount of freezing had occurred, the furnace temperature was held constant and the thermocouple was read until steady. Subsequent raising of the furnace temperature and then maintaining it constant slightly above the sample temperature, gave another set of data that provided a direct empirical determination of the thermocouple sensitivity for measuring the difference in temperature between the furnace and the NaOH solid-liquid interface, assuming that the temperature of the latter had not changed appreciably. As this sensitivity was considerably lower than such a thermocouple would ordinarily give, it was evident that the thermocouple was measuring only a fraction of the desired temperature difference, owing to an unavoidable thermal resistance between the thermocouple junction and the NaOH solid-liquid interface. The calibration just referred to, however, should have eliminated most of the error from this source.

In order to estimate the amount of liquid-soluble, solid-insoluble impurity in the sodium hydroxide sample, the temperature of the furnace was maintained several degrees below that of the sample itself for the time necessary to freeze about half of it. After again raising the furnace temperature to slightly below and then to slightly above the sample, and repeating the readings described in the preceding paragraph, the temperature of the sample was found to have dropped from approximately 317.1° to 315.8° C. Approximately the same temperatures were found for both samples of sodium hydroxide. In the present investigation the solid-solid transition point was similarly determined and for both samples was found to be 292.8° C.

In order to estimate how long to cool the sodium hydroxide so as to freeze a certain fraction of it, it was necessary to establish the heat-leakage rate of the sample in the given experimental environment. This rate was measured by substituting a sealed sample of sodium metal, in which the thermal gradients could be assumed negligible, and following the rate of change in the difference between the temperature of the completely melted sodium and that of the furnace. As in all cases, the differential thermocouple readings were corrected by the reading obtained after the two were known to have reached

same temperature. The heat-leakage rate was readily calculated from the known masses and specific heats of the component parts of this system.

Table 1 summarizes the data obtained in measuring the transition and freezing points of the two samples of sodium hydroxide.

The obvious small inconsistencies in table 1 between the fractions frozen and the corresponding sample temperatures indicate that these measurements can be only roughly correct. Fortunately, the enthalpy measurements later made in this temperature region furnish independent data for determining the same relationships, and an estimate of the amount of impurity present will thus be deferred to section 4.

TABLE 1. *Equilibrium temperatures during transition and freezing of two samples of sodium hydroxide*

Sample	Furnace temperature	Temperature of sample holder relative to furnace	Interpolated temperature of sample	Phase change involved	Estimated fraction frozen	Effective sensitivity of differential thermocouple
	°C	μV	°C			μV/° C
3	292.8	−30	292.8	Transition	.....	42
	293.75	−40				
	292.25	+23				
	293.65	−20				
3	316.35	+18	316.9	Freezing	0.04	27
	317.8	−20.5				
	316.4	+15				
	316.9	−4				
3	316.4	+20	317.2	do	.05	24
	317.8	−14				
3	314.25	+54	315.8	do	.60	38
	316.4	−26				
	315.6	+8				
4	316.5	+11.5	316.9	do	.10	30
	317.8	−28				
4	316.5	+28.5	315.8	do	.44	41
	315.6	+8.5				
4	292.3	+20	292.8	Transition	.....	38
	291.4	+54				

3. Enthalpy Measurements

The method of enthalpy measurement and apparatus used were described in detail in two early papers [2]. Two more recent publications [3,4] describe the improved apparatus used in the present investigation. Briefly, the sample is heated in a silver-core furnace to a known temperature, and is then dropped into a Bunsen ice calorimeter that measures the heat evolved by the sample in cooling to 0° C. Repetition at a number of furnace temperatures enables the heat capacity to be derived over a temperature range. Carrying out such measurements also on the empty container gives "blank" values that correct for the heat evolved by the container.

The sealed silver vessel was contained in an outer vessel, partly for mechanical support at the high temperatures where silver becomes quite soft and partly to protect the apparatus in case the silver container bursts open. The outer vessels used were evacuated, filled with helium, and closed (almost tight) by a screw lid before insertion into the furnace. Three such outer vessels were used, two of commercial nickel and the other of a stainless-steel type 446. The use of a nickel container at 500° and 600° was dictated by earlier work by the authors with the stainless-steel type-446 containers, which were found to give results of inferior reproducibility in this range of furnace temperatures, owing to a transition in the steel.

Beside each sample of sodium hydroxide measured was placed a small piece of annealed silver such as to make the total mass of silver exactly 12 g. In measuring the blanks, a 12-g annealed piece of the same pure silver was put into the appropriate empty outer container. In this way the results were made independent of the explicit heat capacity of silver alone. Small corrections were applied to place the results for containers with and without sodium hydroxide on the basis of the same mass of each material entering the calorimeter. The corrected values of enthalpy obtained in individual runs are given in table 2. No corrections for the effects of impurities are included in the results in table 2; these corrections are large at a few of the temperatures, as shown in section 4.

TABLE 2. *Enthalpy measurements*

Furnace temperature (t)	Outer container No.	Sample No.	Mass of sample	Measured heat		$H_t-H_0°$, net for sample
				With sample	Empty containers	
°C			g	*abs j*	*abs j*	*abs j g*$^{-1}$
100.00	3	4	4.1074	1720.6 1725.5 1722.8	1093.4 1094.4 1098.8	152.8
200.00	3	4	4.1074	3593.7 3597.1 3596.7 3603.1	2271.6 2274.2 2274.0	322.4
280.00	3	3	4.2007	5316.0 5316.1	3270.8 3271.4	486.5
		4	4.1074	5268.9 5268.7	3273.2	486.0
298.00	2	3	4.2007	6326.3 6327.3	3437.4 3438.2	687.7
313.00	2	3	4.2007	6790.3 6789.5	[b](3625.5) 3612.3 3609.7 3614.1 3610.2	756.6
316.00	1	3	4.2007	[a](7137.4) [a](7150.5) 7165.3 7169.3	3711.6 3712.6	822.5
325.00	3	4	4.1074	7497.5 7505.8 7502.4 7503.8	3859.1 3863.6 3859.5 3857.7	886.9
400.00	2	4	4.1074	8986.4 8988.3 8991.3 8988.3	4678.5 4675.7 4676.9 4675.8	1049.8
500.00	2	4	4.1074	11099.1 11104.6 11101.8	5923.0 5924.7 5923.1	1260.8
600.00	2	4	4.1074	13258.3 13259.0 13260.4	7205.6 7204.8 7205.2	1473.9
701.2	3	4	4.1074	16615.6	9684.9 9682.4 9693.8 9695.2 9687.3 9692.8	1686.3
	2	5	4.1840	15610.4	8546.0 8556.1 8553.1 8556.4	1686.8

[a] These two results were rejected because the lengths of time the sample was held in the furnace (92 and 86 min, respectively) were thought inadequate for equilibration under these particular conditions. In the third and fourth runs at 316° the sample was in the furnace for 142 and 116 min, respectively.

[b] Rejected for lack of precision.

As will be noted from table 2, measurements were made on two samples of sodium hydroxide at each of the furnace temperatures 280° and 701.2°. The agreement within 0.03 percent at 701.2° is considered somewhat fortuitous, in view of the precision and of the uncertainties in several corrections applied. Two samples were run at 280° to check on the accuracy of the sample masses, a large error in which would otherwise go undetected. The two runs on each sample at 280° agree closely, so that the difference between the means for the two samples (only 0.1 percent in that part of the enthalpy change attributed to the sample) furnishes evidence that the two sample masses were not much in error. There may thus be a 0.1-percent discrepancy between the masses of the two samples. However, this interpretation of the discrepancy at 280° is uncertain, as it rests on the assumption that the concentration of impurity is practically the same in the two samples. Actually, the corrections derived in section 4 show that at 280° the measured enthalpy of each sample is about 2 percent too high because of the impurity.

The silver vessel containing the sample (No. 5) opened during the second run at 701.2°. There proved to have been no loss of sample, however, so the heat measurement was accepted. On the other hand, in an effort to extend the measurements above 700° two runs were made on a different sample at a furnace temperature near 800° C. A considerable quantity of sodium hydroxide escaped not only from the silver container but from the outside container as well, so that the calorimetric results for 800° are of no value and were discarded.

The reason for the consistent escape of sodium hydroxide from the sealed silver vessels at approximately 700° and 800° is not known. The partial pressure of water, present as an impurity, may have become sufficiently high to blow open the relatively soft silver. Or the experience of two earlier investigators [5] may have been repeated. They found that after prolonged contact of the two substances near 700°, silver was no longer impervious to molten sodium hydroxide.

The two silver containers that opened after a few hours at high temperatures were later examined for any apparent action on them by the sodium hydroxide. Neither container showed any visible signs of having been attacked. However, the silver that had been heated to 800° C was very brittle; it was not possible to remove it quantitatively for weighing. But the silver that had been in contact with sodium hydroxide only up to 700° (and for a shorter time) appeared to be no more brittle than pure annealed silver; after washing and drying, its weight was within 1 mg (0.01 percent) of that before filling with sodium hydroxide and sealing. Thus it appears that under this limited treatment near 700° no appreciable silver loosened and became dispersed in the molten sodium hydroxide.

The same nickel container was used as an outer vessel for both these silver containers at their highest temperatures. There was no detectable loss of nickel at 700°. But at 800° a hole developed in the nickel at one point where the silver had apparently been in contact with it. According to the literature [6], nickel and silver form a nickel-rich solid alloy, but no liquid phase, at this temperature. On the other hand, nickel and silver may have formed an electrochemical couple in the presence of the sodium hydroxide. Otherwise the nickel appeared unattacked, except for a thorough removal of its thin oxide coating where it had come in contact with sodium hydroxide.

4. Correction for Impurity: Final Values

It has been known for a long time that anhydrous sodium hydroxide undergoes a solid-solid first-order transition at some temperature between 290° and 300° C, the high-temperature crystalline form melting in the neighborhood of 320°. Accurate enthalpy measurements on a pure sample of this substance at enough temperatures in the range of the present investigation, 0° to 700°, should obviously be sufficient to determine the heat capacities of the two crystalline forms and the liquid (over the respective temperature ranges in which they are stable), as well as the heats of transition and fusion.

The unexpectedly large amounts of impurities found in the samples analyzed (section 1) make it necessary to consider carefully the errors thereby introduced into the thermal results and to correct for these undesired effects as well as possible. The impurities will for the present be taken as consisting of 0.3 percent of sodium carbonate, as found by chemical analyses, and 0.4 percent not accounted for but assumed to be water. The sources of error thereby created in the measured heat capacities are three: (1) differences between the heat capacity per unit mass of the impurities and that of the sodium hydroxide, (2) the extra heat absorbed or evolved in evaporating or condensing water in the gas space available, and (3) the extra heat absorbed below the melting point because of "premelting" of part of the sodium hydroxide caused by the impurities.

The first is a minor source of error here. Using an estimated heat-capacity equation of Kelley [7] for crystalline sodium carbonate given for the temperature range 25° to 225° C, it was estimated that 0.3 percent of sodium carbonate contributes in this way an error in heat capacity no greater than about 0.1 percent. The apparent specific heat of water (when saturated with sodium hydroxide below the freezing point of the sample) is probably comparable to that of sodium hydroxide and may contribute in this way no greater error than that due to the sodium carbonate.

The second source of error also is of minor importance below the melting point, as the gas space is only about 1 cm ^{3}/g of sample, and the partial pressure of water vapor over saturated aqueous sodium hydroxide solutions does not exceed approximately one-third atmosphere at any temperature [8]. As the temperature rises above 260° C, this partial pressure decreases rapidly, and in the present case is very small, possibly of the order of 0.001 mm, at the freezing point of the sample.

Above the freezing point the concentration of water in the liquid sodium hydroxide cannot become smaller through melting of additional crystalline phase, and as the temperature rises the partial pressure of water vapor must increase many-fold. How great this pressure becomes at the highest temperature of the present measurements, 700°, is difficult to estimate even approximately from the data referred to above [8], as such an estimation involves extrapolating to much higher temperatures and much lower concentrations of water than covered by the data. An estimate made it seem probable, however, that not enough water evaporated up to 700° from the samples measured to contribute an error as great as 2 percent in any smoothed value of heat capacity of liquid sodium hydroxide obtained in the present investigation. This conclusion is supported by two additional facts: (a) One sample that became unsealed in a 700° run was found afterward to have lost in mass, if any, not more than 5 mg that might be water, instead of the 15 mg or so that was inferred from chemical analyses as having been present originally, and (b) it will be seen later in this paper (fig. 3) that the relative enthalpies measured in the liquid range give by difference four "observed" heat-capacity values that fit randomly the adopted linear variation of heat capacity with temperature within about 1 percent, instead of showing the upward curvature that would certainly be expected if the partial pressure of water increased so fast with rising temperature as to evaporate most of the water at or below 700°.

The third source of error, that involving an extraneous "heat of premelting" below the melting point, obviously caused no error in the values obtained for liquid sodium hydroxide. However, the errors in some of the enthalpy values obtained below the melting point are large. These will now be corrected for, by a procedure that makes no assumption as to the identity, the amounts, or the effective molecular weights of the impurities present. Three reasonable simplifying assumptions are made, as follows:

(1) The crystalline form of sodium hydroxide that is stable below the transition temperature will be designated as "alpha," and that stable above as "beta." [4] It will be assumed that at equilibrium at any temperature except the transition temperature, all the crystalline sodium hydroxide present in the sample is in the form of one of these two pure phases. (In this circumstance the transition point found, 292.8° C (section 2), is uninfluenced by the impurities.) In a careful study of the $NaOH$-Na_2CO_3 system [9] an earlier investigator was unable to detect any solubility of Na_2CO_3 in crystalline $NaOH$; and according to the literature, no solid hydrate of sodium hydroxide is stable above 60° C [8]. The existence of a solid solution of sodium hydroxide and water seems even less likely.

(2) The liquid solutions formed by sodium hydroxide and the impurities soluble in it will be assumed to obey Raoult's law, and therefore also to exhibit no heat of mixing as liquids. It thus becomes a simple matter of deducing from the thermal data the fraction of the sodium hydroxide in liquid solution with the impurities at each temperature (fraction "premelted"), and of identifying the extra enthalpy (which the sample possesses) with the heat of fusion of that amount of liquefied sodium hydroxide. Below the transition temperature this heat of fusion is then actually the true heat of fusion (of the "beta" form) plus the heat of transition.

It is claimed [9] that liquid sodium hydroxide forms nearly ideal solutions with sodium carbonate. On the other hand, the solutions with water are certainly far from ideal, as shown by the partial-pressure data [8]. Nevertheless, from the foregoing treatment it may be shown that between the transition and melting points the mole fraction of sodium hydroxide in the liquid solution is not less than about 0.95, so that the deviations from Raoult's law are probably minor. At lower temperatures the deviations from this law become increasingly greater, of course, because of the larger proportions of water; but the thermal corrections become much smaller, so that errors in them are correspondingly less consequential. The data on the $NaOH$-H_2O system [8] seemed too inconsistent to allow any estimate of the error due to this lack of ideality, beyond leading to the belief that most of the thermal corrections to be deduced are in error by not more than a few percent of themselves.

At this point it may be mentioned that the water in the sample is no doubt present at 0° C, the reference temperature of all the enthalpy values, in the form of hydrates of sodium hydroxide. Thermochemical data [10] indicate that for any of the several common hydrates the heat of hydration (referred to pure liquid water) amounts to approximately 4 joules for the 0.004 g of water that may be associated with each gram of sodium hydroxide. However, it seems reasonable to assume that as the temperature rises the heat of dehydration will be more or less balanced by a heat of mixing, as dehydration in the liquid phase is a more gradual process. Thus no corresponding correction seems in order here.

(3) The third assumption is that the heat capacities of the alpha, beta, and liquid forms of sodium hydroxide are equal and independent of temperature, the value taken being 2.15 abs j g^{-1} deg K^{-1}, which is the observed heat capacity of the liquid extrapolated to the temperature region between the transition and melting points.

As the thermal corrections are large enough to make this assumption of consequence only between the transition and melting points, and as the heat capacities of the alpha and liquid forms would be found, regardless of this assumption, to be almost equal at the boundaries of this temperature region (fig. 3), the principal assumption being made here is essentially that the heat capacity of the beta form, otherwise entirely undetermined, is equal to that of the other two forms. This assumes without proof that the enthalpy of the beta form increases between

[4] Some authors have used these names in the reversed sense as applied to sodium hydroxide.

the transition and the melting point by approximately 57 j/g—a substantial amount of heat. However, it seems unlikely that this is considerably in error, as the heat capacities of most substances change by only a few percent on passing the melting point. Enough data were obtained to determine in principle a value for the heat capacity of the beta form; but, as was anticipated, such an indirect method is so sensitive to small errors in the thermal data (aside from deviations from the ideal solution laws) that these errors were sufficient to lead to an incredible value for this constant (actually a negative value).

This third assumption is equivalent to treating the heats of transition and fusion as independent of temperature.

The symbols used in the subsequent quantitative treatment will first be defined:

t = temperature (°C)
T = temperature (°K) ($=t+273.2$)
T_m = melting point of pure sodium hydroxide (°K)
T_t = transition point of pure sodium hydroxide (°K)
T_f = freezing point of the sample measured (°K) (that is, temperature at which $m=1$)
L_f = heat of fusion of pure (beta) sodium hydroxide (abs j g^{-1})
L_t = heat of transition of pure sodium hydroxide (abs j g^{-1})
n = total moles of liquid-soluble impurity in sample measured, per gram of sodium hydroxide present
m = grams of sodium hydroxide in liquid solution at temperature T, per gram of total sodium hydroxide
a_1 = activity of alpha sodium hydroxide relative to the pure liquid at the same temperature
a_2 = activity of beta sodium hydroxide relative to the pure liquid at the same temperature
M = effective molecular weight of sodium hydroxide vapor in any given case
R = gas constant ($=8.3144$ abs j $mole^{-1}$ deg K^{-1})
H = observed enthalpy (at a given temperature T) of sample measured, above that at 0°C (abs j g^{-1})

The variation of activity with temperature for the two crystallline forms of sodium hydroxide is given by the two equations [11]:

$$d \ln a_1/dT = M(L_t+L_f)/RT^2 \quad (1)$$

$$d \ln a_2/dT = ML_f/RT^2 \quad (2)$$

Integration of eq (1) and (2) and imposition of the conditions that when $T=T_m$, $a_2=1$, and when $T=T_t$, $a_1=a_2$, lead to the equations

$$\ln a_1 = -[M/R][L_t(1/T-1/T_t)+L_f(1/T-1/T_m)] \quad (3)$$

$$\ln a_2 = -[M/R][L_f(1/T-1/T_m)]. \quad (4)$$

The activity of each solid is equal to that of the sodium hydroxide in the liquid solution with which the solid is in equilibrium, and this in turn is, according to Raoult's law, equal to the mole fraction of sodium hydroxide in the solution, $1-n/(m/M-n)$. As n is relatively small here, it proves sufficiently accurate to replace $\ln[1-n/(m/M+n)]$ by $-nM/m$, which, when substituted for the left-hand members of eq (3) and (4), gives two equations independent of M:

$$nR/m = L_t(1/T-1/T_t)+L_f(1/T-1/T_m) \quad (T \leqq T_t) \quad (5)$$

$$nR/m = L_f(1/T-1/T_m) \quad (T_t \leqq T \leqq T_f) \quad (6)$$

When $T=T_f$, $m=1$. Substituting into eq (6),

$$nRT_mT_f = L_f(T_m-T_f) \quad (7)$$

Before proceeding further, smoothed values of the relative enthalpy of liquid sodium hydroxide, based on the results of this investigation, will be obtained. The last six values of relative enthalpy in the last column of table 2 (section 3) gave by the method of least squares the equation (in abs j g^{-1} at t°C):

$$H_t(\text{liquid}) - {}_0{}^\circ H(\text{alpha}) = 180.6+2.1990t - 7.31(10^{-5})t^2 \quad (319° \text{ to } 700° \text{ C}) \quad (8)$$

The smoothed values given by this equation differ from the observed values on which the equation is based by the amounts shown in table 3. (The temperature of the melting point, T_m, is anticipated from the calculations that follow.) The differentiation of eq (8) gives for the heat capacity of liquid sodium hydroxide the equation (in abs j g^{-1} deg C^{-1} at t°C):

$$C_p = 2.199 - 1.46\ (10^{-4})t \quad (319° \text{ to } 700° \text{ C}) \quad (9)$$

Using for the heat capacity a constant value of 2.15 abs j g^{-1} deg K^{-1}, which eq (9) gives at the temperatures between the transition and melting points, an equation may now be formulated giving the relation among the observed enthalpy H of the sample measured, the enthalpy at the same temperature if all were liquid, and the fraction of the sodium hydroxide remaining frozen (as beta) in the sample:

$$(1-m)L_f = 874.8 - 2.15(592.3-T) - H. \quad (T_t \leqq T \leqq T_f) \quad (10)$$

TABLE 3. *Enthalpy of liquid sodium hydroxide*

Temperature (t)	Relative enthalpy, $H_t(\text{liq}) - H_0(\alpha)$		
	Observed	Calculated from eq (8)	Difference
°C	abs j g^{-1}	abs j g^{-1}	abs j g^{-1}
[a]319.1	----	874.8	----
325.0	886.9	887.6	−0.7
400.0	1049.8	1048.5	+1.3
500.0	1260.8	1261.8	−1.0
600.0	1473.9	1473.7	+0.2
701.2	1686.6	1686.6	0.0

[a] Melting point.

Elimination of m and n among eq (6), (7), and (10) gives

$$T_m - T_f - T)L_f/[T_f(T_m - T)] = 874.8 - 2.15(592.3 - T) - H. \quad (T_t \leqq T \leqq T_f) \quad (11)$$

The successive substitution into eq (11) of the observed enthalpy values (last column of table 2) for 298°, 313°, and 316° C, together with the corresponding absolute temperatures, gives three equations whose simultaneous solution gives for T_f a value of 589.9° K (316.7° C). The independent cryoscopic measurements described in section 2 gave a freezing point of these samples of 317.1° C. Adopting as a mean 316.9° C (T_f=590.1), the three equations just referred to will give consistent values for the melting point of pure sodium hydroxide and the heat of fusion if the observed enthalpies H are altered by small amounts that are within the accuracy of the measurements: Increasing the observed enthalpy at 313° C by 2.5 abs j g^{-1} and decreasing each of the observed enthalpies at 298° and 316° by half this amount lead to: T_m=592.3 (319.1° C); L_f=158.9. (These constants are very close to those that would have been obtained from the cryoscopically observed freezing point and only the two observed enthalpies at 298° and 313°.) These two values, together with the adopted value for T_f of 590.1, then give, when substituted into eq (7), a value for the impurity in the sample, in moles per gram of sodium hydroxide: n=0.00012.

A value for the heat of transition, L_t, may now be found. Substituting the values of the constants so far found, eq (6) gives, at the transition point (T_f=566.0), m=0.080, corresponding to 8.0 percent of the sodium hydroxide liquefied at this temperature. Equation (10) then gives an "observed" enthalpy at this temperature, with all the solid in the beta form, of 672.1 abs j g^{-1}. Removal as heat of 92.0 percent of the heat of transition per gram of pure sodium hydroxide should then give the "observed" enthalpy at the same temperature with all the solid in the alpha form. Extrapolation of the observed enthalpies at 100°, 200°, and 280° C (last column of table 2, section 3) gives for this enthalpy (at 292.8° C) a value of 525.9 abs j g^{-1} (actually after a slight adjustment by means of a second approximation in order to make all the results entirely consistent). Thus

$$L_t = (672.1 - 525.9)/0.920 = 158.9.$$

Substitution into eq (5) then gives values of m at 100°, 200°, and 280° C, and when these are multiplied by the sum of the heats of transition and fusion and then subtracted from the observed enthalpies at these temperatures, three values of relative enthalpy of pure alpha sodium hydroxide are obtained that determine the empirical equation (in abs j g^{-1} at t° C):

$$H_t(\text{alpha}) - H_{0°C}(\text{alpha}) = 1.4764t + 2.195(10^{-4})t^2 + 1.968(10^{-6})t^3 \quad (0° \text{ to } 292.8° \text{ C}) \quad (12)$$

(As was intended, this equation gives at 292.8° C a value that is consistent with the "observed" value of 525.9 abs j g^{-1} used above.)

It is of interest to solve eq (3) for the temperature at which a_1=1. This gives 305.7° C, which is the temperature at which the alpha form would melt if the beta form, which is the more stable at this temperature, did not appear. Such metastability is very important in the case of some substances; but only a slight amount (brief supercooling once at the transition point) was detected in all the present cryoscopic and thermal measurements on sodium hydroxide, and this is in accord with the report of another investigator [9].

Some of the results of the preceding treatment may now be compared with those found in the cryoscopic measurements (section 2) and by chemical analysis (section 1). It will be noted from table 1, section 2, that for the two samples the estimated fractions frozen at 315.8° show poor agreement, though the values found for the freezing points of the two samples approximately agree. This is thought to be due to the crude method of determining from time interval and average temperature difference the total heat passing from sample to furnace in such partial freezing, particularly as the solid-liquid interface of the sample was no doubt moving constantly toward the center of the sample, setting up an extra temperature gradient across the solid that for so poor a thermal conductor was difficult to estimate and allow for correctly. The above treatment, in comparison, gives at 315.8° a still somewhat lower fraction present as solid than the two cryoscopic figures, and hence a somewhat greater proportion of impurity in the sample, though of the same order of magnitude.

As shown above, the treatment of this section gives for the moles of impurity per gram of sodium hydroxide (n) a value of 0.00012. On the other hand the chemical analyses referred to in section 2 give a value approximately twice as great if the effective molecular weights of H_2O and Na_2CO_3 be taken equal to their formula weights. It is not known whether the last assumption is unjustified here or whether the samples chemically analyzed contained more impurity than the samples measured thermally.

At any rate, the samples contained several tenths of one percent of impurity, and the derived heats of transition and fusion are proportionately too low because this fact was not taken into account. The uncertainties due to the assumptions of the above treatment, however, are probably more serious and must be considered to render the derived heats of transition and fusion uncertain by perhaps as much as 5 percent. However, the observed enthalpy for liquid sodium hydroxide near the melting point should possess considerable accuracy. Thus the total enthalpy change in the conversion of pure sodium hydroxide from the alpha form at the transition point to liquid at the melting point should be given rather accurately by the results of the present investigation. And as this relatively large enthalpy change occurs over a range of only 26 degrees, its contribution can hardly produce much error in the

absolute entropy and free energy of the liquid, as tabulated in section 6.

The accuracy of the treatment carried out in the present section cannot be expected to equal that of accurate enthalpy measurements on a highly pure sample, though such a treatment would give more accurate corrections the purer the sample measured. Nevertheless, it is believed that the present corrected results are more accurate than have been published to date for sodium hydroxide over this temperature range.

The final results for pure sodium hydroxide, based on the present investigation only, will now be summarized (with enthalpy in abs j g^{-1} and heat capacity in abs j g^{-1} deg C^{-1}, at $t°$ C).

Alpha NaOH, 0° to 292.8° C

$$H_t - H_{0°} = 1.4764t + 2.195(10^{-4})t^2 + 1.968(10^{-6})t^3$$

$$C_p = 1.476 + 4.39(10^{-4})t + 5.90(10^{-6})t^2$$

Transition, 292.8° C

Heat of transition, 158.9

Beta NaOH, 292.8° to 319.1° C

$$H_t(\beta) - H_{0°}(\alpha) = 29.9 + 2.15t$$

$$C_p = 2.15$$

Melting, 319.1° C

Heat of fusion, 158.9

Liquid, 319.1° to 700° C

$$H_t(\text{liquid}) - H_{0°}(\alpha) = 180.6 + 2.1990t - 7.31(10^{-5})t^2$$

$$C_p = 2.199 - 1.46(10^{-4})t$$

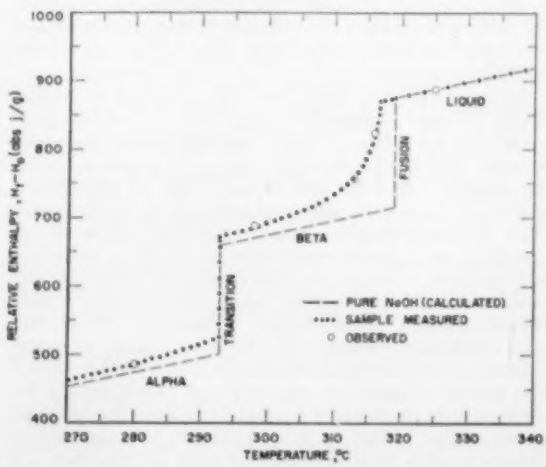

FIGURE 2. *Observed and corrected enthalpy of sodium hydroxide.*

It is interesting to compare the above (corrected) enthalpy-temperature relations with those observed on the samples measured. This comparison is shown in figure 2 for the temperature region in which the difference is significantly large. The dotted path deviates from the observed points to the extent necessary to make it consistent with the simplifying assumptions made in this section.

5. Comparison With Other Measurements

Various values for the transition and melting points of sodium hydroxide have been reported in the literature. Together with the values for these obtained in the present investigation, they are given in table 4. Some of these temperatures were apparently determined on samples containing considerable impurity whose effect was not allowed for.

The present work gives the same value, 159 abs j g^{-1}, for the heat of transition and the heat of fusion. The only values that were found in the literature are those of von Hevesy [12] and Seward [9]. Von Hevesy obtained from cooling curves 104 and 168 abs j g^{-1}, respectively. Seward did not attempt to measure the heat of transition, but calculated from the effect of sodium carbonate on the melting point a value of 175 abs j g^{-1} for the heat of fusion. Though Seward's measurements were apparently made with considerable care, his assumption of the effective molecular weight of Na_2CO_3 in these solutions being equal to the formula weight is open to question for so strong an electrolyte. His value for the heat of fusion of sodium hydroxide depends directly on this assumption.

A few investigators have measured the heat capacity of sodium hydroxide. Blümcke [17] obtained 3.26 abs j g^{-1} deg C^{-1} between 0° and 98° C, a value that is undoubtedly much too high. Terashkevich and Vishnevskii [18] covered the range 20° to 600° C, using samples of sodium hydroxide of 99 and 96 percent purity. Their results have been systematically formulated by Hulme [19]. Recently (1951) the enthalpy of the liquid from the melting point to 990° C was measured at the Oak Ridge National Laboratory using a Bunsen ice calorimeter [20]. The results of this work were expressed by an equation which when converted to terms of abs j g^{-1} is:

$$H_t(\text{liquid}) - H_{0°}(\text{alpha}) = 275.3 + 2.067t.$$

TABLE 4. *Transition and melting points of sodium hydroxide*

Transition point	Melting point	Reference
°C	°C	
292.8	319.1	This investigation.
294	320	[9]
299.6	318.4	[12]
295	327.6	[13]
.....	296	[14]
304	322	[15]
.....	310-	[16]

The corresponding heat capacity, 2.07 ± 0.08 abs j g^{-1} $deg\ C^{-1}$, agrees within the precision with that of the present measurements over the entire temperature range covered by both; but the values of enthalpy referred to 0° differ considerably (by 60 j g^{-1} at 325°). Using an adiabatic calorimeter and sodium hydroxide said to be at least 99.84 percent pure, Kelly and Snyder [21] measured the heat capacity from 60° to 300° K.

The heat capacity, as measured in the present investigation and corrected below the melting point in section 4, is compared with the values of the other investigators in figure 3.

The curve representing the present results for the alpha form fits fairly smoothly (above 25° C) to that obtained from the precise low-temperature measurements of Kelly and Snyder [21], and shows at higher temperatures an upward curvature similar to that found by the present authors for crystalline lithium fluoride near its melting point [4]. As has already been pointed out in section 4, the heat capacities of solid and liquid sodium hydroxide show the customary behavior of being roughly the same near the melting point. Finally, attention may be called to the gradually decreasing heat capacity of liquid sodium hydroxide with temperature, according to the present measurements. Such a gradual decrease not far above the melting point has been found for numerous other liquids whose heat capacities have been measured in this laboratory—for all liquid metals measured, and very recently for the eutectic mixture of lithium and potassium chlorides over a range of 450 deg above the eutectic temperature. The decrease of heat capacity with rising temperature has a theoretical basis in the case of simple liquids.

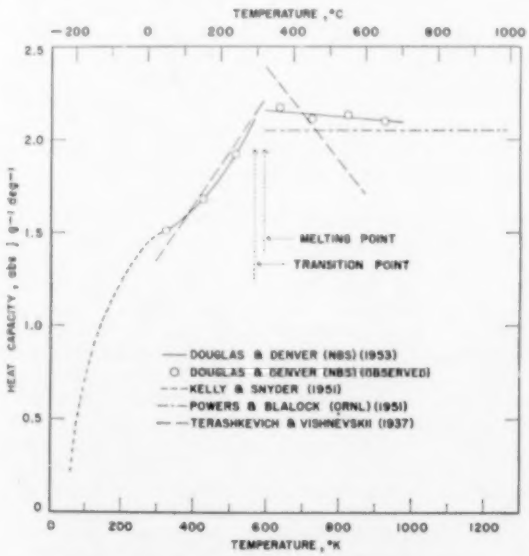

FIGURE 3. *Heat capacity of sodium hydroxide.*

6. Thermodynamic Functions of Sodium Hydroxide, 298.2° to 1,000° K

Using the corrected enthalpy results summarized at the end of section 4, together with Kelly and Snyder's value of 15.34 ± 0.1 cal/mole-deg K for the absolute entropy at 298.2° K [21][5], some of the common thermodynamic properties of sodium hydroxide (relative enthalpy, relative free energy, entropy, and heat capacity) were computed from 298.2° to 1,000° K and are given in table 5. It will be noted that the values of enthalpy and free energy given are relative to the enthalpy at 298.2° K, whereas the entropy as given is the absolute entropy (that is, relative to 0° K).

TABLE 5. *Thermodynamic functions of sodium hydroxide*[a]

Temperature	Physical state	$\frac{H^\circ - H^\circ_{298.2}}{T}$	$-\left(\frac{F^\circ - H^\circ_{298.2}}{T}\right)$	S°	C_p°
°K		*cal deg⁻¹ mole⁻¹*	*cal deg⁻¹ mole⁻¹*	*cal deg⁻¹ mole⁻¹*	*cal deg⁻¹ mole⁻¹*
298.2	Alpha	0	15.34	15.34	14.26
300	do	0.086	15.34	15.43	14.27
325	do	1.184	15.40	16.58	14.49
350	do	2.144	15.52	17.66	14.77
375	do	2.998	15.69	18.69	15.13
400	do	3.769	15.91	19.68	15.56
425	do	4.477	16.16	20.64	16.05
450	do	5.135	16.44	21.57	16.62
475	do	5.756	16.73	22.49	17.26
500	do	6.349	17.04	23.39	17.97
525	do	6.921	17.37	24.29	18.75
550	do	7.478	17.70	25.18	19.60
566.0	do	7.829	17.92	25.75	20.18
566.0	Beta	10.513	17.92	28.43	(20.56)
575	do	10.670	18.04	28.76	(20.56)
592.3	do	10.959	18.41	29.37	(20.56)
592.3	Liquid	13.524	18.41	31.93	20.58
600	do	13.615	18.58	32.20	20.57
650	do	14.147	19.69	33.84	20.50
700	do	14.598	20.76	35.36	20.43
750	do	14.984	21.78	36.76	20.36
800	do	15.318	22.76	38.08	20.29
850	do	15.609	23.69	39.30	20.22
900	do	15.863	24.60	40.46	20.15
950	do	16.087	25.45	41.54	20.08
1,000	do	16.284	26.29	42.57	20.01

[a] 1 calorie = 4.1840 abs j. Molecular weight of NaOH = 40.005. 0° C = 273.2° K

The sodium hydroxide was supplied by members of the Oak Ridge National Laboratory. Credit is due several members of the National Bureau of Standards: To S. W. Clabaugh and J. W. Donovan for investigating means of preparing pure sodium hydroxide, as well as for analyses of samples; to J. M. Sherfey for making available a special dry box.

[5] The other source of entropy data is the emf measurements of Shibata, who in two papers [22] gave values of 17.5 and 12.43 for this entropy. Kelley [23] lists 14.2 ±1.5, based on this work. Kelly and Snyder [21] gave a table of thermodynamic functions of sodium hydroxide from 60° to 300° K, based on their own measurements.

7. References

[1] T. B. Douglas, J. Research NBS **52,** 223 (1954) RP2493.

[2] D. C. Ginnings and R. J. Corruccini, J. Research NBS **38,** 583, 593 (1947) RP1796 and RP1797.

[3] D. C. Ginnings, T. B. Douglas, and A. F. Ball, J. Research NBS **45,** 23 (1950) RP2110.

[4] T. B. Douglas and J. L. Dever, Lithium fluoride: Heat content from 0° to 900°, melting point and heat of fusion, J. Am. Chem. Soc. (in press).

[5] M. LeBlanc and L. Bergmann, Ber. deut. chem. Ges. **42,** 4728 (1909).

[6] M. Hansen, Der Aufbau der Zweistofflegierungen, p. 42 (Julius Springer, Berlin, 1936).

[7] K. K. Kelley, U. S. Bur. Mines Bul. **476,** 211 (1949).

[8] International critical tables, vol. 3, p. 369, 370 (McGraw-Hill Book Co., New York, N. Y., 1928).

[9] R. P. Seward, J. Am. Chem. Soc. **64,** 1053 (1942).

[10] F. R. Bichowsky and F. D. Rossini, The thermochemistry of the chemical substances, p. 137, 138 (Reinhold Publishing Corp., New York, N. Y., 1936); F. D. Rossini, D. D. Wagman, W. H. Evans, S. Levine, and I. Jaffe, Selected values of chemical thermodynamic properties, NBS Circular 500, p. 448, 449 (U. S. Government Printing Office, Washington, D. C., 1952).

[11] G. N. Lewis and M. Randall, Thermodynamics and the free energy of chemical substances, p. 282, equation (11) (McGraw-Hill Book Co., New York, N. Y., 1923).

[12] G. von Hevesy, Z. physik. Chem. **73,** 667 (1910).

[13] F. Halla and H. Tompa, Z. anorg. allgem. Chem. **219,** 321 (1934).

[14] B. Neumann and E. Bergve, Z. Elektrochem. **20,** 271 (1914).

[15] A. von Antropoff and W. Sommer, Z. physik. Chem. **123,** 161 (1926).

[16] G. Scarpa, Atti accad. nazl. Lincei Mem., Classe sci. fis., mat. e nat. I. **24,** 955 (1915).

[17] A. Blümcke, Ann. Physik. [3] **25,** 417 (1885).

[18] V. R. Terashkevich and A. I. Vishnevskii, Zhur. Obshchet Khim. **7,** 2175 (1937).

[19] R. E. Hulme, Chem. Eng. **57,** 139 (1950).

[20] W. D. Powers and G. C. Blalock, Oak Ridge Natl. Lab. Report 1653 (1954).

[21] J. C. R. Kelly and P. E. Snyder, J. Am. Chem. Soc. **73,** 4114 (1951).

[22] F. L. Eiichi Shibata, J. Chem. Soc. Japan **50,** 523 (1929); J. Sci. Hiroshima Univ. [A] **1,** 215 (1931).

[23] K. K. Kelley, U. S. Bur. Mines Bul. **434,** 71 (1948).

WASHINGTON, March 19, 1954.

Heat Content of Molybdenum Disilicide From 0° to 900° C[1]

Thomas B. Douglas and William M. Logan

The heat content relative to 0° C of a sample of molybdenum disilicide ($MoSi_2$) was measured at 100-degree intervals up to 900° C, using a nichrome-V container for the sample, a silver-core furnace, and a precision ice calorimeter. Corrections were applied for the impurities (approximately 2 percent) reported to be in the sample. The equation

$$H_t - H_0 = 0.48560t + 3.586(10^{-5})t^2 - 41.78 \log_{10}[(t + 273.16)/273.16],$$

giving between 0° and 900° C the heat content in absolute joules per gram at t° less that at 0° C, represents the unsmoothed corrected mean values, with an average deviation of 0.24 absolute joule gram $^{-1}$. This equation is believed to have an absolute accuracy within 2 percent between 100° and 800°. Values of the relative heat content, heat capacity, and relative entropy derived from this equation are formulated and tabulated at even temperatures.

1. Introduction

There are several compounds of molybdenum and silicon, of which the best known is the disilicide. This substance has considerable resistance to oxidation, and because of this and other properties, shows promise as a high-temperature structural material. No measurements of its heat capacity were found in the literature.

2. Experimental Procedure

The sample of molybdenum disilicide, broken into pieces of about 2- or 3-mm diameter, was furnished by the Lewis Flight Propulsion Laboratory, National Advisory Committee for Aeronautics, Cleveland, Ohio. This laboratory stated that the impurities were approximately as follows: Iron, 0.8 percent; oxygen, 0.50 percent; nitrogen, 0.34 percent; and carbon, 0.17 percent.

A preliminary test of a separate portion of the sample was conducted to determine its apparent behavior at high temperatures toward oxygen and toward nichrome V, in anticipation of using the latter as a container material. Simple heating at about 1,000° C for a few minutes on a nichrome plate in air gave no obvious evidence of oxidation of the $MoSi_2$ nor of its attack of the nichrome.

The method and apparatus employed for the heat-content measurements were described in detail in an earlier paper.[2] Briefly, the procedure involved heating the sample, in its helium-filled container of nichrome V, to a known temperature in the furnace. The sample and container were then dropped into the ice calorimeter, which measured the heat delivered in cooling to 0° C. Repetition of the same procedure on the empty container measured the part of the heat that had not been delivered by the sample itself. From such measurements of relative heat content at a sufficient number of furnace temperatures, the heat capacity over the temperature range covered can be derived by one of the usual methods.

The furnace temperature was measured up to 600° C by a platinum resistance thermometer, and above 600° by a platinum-platinum-10-percent-rhodium thermocouple. The calibration factor of the ice calorimeter, as determined earlier by numerous electrical calibrations, and with the same apparatus, is 270.48 abs j/g Hg.[3]

3. Heat-Content Data and Corrections Applied

Several very small corrections to the measured heats were made whenever significant, especially for the small heat leak of the calorimeter (usually about 2 j/hr) and for slightly varying masses of container materials entering the calorimeter. Two major corrections, however, had to be applied. These were (a) for increases in weight of the container itself, totaling several milligrams throughout the series of measurements, due to oxidation at the higher temperatures by traces of oxygen in the furnace atmosphere, and (b) for the impurities in the sample of molybdenum disilicide listed in section 2.

The corrections for oxidation of the container were computed from the differences in heat content of Fe_3O_4 and metallic iron.[4] The corrections themselves were relatively small (in no instance exceeding 0.7 percent of the total heat measured), and should be sufficiently accurate for this purpose, as the increase in heat content during oxidation of iron or one of the metals composing nichrome V depends largely on the amount of oxygen acquired, regardless of which metal is involved or which of its oxides is formed.

[1] This work was supported by the United States Air Force, Wright Air Development Center, Wright-Patterson Air Force Base, Ohio.

[2] D. C. Ginnings, T. B. Douglas, and Anne F. Ball, J. Research NBS **45**, 23 (1950) RP2110.

[3] The factor, differing slightly from the previously published value of 270.46 (footnote 2), was arrived at by a correction of the circuit constants applicable in all the calibration experiments.

[4] K. K. Kelley, Contributions to the data on theoretical metallurgy, X. Entropy data for inorganic compounds, U. S. Bureau of Mines Bulletin 476, U. S. Government Printing Office, Washington 25, D. C., 1949.

The heats found were corrected for the approximately 2 percent of reported impurities by calculating in a similar way the approximate differences in heat content that would occur were the impurities replaced by the same mass of pure molybdenum disilicide. Taking advantage of the roughly approximate equality of the gram-atomic heat capacities of many elements at temperatures not too low, the effects of the impurities oxygen, nitrogen, and carbon were corrected for as though these elements were present in the form of the same total number of gram atoms of oxygen only, and in the manner described above. The effect of the impurity iron was corrected for, using the heat-content values of this element given by Kelley (see footnote 4). Making the total correction for the impurities at each furnace temperature was equivalent to decreasing the net measured heat content of the molybdenum disilicide sample by approximately 3 percent. The greatest part of this correction can be attributed to the fact that the average atomic weight of the impurity content is much smaller than that of $MoSi_2$.

The corrected measured heats from individual runs are given in table 1 in absolute joules, and at each temperature in the chronological order in which they were obtained. The mass of molybdenum disilicide was 16.560 g in each case. For each temperature the last three columns afford a comparison between the observed mean net heat content per gram and the corresponding smoothed value calculated as described in section 4.

TABLE 1. *Individual heat content measurements*

Furnace temperature t	Measured heat		Mean net heat content of $MoSi_2$, $H_t - H_0$		
	Sample and container	Empty container	Observed	Calculated	Difference
°C	abs j	abs j	abs j g^{-1}	abs j g^{-1}	abs j g^{-1}
100.0	1245.7 1243.2	[a]535.6	42.81	43.26	−0.45
150.0		816.4 815.4			
200.0	2573.7 2572.7	[a]1101.9	88.85	88.59	+0.26
300.0	[b](3950.7) 3939.5 3939.7 3939.3	1689.0 1686.1 1702.3 1684.6 1693.6 1686.1	135.62	135.46	+.16
400.0	5351.2 5351.6	2316.8 2306.2 2316.1 2306.7	183.57	183.61	−.04
500.0	6791.0 6794.1 6787.8	2933.4 2931.4	233.01	232.89	+.12
600.0	8262.8 8266.9 8281.7 8286.8 8278.1	3590.8 3590.0 3593.3 3590.1	282.87	283.18	−.31
701.7	9847.5 9853.4 9842.9	4298.6 4298.7	335.11	335.32	−.21
796.2	11349.8 11343.7	4975.1 4967.5 4969.7	385.03	384.60	+.43
895.5	12934.3 12939.5	5694.7 5700.7 5696.6	437.09	437.24	−.15

[a] Not measured directly, but found by interpolation.
[b] Excluded from the mean because of inferior precision.

. Heat Content, Heat Capacity, and En py

The corrected smooth values of the heat co ent of molybdenum disilicide, in excess of that at °C, are represented from $t=0°$ to $t=900°C$ by the equation (in absolute joules per gram)

$$H_t - H_0 = 0.48560t + 3.586(10^{-5})t^2 - 41.78 \log_{10}[(t+273.16)/273.16], \quad (1)$$

whose coefficients were found by least squares from the observed values of the fourth column of table 1. Differentiation of eq (1) gives the heat capacity (in absolute joules per gram deg C)

$$C_p = 0.4856 + 7.17(10^{-5})t - 18.14/(t+273.16). \quad (2)$$

Values of heat content calculated from eq (1) are listed in the fifth column of table 1, and smoothed values of heat capacity calculated from eq (2) are listed in table 2.

Figure 1 affords a graphical comparison between the heat capacity in calories per gram-atom degree C,[5] as calculated from eq (2), and the "observed" values calculated from successive differences of mean

[5] One gram-atom of $MoSi_2$ (50.71 g) = one-third the gram-molecular-weight. One calorie = 4.1840 abs j.

TABLE 2. *Heat capacity of molybdenum disilicide*

Temperature	Heat capacity	Temperature	Heat capacity
°C	abs j g^{-1} deg C^{-1}	°C	abs j g^{-1} deg C^{-1}
0	0.419	500	0.498
50	.433	550	.503
100	.444	600	.508
150	.453	650	.513
200	.462	700	.517
250	.469	750	.522
300	.476	800	.526
350	.482	850	.531
400	.487	900	.535
450	.493		

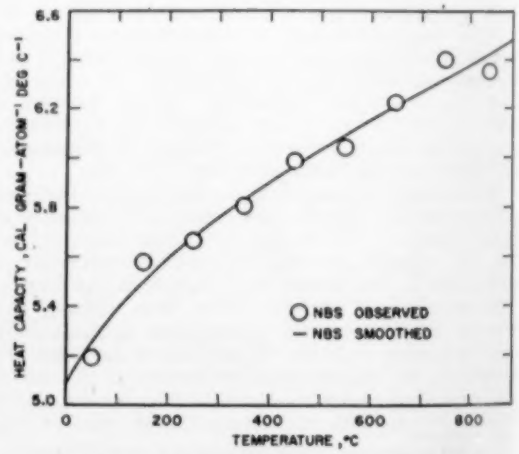

FIGURE 1. *Heat capacity of molybdenum disilicide.*

heat content given in the fourth column of table 1. Very small corrections for curvature[6] have been applied to the latter values. The heat-capacity values of figure 1 may be compared with 6.3 cal/g-atom deg C, a value that holds approximately for a large number of chemical elements and compounds at these temperatures. This simple generalization, which is very useful for rough estimates, predicts too high a heat capacity at room temperature for substances containing elements of low atomic weight (even silicon), as the tendency for the Debye temperatures to be unusually high in these cases causes the heat capacities to approximate this predicted value only at higher temperatures.

The precision of measuring the net heat content of molybdenum disilicide at any given temperature, as determined by the variation of individual measurements recorded in table 1, corresponded to a probable error of the mean averaging ± 0.05 percent. The corresponding probable error of the mean "observed" heat-capacity values calculated from the enthalpy values at two successive furnace temperatures was found to average ± 0.35 percent. The difference between these "observed" heat capacities and those given by eq (2) average 0.8 percent. Considering also the possible systematic errors, it is believed that the absolute error of eq (1) does not exceed 2 percent between 100° and 800° C.

The increased uncertainty in evaluating a derivative (here the heat capacity) near the ends of the range of measurement is exemplified by comparison of eq (2) with the best corresponding quadratic equation, the disagreement between the two equations being less than 0.5 percent between 100° and 800° but amounting to 1.7 percent at 0°. The best quadratic equation fits the "observed" values with the same average deviation as eq (2), but has a less plausible form, as it would lead to a maximum in the heat capacity at some temperature above 900°.

Taking the "molecular weight" of $MoSi_2$ as 152.13, equations for the relative heat content, relative entropy, and heat capacity may be readily derived from eq (1). In terms of calories $mole^{-1}$ and at $T°$ K, these equations are as follows:

$$H^\circ_T - H^\circ_{298.16} = 16.944\,T + 0.001304\,T^2 - 1519.2\,\log_{10} T - 1409; \quad (3)$$

$$S^\circ_T - S^\circ_{298.16} = 39.016\,\log_{10} T + 0.00261\,T + 660/T - 99.53; \quad (4)$$

$$C^\circ_p = 16.94 + 0.00261\,T - 660/T. \quad (5)$$

Values up to 1,200° K, calculated from eq (3), (4), and (5), are given in table 3.

TABLE 3. *Heat content, heat capacity, and relative entropy of* $MoSi_2$

T	$H^\circ_T - H^\circ_{298.16}$	C°_p	$S^\circ_T - S^\circ_{298.16}$
° K	*cal mole*$^{-1}$	*cal mole*$^{-1}$ *deg K*$^{-1}$	*cal mole*$^{-1}$ *deg K*$^{-1}$
298.16	0	15.50	0.00
300	28	15.52	.10
350	816	15.97	2.53
400	1,624	16.33	4.69
450	2,449	16.65	6.63
500	3,289	16.92	8.40
550	4,142	17.18	10.02
600	5,006	17.41	11.53
650	5,882	17.62	12.93
700	6,768	17.82	14.24
750	7,665	18.02	15.48
800	8,570	18.20	16.65
850	9,485	18.38	17.76
900	10,409	18.56	18.82
950	11,341	18.72	19.82
1,000	12,281	18.89	20.79
1,050	13,230	19.05	21.71
1,100	14,187	19.21	22.60
1,150	15,151	19.37	23.46
1,200	16,124	19.52	24.29

WASHINGTON, March 2, 1954.

[6] N. S. Osborne, H. F. Stimson, T. S. Sligh, and C. S. Cragoe, BS Sci. Pap. **20**, 65 (1925) S501.

Journal of Research of the National Bureau of Standards Vol. 53, No. 2, August 1954 Research Paper 2521

Precise Comparison Method of Testing Alternating-Current Watthour Meters

A. W. Spinks and T. L. Zapf

A brief description of the basic method of testing alternating current watthour meters at the National Bureau of Standards is given, followed by a description of equipment for a faster and less laborious method.

Equipment with several novel features has been assembled for making precise tests of alternating-current watthour meters by a comparison method employing a group of carefully selected alternating-current watthour meters, which serve as a secondary standard group. One of this group, designated the "Standard Watthour Meter", is used with multirange instrument transformers as a reference standard to test other watthour meters with good precision. The testing procedure is explained, and the formulas used in computing the results of the tests are derived.

An analysis of the possible errors of measurement and data from numerous tests indicate that the measurement of energy applied to a watthour meter under test can be relied upon to better than 0.06 percent.

1. Introduction

For many years the National Bureau of Standards has employed a method of testing alternating-current watthour meters, which, although very precise and accurate, is tedious and time consuming. By this method, the energy indicated by the watthour meter under test is compared with the true value of energy as measured in terms of a constant and accurately known power and an accurately determined time interval. The power is held constant with the aid of a standard electrodynamic wattmeter [1] which is calibrated on reversed direct current before and after each run. For this test, a very stable, manually controlled alternating-current source is required to insure a steady value of power.

In the midthirties it was observed that repeated tests on particular watthour meters showed remarkably small deviations from the initial test values. This suggested the possibility of using a group of watthour meters of demonstrated good repeatability as secondary standards. The register and gear train could be removed from each meter to reduce friction. Disk revolutions would be counted photoelectrically.

Four such meters were obtained, but unfortunately, work on this project was interrupted, and construction of a permanent setup and the apparatus for intercomparing the meters was delayed. In 1940 the paper of Goss and Hansen [2] describing the excellent performance of a group of watthour meters caused a revival of interest in this project. Further experimental work led to detailed plans, but actual shop construction was interrupted by duties imposed by World War II.

Work was resumed after the war, and the equipment, except for minor modifications, was constructed as originally planned. This apparatus has been under observation for several years, and its reliable performance has been verified. The new equipment is now used at the National Bureau of Standards in preference to the older equipment for practically all of the testing of a-c watthour meters. This paper describes the equipment, the procedures followed in its calibration and use, and the results obtained.

[1] John H. Park and Arthur B. Lewis, Standard electrodynamic wattmeter and ac-dc transfer instrument, J. Research NBS **25**, 545 (1940) RP1344.

[2] J. H. Goss and A. Hansen, Jr., A precision rotating standard for the measurement of kilowatt hours, Trans. AIEE **59**, 412 (1940).

2. Equipment

Basically, the complete equipment consists of a group of modified commercially available portable watthour meters maintained at a constant temperature, and the means for their calibration and intercomparison with a high degree of precision. In order to eliminate friction except at the top and bottom bearings, the meters are not equipped with registers. Instead, phototubes serve for counting revolutions of these meters, which are operated continuously during a test. For any direct intercomparison, some means of reading the registration of at least one meter of the group to a fraction of a revolution is extremely desirable. This is accomplished by providing a light-beam pointer and a special circular phosphorescent scale for one of the meters. At the beginning and again at the end of each run the light source for the pointer (a mercury-vapor lamp) is flashed, leaving spots on the phosphorescent scale that persist for several seconds. The standard meters are always operated at the same voltage and current. Other ranges are provided by special voltage and current transformers.

Originally it was intended to use four house-type meters, one from each of four American manufacturers. Each of the manufacturers was consulted, and asked for advice in the selection of the meters. Two of the manufacturers recommended their portable standards rather than selected house-type meters. As a result, the original setup was designed to accommodate two portable standards and two (or more) house-type meters. More recently, however, a different type of watthour meter has proved to be so much more stable than the older house-type meters originally procured, that the latter have been replaced by two of the newer type.

The two original portable standard meters were individually housed in separate temperature-controlled enclosures, each enclosure consisting essentially of a Bakelite housing completely surrounding the aluminum case of the meter, a mercury thermoregulator to control the temperature, and four small lamps distributed inside the aluminum case to serve as heaters. The temperature is regulated at approximately 35° C to better than ±0.2 deg C. The upper end of the meter shaft projects through the top of the Bakelite enclosure. The mirror for the light-beam pointer is attached to this end of the shaft at an angle of 45° to the axis of the shaft. Each meter enclosure is assembled on a brass base plate to make a complete unit for interchangeable mounting in the housing that holds the phosphorescent scale. The particular portable watthour meter that is used with the circular scale is referred to in this discussion as the Standard Watthour Meter, as distinguished from the Comparison Standard Watthour Meters.

The cast-aluminum base of the circular-scale housing is equipped with leveling screws. The circular scale, approximately 26 inches in diameter, is assembled on brackets attached to the base of the housing. The meter enclosure rests on screws for leveling the meter and adjusting its height for proper scale alinement. These screws, in turn, are mounted on an adjustable centering plate, which permits centering the axis of the meter shaft with respect to the scale.

The mercury-vapor lamp is mounted on a hinged arm above the meter. A diaphragm below the lamp has a ½-mm aperture that serves as a point source of light. Adjustments are provided for centering the light beam. The light path is vertically downward from the aperture through a lens to the mirror on the end of the meter shaft where it is reflected horizontally to the circular scale, a curved brass strip coated with phosphorescent paint. The dark-blue component of light from the aperture is focused by the lens to provide a well-defined image of 1-mm diameter when a flash occurs. Flush with this strip and directly below it is a circular strip of Lucite engraved with 1,000 small divisions (about 2 mm per division). Every tenth division is numbered. Effective use of the phosphorescent scale requires that the room be semidark; therefore, the Lucite scale is provided with edge illumination by 12 small panel lamps spaced at regular intervals. The zero mark on the scale, which is also the 1,000 division mark, is centered on the bracket supporting the mercury lamp. There is a narrow slit cut through the scale and bracket at this point. A phototube, which is used with auxiliary apparatus for counting revolutions, is mounted directly behind this slit. Figure 1, a photograph of the Standard Watthour Meter, shows most of these features.

The temperature-controlled cabinet originally designed for the house-type meters is now being used to house the newer type watthour meters, which serve as comparison standards. Its dimensions are approximately 112 cm long, 37.5 cm wide, and 30 cm high. It consists of a wooden cabinet with a removable glass top, a thermoregulator, electric heating coil, and a small blower for circulating the air within the cabinet. Temperature is maintained at approximately 40° C to within ±1 deg C.

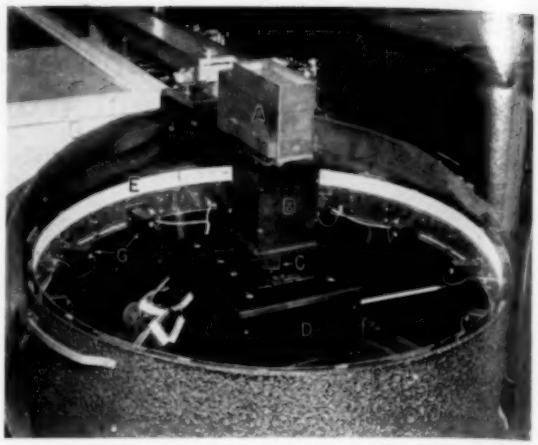

FIGURE 1. *Standard Watthour Meter with circular phosphorescent scale used as a reference standard for the testing of watthour meters by a comparison method.*

The light beam "pointer" is produced by a mercury vapor lamp and lamp combination located above the Standard Watthour Meter.
a, Mercury vapor lamp housing; b, lens box; c, mirror; d, Standard Watthour Meter; e, phosphorescent scale; f, engraved plastic scale; g, lamps.

The accessory electronic equipment performs three functions. The first function, that of counting, is accomplished by a relay pulse-counting circuit by means of which either a predetermined length of time or a predetermined number of revolutions of a watthour meter may be used to make or break electric circuits. The counting circuit may be preset to count seconds or revoltuions from 1 to 999. When calibrating the Standard Watthour Meter, using the Standard Wattmeter to aid in maintaining constant power, the counting circuit is operated by pulses accurately spaced 1 second apart. These pulses, or seconds signals, are derived from the quartz-crystal-controlled frequency standards maintained at the National Bureau of Standards, and, as a basis for timing, are reliable to better than a part in a million. With the aid of phototubes the pulse counter can be used for counting the revolutions of the disk of either a comparison standard, the reference standard, or a watthour meter under test.

The second function of the accessory electronic equipment is that of flashing the mercury-vapor lamp. The pulse counter completes a circuit for the starting pulse to trigger a thyratron whose plate circuit discharges a capacitor through the mercury-vapor lamp. The capacitor is charged to approximately 1,000 v by means of a conventional high-voltage power supply. The lamp is normally supplied with a current of 0.7 amp from a 240-v d-c power circuit. Normal voltage provides sufficient light intensity in the beam to trigger the phototube each time it passes over the slit in the scale. A large choke prevents the capacitor discharge from entering

the power circuit. Just before the end of the preset time interval (or preset number of revolutions of a meter) the pulse counter again completes the circuit, so that the last or stopping pulse fires the thyratron. Thus the flashing is entirely automatic; the timing of the flash depends on the signal pulse, which in the case of the seconds signals is accurate to better than a part in a million.

The third function of the accessory electronic equipment is that of counting the disk revolutions of the Standard Watthour Meter. This, too, is automatic. During a run the constant light actuates the phototube behind the slit in the scale. This operates an electromagnetic counter by means of an amplifier and a small thyratron. An electronic switch opens the cathode circuit of the thyratron tube to prevent counting except during the run. The pulse that flashes the mercury lamp is also fed to the grids of the electronic-switch tubes. The first, or starting, pulse that flashes the lamp also enables conduction in the counter thyratron and allows counting to start. The second, or stopping, pulse that flashes the lamp again at the end of the preset timing or counting interval, disables the thyratron and stops the counting.

3. Testing

The accuracy of a test of a watthour meter, using the apparatus described is directly dependent upon the latest previous calibration of the reference standard, the stability of which is substantiated by more recent intercomparison tests. Phantom loading is employed in all tests. Correct circuit connections are made rapidly by means of links on an otherwise permanently wired circuit board.

3.1. Calibration of the Standard Watthour Meter

The word "calibration" usually implies not only a carefully made test, but also an initial careful adjustment or marking of the apparatus under test. For the purpose of this discussion, however, a calibration of the Standard Watthour Meter implies a test to determine accurately its percentage registration and possibly, but not necessarily, an adjustment of its mechanism in order to bring the percentage registration within certain limits.

The Standard Watthour Meter is periodically calibrated with 120 v, 5 amp applied, at unity power factor, and at 0.5 power factor with the current lagging the voltage. During calibration, a measured value of a–c power is maintained constant for an accurately determined time interval.

The testing circuit is shown in figure 2. In the potential circuit it is important that the effective terminals of the Standard Wattmeter be located precisely at the Standard Watthour Meter terminals on alternating current, and at the volt-box terminals on direct current. Hence the lead resistance from the a–c—d–c switch to the Standard Watthour Meter potential terminals and to the volt-box terminals must be equal to prevent errors that would otherwise be caused by a difference in IR drops in

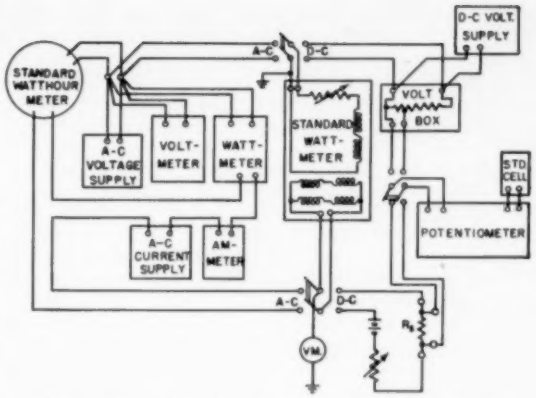

FIGURE 2. *Calibration of Standard Watthour Meter.*

the leads. It is also important that the voltage supplies be connected to these same terminals, otherwise a phase-angle error in the watthour-meter-potential circuit might result from an IR drop in the leads. Lead resistances are checked and adjusted, if necessary, just before each calibration. Note also in figure 2 that the moving-coil side of the Standard Wattmeter potential circuit is grounded, and that the current circuit is connected to ground through a rectifier-type voltmeter, a 300-v instrument having a total resistance of 300,000 ohms. This serves as an electrostatic tie to ground, which minimizes electrostatic forces between fixed and moving coils of the wattmeter, and provides an indication of the presence of leakage current and its magnitude.

In calibrating the Standard Watthour Meter the procedure is as follows. First, temperature equilibrium of the entire equipment is established by applying a–c power adjusted (in the case of the wattmeter and watthour-meter circuits) to approximately the values required for the test and then waiting for an hour or two before proceeding. After temperature equilibrium has been attained, the Standard Wattmeter is calibrated on reversed direct current to indicate the desired value of power. Alternating-current power is restored to the Standard Wattmeter and Standard Watthour Meter circuits and adjusted to give the same deflection of the Standard Wattmeter as that obtained on direct current. The a–c power is held substantially constant throughout the run.

The pulse-counting circuit is then energized. The next seconds signal flashes the mercury-vapor lamp and starts the run. The position of the spot on the phosphorescent scale is recorded to the nearest division. At the end of the preset interval (usually 100 seconds) the final seconds pulse again flashes the mercury-vapor lamp, thereby ending the run. The position of this last spot is recorded as well as the reading of the revolution counter, which indicates the number of complete revolutions. Thus, the number of revolutions of the Standard Watthour Meter's disk equals the reading of the revolution counter plus the scale reading at the end of the run

minus the scale reading at the beginning of the run. For example, if the reading at the start of the run were 872 divisions, and at the end of the run, 493 divisions, and the revolution counter read 10, the number of revolutions would be $10+0.493-0.872=9.621$. After the a-c run, two additional readings of the Standard Wattmeter on reversed d-c power are obtained in the same manner as at the start, giving a total of four d-c readings. Care is taken to insure a minimum of delay between the d-c readings and the run with alternating current. If this is done, any small linear drift that may be present in the deflection of the Standard Wattmeter causes no significant error in the result. The d-c readings are averaged and a correction applied for the difference between the a-c setting and the average d-c reading. Corrections are also applied for known errors in the resistance standard, volt box, wattmeter (phase-defect angle), and for deviations from normal of the average frequency of the source, if significant.

The formula used in this calibration for computing percentage registration is

$$\mathscr{R}=100\left[\frac{KR_s n3600}{E_p N_{vb} E_c t}+\frac{D_{dc}-D_{ac}}{D_{dc}}+c_s-c_{vb}+c_f-T_w\tan\theta\right] \quad (1)$$

where

K = disk constant of the watthour meter, in watthours per revolution.
R_s = nominal resistance of resistance standard, in ohms.
n = number of disk revolutions of watthour meter.
E_p = potentiometer setting, in volts, when adjusting the d-c voltage.
N_{vb} = nominal volt box ratio.
E_c = potentiometer setting, in volts, when adjusting the d-c current.
t = time of run in seconds.
D_{dc} = average of the four deflections of the Standard Wattmeter, in centimeters, observed during the d-c calibrations before and after each run.
D_{ac} = average deflection of Standard Wattmeter, in centimeters, maintained during the a-c run.
c_s = correction to the resistance standard, in parts per unit.
c_{vb} = correction to the volt box, in parts per unit.
c_f = frequency correction to the Standard Watthour Meter, determined from the reading of the synchronous timer, the time duration of the run, and a frequency correction factor obtained in a separate test of the Standard Watthour Meter.
T_w = phase defect angle of the Standard Wattmeter, in radians, positive if the moving coil current leads the supply voltage.
θ = power factor angle, which is the angular phase difference between the voltage, E, applied to the Standard Wattmeter, and the current, I, in the Standard Wattmeter current coils, and is positive if the current lags the voltage.

A complete derivation of this equation appears in the appendix.

3.2. Tests of the Comparison Standard Watthour Meters

The watthour meters used as Comparison Standards are tested with 120 v and 5 amp applied, at unity power factor, and at 0.5 power factor, with the current lagging the voltage. The method of testing a Comparison Standard Watthour Meter involves a comparison with the Standard Watthour Meter immediately following or during its calibration and periodically between calibrations. Figure 3 is a diagram of the circuit involved in the intercomparison of the standard watthour meters.

The similarity between the circuit shown in figure 3 and the alternating-current portion of figure 2 should be noticed. When a calibration of the Standard Watthour Meter is in progress the Comparison Standard Watthour Meters shown in figure 3 are incorporated in the circuit of figure 2, although in the interest of simplicity, this modification is not shown in the figure. With the circuit revised in this manner, the Standard Watthour Meter, the Comparison Standard Watthour Meters, and the Standard Wattmeter are energized simultaneously, and the calibration runs on the reference standard can be performed alternately with intercomparison test runs, thereby insuring nearly identical conditions for both tests. Truly simultaneous testing of the reference standard (having the circular phosphorescent scale) and the comparison standards is possible with the addition of more equipment, but it is believed that any improvement that might accrue from simultaneous testing would be too small to detect with certainty.

There is a phototube-lamp combination associated with each Comparison Standard, but only one of these combinations is energized at a time. The phototube produces a pulse for each revolution of the disk of the Comparison Standard under test. This pulse is amplified and used in conjunction with the pulse-counting circuit to start and stop the run.

To start the run, a pulse from the phototube associated with the Comparison Standard Watthour

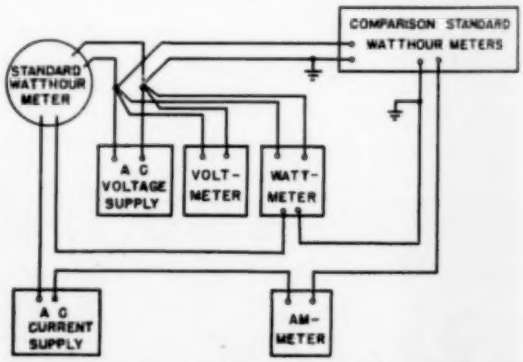

FIGURE 3. *Intercomparison of Standard Watthour Meters.*

Meter is used to flash the mercury-vapor lamp and a spot is left on the phosphorescent scale of the Standard Watthour Meter. The position of this spot is recorded on the data sheet. When the preset number of turns have been completed, the mercury-vapor lamp again flashes; another spot is left, and its position is recorded together with the reading of the revolution counter. From these readings the number of revolutions of the Standard Watthour Meter's disk is computed. The average percentage registration of the Comparison Standard obtained from several runs is taken as the most probable value. The other Comparison Standard Watthour Meters are tested in the same way.

The formula used in this test for computing the percentage registration of the Comparison Standards is

$$\mathscr{R}_c = \frac{n_c K_c}{K_s} \frac{\mathscr{R}_s}{n_s}, \qquad (2)$$

where

n_c = number of disk revolutions of the Comparison Standard Watthour Meter.
n_s = number of disk revolutions of the Standard Watthour Meter.
K_s = disk constant of the Standard Watthour Meter, in watthours per revolution.
K_c = disk constant of the Comparison Standard Watthour Meter, in watthours per revolution.
$\mathscr{R}_s$ = percentage registration of the Standard Watthour Meter.

A derivation of this equation appears in the appendix.

3.3. Tests of Other Watthour Meters, Using the Standard Watthour Meter

Alternating-current watthour meters that are sent to the National Bureau of Standards for test are compared with the Standard Watthour Meter in the following manner. The current and potential circuits of the Standard Watthour Meter are energized from the secondaries of a current transformer and a potential transformer having multiple ranges. The primary windings of these transformers and the watthour meter under test are excited by the a-c power supplies, as shown in figure 4.

The resistance of the leads that connect the potential circuit of the watthour meter under test to the primary of the voltage transformer is made small enough to render negligible the error in phase angle caused by the voltage drop in the leads. A voltmeter, ammeter, and a wattmeter of good quality are connected in the secondary circuit, and they enable an observer to set the secondary voltage, current, and power factor.

A phototube-lamp combination is arranged to produce a pulse at each revolution of the disk of the watthour meter under test if this is conveniently possible. The pulses are amplified, and, in conjunction with the pulse counter, are used to determine the duration of the run.

An alternative method of testing meters, particularly those that have no good means of operating a phototube, is to let the duration of the run be determined by the Standard Watthour Meter. This is accomplished by connecting the pulse counter to the output of the phototube located behind the slit in the scale of the Standard Watthour Meter. The potential circuit of the watthour meter under test is then closed at the beginning of the run and opened at the end by relays operated by the pulse counter. Contacts on one of the relays, when energized, close the potential circuit; while normally closed, contacts on the other relay, when energized, open the circuit. The time lags in the operation of these relays are carefully equalized to reduce timing errors to a negligible amount.

As the percentage registration of the Standard Watthour Meter is accurately known, the percentage registration of the watthour meter under test can be computed. Corrections are applied for the ratio and phase-angle errors of the current and potential transformers.

The procedure followed in making a test of this sort is practically identical to that followed in testing a Comparison Standard Watthour Meter.

The formula used in this test for computing the percentage registration of the test watthour meter is

$$\mathscr{R}_t = \frac{K_t n_t \mathscr{R}_s}{K_s N_{pt} N_{ct} n_s} + 100[c_\theta - c_{ct} - c_{pt}], \qquad (3)$$

where

K_t = disk constant of the watthour meter under test, in watthours per revolution.
n_t = number of disk revolutions of the test watthour meter.
$\mathscr{R}_s$ = percentage registration of the Standard Watthour Meter.
K_s = disk constant of the Standard Watthour Meter, in watthours per revolution.
N_{pt} = nominal potential transformer ratio.
N_{ct} = nominal current transformer ratio.
n_s = number of disk revolutions of Standard Watthour Meter.
c_{ct} = correction for the current transformer ratio (= ratio factor − 1), in parts per unit.
c_ϕ = correction for the potential transformer ratio (= ratio factor − 1), in parts per unit.
c_φ = correction for the phase angle, in parts per unit. It is equal to $(\beta - \gamma) \tan \theta_s$.
β = phase angle of the current transformer, in radians, considered positive when the reversed secondary-current vector leads the primary-current vector.
γ = phase angle of the potential transformer, in radians, considered positive when the reversed secondary-voltage vector leads the primary-voltage vector.
θ_s = power-factor angle at the Standard Watthour Meter, considered positive when the current vector lags the voltage vector.

A complete derivation of this equation appears in the appendix.

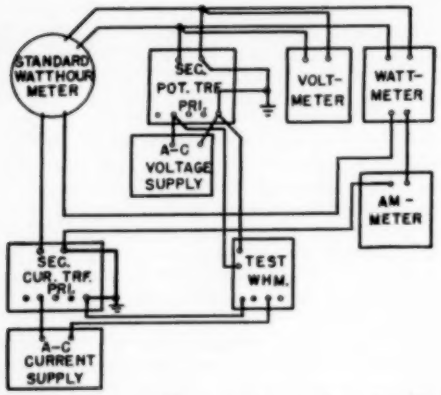

FIGURE 4. *Testing watthour meters, using the Standard Watthour Meter.*

4. Calibration and Testing Schedule

The periodic primary calibrations of the Standard Watthour Meter serve to accurately ascertain its percentage registration. Primary calibrations performed at monthly intervals for a period of time have indicated a long-time stability of the reference standard that will permit an increase in the interval between calibrations to 6 months or longer. A graphical record is kept of the intercomparison tests, which are performed at more frequent intervals, to detect any appreciable drifts or erratic changes in registration of any one of the group relative to the others, and possibly, to form a basis for a revision of the registration assigned to the Standard Watthour Meter if an observed change is not large enough to warrant a primary calibration. When a revision of the registration of reference standard is warranted on the basis of intercomparison tests and the evidence does not indicate gross instability in any one particular meter, the computation of registration is performed on the assumption that the mean registration of all meters remains unchanged between calibrations. With this assumption, the entire group of meters is useful in maintaining the unit of energy, although transfer of the unit to a watthour meter under test is accomplished through only one member of the group.

5. Precision and Accuracy Attainable

Both systematic and random errors limit the accuracy of test results obtained with the Standard Watthour Meter and its associated apparatus. Systematic errors, those which cannot be considered accidental, can be further classified into several types. First, there are the errors that have escaped the attention of the observers. After a careful analysis of all possible sources of error and the comparison of the results of tests made by several methods, it is believed that unknown systematic errors of magnitudes larger than about 0.01 percent are highly improbable.

Second, there are residual errors from the application of imperfect corrections. These errors are systematic in nature and have been minimized in the present work by carefully calibrating each piece of apparatus for which a correction must be applied in terms of the National Electrical Standards, which are readily available. The largest systematic errors of this type result from the uncertainty in the ratio and phase-angle corrections of the current and potential transformers. Other residual errors of this type, such as those associated with the standard cell, potentiometer, and volt box, occur in the primary calibrations of the Standard Watthour Meter, and are rather small. The history of the components used in the measurements circuit is well known. The maximum net change in value of the components between their periodic tests, for the last several years, is listed in table 1.

The third type of systematic error is, in a sense, similar to the second type, in that it arises from the imperfect application of corrections, but in this case the corrections are for the compensation of fluctuating errors. Such errors may vary with certain parameters in a definite though unknown manner. On the other hand, the fact that an error exists and that it is a function of a certain parameter may be known, but its effect may be negligibly small (and a correction impractical to apply) compared with that of the other errors. Varying systematic errors are evident in the Standard Watthour Meter as well as the Comparison Standard Watthour Meters and, in fact, sharply limit the accuracy of which any watthour meter is capable. Reference is here made to the effect on the percentage registration of a watthour meter of such factors as incorrect magnitude of applied voltage and current, incorrect phase angle, incorrect frequency, or the presence of harmonics in the applied voltage or current. Studies have been made of the effect of each of these variables on the meters used as standards. It has been found feasible to use a good quality voltmeter, ammeter, and wattmeter, to facilitate setting the voltage, current, and phase angle. The power supplies are electronically regulated to maintain the initial adjustment of voltage and current, and are operated and loaded in such a manner as to minimize harmonics.

TABLE 1. *Observed maximum net change in the value of the components necessary for the accurate standardization of the Standard Electrodynamic Wattmeter*

Component	Maximum net change in value
	ppm
Standard cell	10
Potentiometer	10
Volt box	11
Total	31
Standard cell	10
Potentiometer	10
Resistance standard	6
Total	26
Grand total	57

A third harmonic of as little as 1 percent of the fundamental in the current circuit of a watthour

meter may cause a registration error of several hundredths of a percent if certain phase relationships exist. This error arises from the existence of a third harmonic flux in the air gap of the electromagnet even if a purely sinusoidal voltage is applied to the potential coil. It is important to realize that even if a watthour meter is tested using alternating current of practically sine wave form it will register inaccurately if used in a circuit in which the wave form is nonsinusoidal. Although it would be unfair to impute errors due to nonsinusoidal wave form to watthour meters, which are designed for use on a sinusoidal waveform, the possibility of an appreciable error arising from this cause should not be overlooked if accurate measurements are desired. Odd harmonics which are present in the wave form of the current and voltage supplied to the Standard Watthour Meter and associated apparatus at the time of this writing are, under most load conditions, considerably less than 1 percent, much less than usually found in commercial power sources.

During calibrations of the Standard Watthour Meter, average frequency of the applied power during a run is measured and a correction applied for any deviation from 60 c/s. In most other tests a measurement of average frequency, and a correction for errors therein, is not conveniently possible, and this probably contributes the greatest share of systematic errors that vary in a definite, but unknown, manner. However, it has been determined that errors arising from customarily observed deviations in frequency are of the order of a few thousandths of a percent. The effect of temperature changes on the watthour meter standards is reduced to a small value by keeping all meters in temperature-controlled enclosures. The standards are not removed from the position in which they are calibrated. Throughout all tests the Standard Watthour Meter is operated continuously, thus eliminating those errors associated with starting and stopping the disk.

Since the scale of the Standard Watthour Meter is marked with 1,000 small divisions, any small variations in the angular speed of the disk which would be undetectable in other meters may very likely be easily discernible. To determine the nature and the magnitude of errors due to angular speed variations, the standard was centered as accurately as feasible in its scale and carefully levelled. It was operated at a reduced speed, and seconds pulses were used to flash the mercury vapor lamp once every second. The applied power was held constant at a value sufficient to cause successive spots from the mercury-vapor lamp to appear on the phosphorescent scale at four points as the disk revolved. Scale readings corresponding to spot positions indicated a regular (nearly sinusoidal) variation of disk speed during each revolution. The variations were such as to cause a maximum shift in scale reading of about 0.005 revolution. A method was devised for aligning the watthour meter in its scale to reduce this error to less than 0.001 revolution, thereby partially compensating for the angular speed variations. An error of 0.001 revolution would cause a scale reading error of only 0.001 percent if the watthour meter is operated for 100 revolutions, as is usually done.

Some of the residual errors thus far discussed will be positive, others will be negative, and the magnitude of many of these systematic errors will appear to vary in a random manner as more and more tests are performed. To this must be added the truly random errors, the distribution of which is entirely by chance, and to which the theory of errors may be applied. The values listed in table 2 include an estimate of the standard deviation of random errors based upon numerous test data, and half the maximum systematic error that it is believed may possibly be present in any one measurement of energy. It is recognized that the errors listed do not represent truly random variations, yet their individual contribution (some being positive and some negative) to the final result partakes of randomness and probably justifies the computation of the total propagated error from the square root of the sum of the squares of the component errors. There is one exception. The error in the standard cell and the error in balancing the potentiometer against the electromotive force of the standard cell occur twice in a single measurement of d-c power; hence, these component errors are not independent, and the propagation of these errors is by simple addition. The potentiometer error also occurs twice, but these are independent, since different resistance sections of the potentiometer are used for the measurement of voltage and current. The total propagated error provides an estimate of expected accuracy with which the applied energy is known, when the Standard Watthour Meter and its associated apparatus is used to test other meters. It is not to be inferred that the other meters are capable of calibration or maintaining their calibration to the degree of accuracy indicated at the bottom of the table.

A test was made to determine the repeatability of results in the comparison testing of the Comparison Standard Watthour Meters against the Standard Watthour Meter. Individual runs of about 100 seconds duration were made about 10 minutes apart until a group of 10 runs had been made. This was repeated the next day, and again 4 days later. The relative percentage registrations of the two Comparison Standards are shown in table 3. The values listed are the means of the groups of 10 runs, and the measure of precision is the standard deviation of a single run of the group.

The precision indices listed in table 3 result from a combination of random errors inherent to (1) the Comparison Standard Watthour Meter being tested, and (2) the Standard Watthour Meter, including observational errors in reading its scale. If it is assumed that each meter contributes equally to the total error, but that the contributions are random, then an index of precision for each meter may be computed. If the total error is considered as 0.012 percent, the individual errors which produce this error are each $0.012/\sqrt{2}=0.008$ percent. From these data it is estimated that the precision of each of the watthour meters in the setup over a period of a few hours is about 0.008 percent.

TABLE 2. *Effect of residual errors on the test of a watthour meter*

Type of measurement and components	Estimated residual error
	%
Measurement of d-c power with a potentiometer, volt box, and resistance standard:	
Standard cell	0.001
Error in standardizing potentiometer	.002
Twice the square root of the sum of the squares from the above sources	0.005
Potentiometer:	
a. Measurement of voltage	.002
b. Measurement of current	.002
Volt box	.001
Resistance standard	.001
Reading deflection of wattmeter on direct current	.002
Calibration of the Standard Watthour Meter:	
Setting and holding deflection of Standard Wattmeter on alternating current	.002
Timing errors	.001
Standard Watthour Meter scale errors	.001
Errors in maintenance and use of the standard meters:	
Maintenance of the unit of electric energy by the Standard Watthour Meter and the Comparison Standard Watthour Meters (long-time stability, see table 4)	.012
Standard Watthour Meter registration variations (short-time stability)	.010
Test of a watthour meter at unity power factor in a comparison test with the Standard Watthour Meter:	
Transformer errors:	
a. Current transformer ratio	.010
b. Potential transformer ratio	.010
Square root of sum of squared residual errors at unity power factor. Total propagated error equals	0.022
Test of a watthour meter at 0.5 power factor in a comparison test with the Standard Watthour Meter:	
Transformer errors (additional errors due to uncertainty of transformer phase angles):	
a. Current transformer	0.010
b. Potential transformer	.010
Square root of sum of squared residual errors at 0.5 power factor. Total propagated error equals	0.026

TABLE 3. *Short-time repeatability of intercomparison tests on the Comparison Standard Watthour Meters against the reference Standard Watthour Meter*

At 0.5 power factor, the current lagged the voltage.

Group	Comparison Standard No. 1				Comparison Standard No. 2			
	1 power factor		0.5 power factor		1 power factor		0.5 power factor	
	Registration	Standard deviation	Registration	Standard deviation	Registration	Standard deviation	Registration	Standard deviation
	C_E	σ_E	C_θ	σ_θ	C_E	σ_E	C_θ	σ_θ
A	100.067	0.014	99.923	0.012	100.140	0.011	100.068	0.007
B	100.085	.001	99.932	.016	100.160	.010	100.064	.010
C	100.056	.010	99.936	.016	100.135	.015	100.082	.018

TABLE 4. *Precision of intercomparison test results over a period of several months (from same data as figure 5)*

At 0.5 power factor, the current lagged the voltage.

Watthour meter	Standard deviation	
	1.0 power factor	0.5 power factor
	Percent	*Percent*
Standard Watthour Meter	0.012	0.014
Comparison Standard Watthour Meter No. 1	.008	.007
Comparison Standard Watthour Meter No. 2	.007	.012

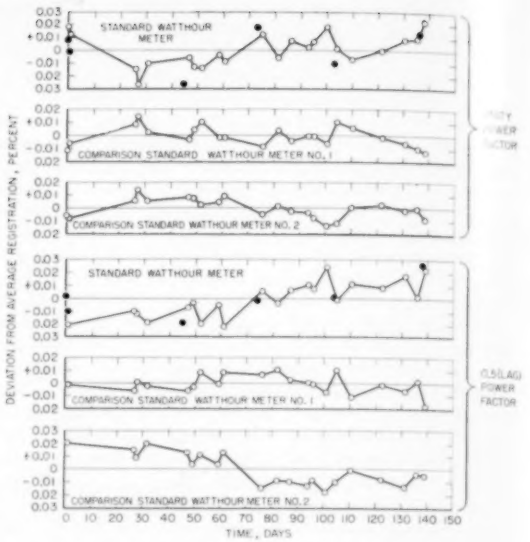
STANDARD WATTHOUR METER
COMPARISON STANDARD WATTHOUR METER NO. 1
COMPARISON STANDARD WATTHOUR METER NO. 2
STANDARD WATTHOUR METER
COMPARISON STANDARD WATTHOUR METER NO. 1
COMPARISON STANDARD WATTHOUR METER NO. 2
UNITY POWER FACTOR
0.5(LAG) POWER FACTOR
DEVIATION FROM AVERAGE REGISTRATION, PERCENT
TIME, DAYS

FIGURE 5. *Percentage registration deviations of the Standard Watthour Meter and Comparison Standard Watthour Meters over a period of several months.*

Connected points are results of intercomparison tests; isolated points are results of calibrations of the Standard Watthour Meter.

As these meters are used to maintain the unit over much longer periods of time than were used in the test described, it might be expected that the long-time stability of the meters should not be as good as that for short intervals because of varying systematic errors. On the other hand, the use of a multiplicity of meters improves the over-all precision. A measurement of the precision with which the unit is maintained is obtained from the records of calibration and intercomparison tests. Figure 5, for example, shows the test results over a period of several months. The points connected by straight lines represent the results of intercomparisons, and are based on an assumed constant mean registration of all three meters. The validity of this assumption is proved by the proximity of the intercomparison test results to the isolated points representing calibrations of the Standard Watthour Meter by the wattmeter method. The standard deviation for each of the meters (assuming all deviations are normally distributed and random) computed from the data shown in figure 5 is given in table 4. From data such as these it is estimated that the unit of the watthour can be maintained over a period of several months with precision represented by a standard deviation of 0.012 percent or better. Many tests that have been run in rapid succession, a few minutes apart, indicate drifts in registration in one direction for a period, then a reversal or rapid change of some sort. Such drifts or changes have been very small (few thousandths of a percent). However, an abnormal distribution of this sort reveals the presence of those

varying systematic errors, discussed previously, which depend upon other parameters. A comparison of tables 3 and 4 shows that the stability over several months is very nearly the same magnitude as that over a period of an hour or two. This implies that any varying systematic errors that may exist vary rapidly and in such a manner that their effect on the mean of a number of observations of percentage registration taken several hours or more apart is negligibly small. Accordingly, when calibrations of the Standard Watthour Meter are performed, the individual runs are taken at time intervals sufficient to extend the duration of the test to several hours.

When the apparatus is used for testing other watthour meters it is believed that the measurement of the energy applied to the test watthour meter is valid and can be relied upon to better than 0.06 percent.

6. Conclusion

At the National Bureau of Standards a set of several carefully selected and prepared watthour meters has been arranged as a standard group for testing alternating-current watthour meters by a comparison method.

Although the initial cost of designing, constructing, and assembling this apparatus would ordinarily deter the general adoption of such an elaborate system of testing watthour meters, the use of the apparatus described has yielded a definite saving in time and labor, without significant loss of accuracy when compared with the primary method used in the past.

Accurate initial calibration of the apparatus is accomplished by averaging the results of a number of primary calibrations of the Standard Watthour Meter, using (1) a transfer wattmeter and potentiometer for measurements in terms of the fundamental electrical units of electromotive force and resistance, and (2) standard seconds signals for time measurements. Assurance of the continued accuracy of the reference standard watthour meter is obtained by intercomparison tests with other members of the standard group. The reference standard, supplemented by calibrated instrument transformers, accurately measures the energy supplied to a watthour meter under test.

J. B. Dempsey initiated the early work in setting up selected watthour meters for secondary standards. F. B. Silsbee proposed the light-beam pointer and phosphorescent scale. F. J. Gross carried out the developmental work and the original design of the comparison apparatus. Most of the mechanical construction of this apparatus was done by C. H. Hochgesang of the Bureau's Instrument Shop. Robert W. Balcom assembled most of the electronic equipment and provided many valuable suggestions. Thomas W. Cushing carried the project forward for a time and designed and supervised the construction of the constant-temperature cabinet for the comparison standards.

7. Appendix

The derivations of eq (1), (2), and (3) proceed most easily from the definition of percentage registration, which is the ratio of the indicated energy as obtained from the reading of the watthour meter to the true energy, expressed in percent.

$$\mathscr{R}=100\,\frac{\text{Indicated energy}}{\text{True energy}}. \tag{4}$$

In a test of the Standard Watthour Meter, using the Standard Wattmeter, the indicated energy in watthours is Kn. The true energy is determined by the readings and settings of the Standard Wattmeter. Because this instrument is very nearly astatic, its sensitivity, s, will be the same for both directions of the direct current, and the average deflection is

$$D_{dc}=sW_{dc}, \tag{5}$$

where W_{dc} is the true power impressed on the Standard Wattmeter.[4] The true power in terms of the potentiometer settings and circuit constants is

$$W_{dc}=\frac{E_pN_{rb}E_c}{R_s}+c \tag{6}$$

where c represents the correction terms for the circuit components. The average a-c deflection of the Standard Wattmeter is

$$D_{ac}=sEI\cos(\theta+T_w), \tag{7}$$

where E is the a-c voltage between the Standard Wattmeter potential terminals causing a potential coil current, I_p, see figure 6. It is the magnetic field from this current that reacts with the magnetic field from the current, I, in the fixed coils of the Standard Wattmeter to produce the deflection, D_{ac}.

The wattmeter sensitivity, s, will be the same on alternating current as on direct current provided all readings are grouped closely on the Standard Wattmeter's scale.

Dividing (5) by (7)

$$\frac{D_{dc}}{D_{ac}}=\frac{sW_{dc}}{sEI\cos(\theta+T_w)}. \tag{8}$$

Solving for EI

$$EI=W_{dc}\,\frac{D_{ac}}{D_{dc}\cos(\theta+T_w)}. \tag{9}$$

The a-c power impressed on the Standard Watthour Meter is

$$W_{ac}=EI\cos\theta \tag{10}$$

and substituting for EI from eq (9)

$$W_{ac}=W_{dc}\,\frac{D_{ac}\cos\theta}{D_{dc}\cos(\theta+T_w)}. \tag{11}$$

[4] The symbols not specifically defined in the appendix have been previously defined in the text.

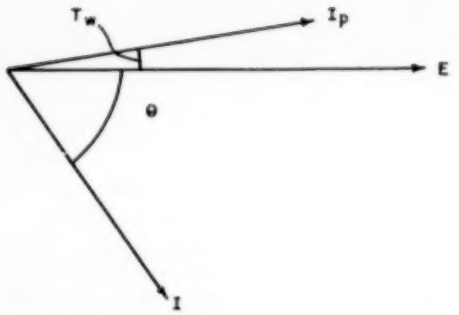

FIGURE 6. *Vector relationships at the Standard Wattmeter terminals during a calibration of the Standard Watthour Meter.*

No scale is intended and the angles indicated are grossly exaggerated for clarity.

This can be rearranged in the form

$$W_{ac}=W_{dc}\left[1+\frac{D_{ac}-D_{dc}}{D_{dc}}\right]\left[1+\frac{\cos\theta}{\cos(\theta+T_w)}-\frac{\cos(\theta+T_w)}{\cos(\theta+T_w)}\right]$$

$$W_{ac}=W_{dc}\left[1+\frac{D_{ac}-D_{dc}}{D_{dc}}\right]\left[1+\frac{\cos\theta-\cos\theta\cos T_w+\sin\theta\sin T_w}{\cos\theta\cos T_w-\sin\theta\sin T_w}\right] \quad (12)$$

$$W_{ac}=W_{dc}\left[1+\frac{D_{ac}-D_{dc}}{D_{dc}}\right]\left[1+\frac{\cos\theta(1-\cos T_w)+\sin\theta\sin T_w}{\cos\theta\cos T_w-\sin\theta\sin T_w}\right]$$

and since T_w is a very small angle (116 microradians at 60 c/s), sin T_w very nearly equals T_w in radians and cos T_w is very nearly 1; therefore, the equation can be simplified by neglecting the extremely small terms.

$$W_{ac}=W_{dc}\left[1+\frac{D_{ac}-D_{dc}}{D_{dc}}\right][1+T_w\tan\theta] \quad (13)$$

and since the second terms in both pairs of brackets are much smaller than 1, the equation may be further simplified by multiplying and then neglecting the smaller second-order terms.

$$W_{ac}=W_{dc}\left[1+\frac{D_{ac}-D_{dc}}{D_{dc}}+T_w\tan\theta\right]. \quad (14)$$

When W_{dc} from eq (6) is substituted and the result is multiplied by $t/3600$ to obtain energy in watthours, the true energy thus obtained may be used in eq (4), and the results, showing all corrections as correction terms, is eq (1) shown in section 3.

The derivation of eq (2), which is used in intercomparison tests, follows logically from eq (4). The indicated energy equals $K_c n_c$. Hence the percentage registration of the Comparison Standard Watthour Meter is

$$\mathscr{R}_c=100\frac{K_c n_s}{\text{True energy}} \quad (15)$$

and that of the Standard Watthour Meter is

$$\mathscr{R}_s\frac{K_s n_s}{\text{True energy}}. \quad (16)$$

Since, in this test, the true energy is identical for both watthour meters, eq (15) and (16) can be combined to yield eq (2), as shown in section 3.2.

In the derivation of eq (3) the following additional symbols will be used:

θ = power factor angle at the test watthour meter, considered positive when the current vector lags the voltage vector. It is equal to $\theta_s+\beta-\gamma$.

E_p = primary voltage applied to the test watthour meter.

I_p = primary current applied to the test watthour meter.

E_s = secondary voltage applied to the Standard Watthour meter.

I_s = secondary current applied to the Standard Watthour meter.

t = time of run, in seconds.

N'_{pt} = true potential transformer ratio = $N_{pt}(1+\epsilon_{pt})$.

N'_{ct} = true current transformer ratio = $N_{ct}(1+\epsilon_{ct})$.

The indicated energy of the watthour meter under test is $K_t n_t$. The true energy that should be measured by the test watthour meter is $E_p I_p t\cos\theta$, or, if E_p and I_p are expressed in terms of secondary voltage and secondary current, the true energy is $E_s N'_{pt} I_s N'_{ct} t\cos\theta$. Substituting these factors in eq (4), the percentage registration of the test watthour meter is

$$\mathscr{R}_t=100\frac{K_t n_t}{E_s N'_{pt} I_s N'_{ct} t\cos\theta}. \quad (17)$$

Now consider the energy measured by the Standard Watthour Meter. Since the percentage registration of the Standard Watthour Meter is known, and the indicated energy is $K_s n_s$, then the true energy measured by the Standard Watthour Meter is

$$\frac{100K_s n_s}{\mathscr{R}_s}=E_s I_s t\cos\theta_s \quad (18)$$

or

$$\frac{1}{E_s I_s t}=\frac{\mathscr{R}_s\cos\theta_s}{100K_s n_s} \quad (19)$$

and substituting eq (19) in eq (17)

$$\mathscr{R}_t=\frac{K_t n_t \mathscr{R}_s}{K_s N'_{pt} N'_{ct} n_s}\frac{\cos\theta_s}{\cos\theta}. \quad (20)$$

In this equation $\cos \theta_s/\cos \theta$ is a correction factor for the phase angles of the current and voltage transformers. To simplify this correction the denominator may be expanded

$$\frac{\cos \theta_s}{\cos (\theta_s+\beta-\gamma)} = \frac{\cos \theta_s}{\cos \theta_s \cos (\beta-\gamma) - \sin \theta_s \sin (\beta-\gamma)}. \tag{21}$$

Dividing both numerator and denominator by $\cos \theta_s$ the correction factor becomes

$$\frac{1}{\cos (\beta-\gamma) - \sin (\beta-\gamma) \tan \theta_s}. \tag{22}$$

Since $(\beta-\gamma)$ is a small angle, $\cos (\beta-\gamma)$ is very nearly 1 and $\sin (\beta-\gamma)$ is very nearly $(\beta-\gamma)$, hence the correction factor is

$$\frac{1}{1-(\beta-\gamma) \tan \theta_s} \tag{23}$$

and when the indicated division is performed, neglecting the extremely small second-order terms, the result is

$$1+(\beta-\gamma) \tan \theta_s. \tag{24}$$

Thus the correction term for the phase angle in parts per unit is $c_\varphi=(\beta-\gamma) \tan \theta_s$, and when the correction terms for the current transformer ratio, potential transformer ratio, and phase angles are shown, the final form of eq (20) is that of eq (3) in part 3.3.

Washington, March 5, 1954.

Mass Spectra of the Deuteroethylenes

Vernon H. Dibeler, Fred L. Mohler, and M. de Hemptinne [1]

Samples of all of the deuteroethylenes have become available in satisfactory purity, and mass spectra have been measured and corrected for isotopic impurities. The mass spectra of *cis* and *trans* dideuteroethylene are nearly identical, and the spectrum of the asymmetrical dideuteroethylene is similar to the symmetrical molecules in the mass range 24 to 30. The probability of removing an H atom from the deuteroethylenes relative to the probability in C_2H_4 is equal to the a priori probability times 1.10, $(1.10)^2$, and $(1.10)^3$ in molecules containing 1, 2, and 3 D atoms, and the relative probability of removing a D atom is 0.90 in C_2D_4 and is nearly equal to the a priori probability times $(0.90)^2$, $(0.90)^3$, and $(0.90)^4$ in molecules C_2HD_3, $C_2H_2D_2$, and C_2H_3D, respectively. As the factors 1.10 and 0.90 are nearly reciprocals, these ratios can be expressed as positive and negative powers of 1.10. The probabilities of removing 2, 3, or 4 atoms are powers or products of the probability of removing single atoms, and thus are also positive and negative powers of 1.10. Similar relations are found in the previously published data on deuteroacetylenes.

1. Introduction

Studies of the mass spectra of hydrocarbon molecules containing one or more deuterum atoms have shown that in the case of paraffins [1 to 5][2] and simple unsaturated molecules [6, 7] the relative probabilities for dissociating hydrogenic atoms from the deuterated molecule relative to the ordinary molecule are not predictable from a priori possibilities alone. In a molecule containing both protium and deuterium, the probability of removing H atoms is increased, and that of removing D atoms is decreased as compared with removing H from the ordinary compound. Schissler, Thompson, and Turkevich [5] describe this by using two parameters, *a* and *b*, which give the relative probabilities of removing H and D from the deuterated compound as compared with removing H from the ordinary compound.

Unfortunately these parameters are different for different compounds and also for the same chemical compound containing different numbers of D atoms. At the present time there is no general theoretical basis for predicting the spectra of deuterated compounds, and the complexity of the problem increases rapidly with the number of carbon and hydrogen atoms in the molecule. For this reason, the availability of samples of all the possible deuterated ethylenes afforded an exceptional opportunity to study the mass spectra of these compounds. The data are useful not only for analytical applications but also to supply additional information on the relation between dissociation probabilities and isotopic structure.

2. Experimental Details

Mass spectra were obtained with a Consolidated 21-103 mass spectrometer. The electron energy was nominally 70 v, with an anode current of 10.5 μa. The temperature of the ion source was maintained at 250° C. The energy filter at the collector end was grounded to permit ions resulting from metastable transitions to reach the collector. Other procedures for introducing the samples and obtaining the spectra were conventional.

The ethylene was Phillips Research Grade with a minimum purity of 99.77 mole percent as stated by the manufacturer.

The deuteroethylenes, C_2H_3D, C_2D_3H, and C_2D_4, were prepared by the same general methods described briefly by de Hemptinne, Jungers, and Delfosse [8] and in greater detail by de Hemptinne [9]; i. e., the photochemical addition of hydrogen bromide to acetylene and vinyl bromide. The reactions are briefly summarized as:

$$\left.\begin{array}{l} HC{\equiv}CH + HBr \rightarrow H_2C{=}CHBr \\ DC{\equiv}CD + HBr \rightarrow HDC{=}CDBr \\ DC{\equiv}CD + DBr \rightarrow D_2C{=}CDBr \end{array}\right\} + DBr \rightarrow$$

$$\left.\begin{array}{l} H_2BrC{-}CHDBr \\ HDBrC{-}CD_2Br \\ D_2BrC{-}CD_2Br \end{array}\right\} + Zn \rightarrow \left\{\begin{array}{l} H_2C{=}CHD \\ HDC{=}CD_2 \\ D_2C{=}CD_2 \end{array}\right.$$

Bryce L. Crawford, Jr. of the University of Minnesota very kindly provided a sample of 1,1-dideuteroethylene. The 1,*trans*-2-dideuteroethylene and 1,*cis*-2-dideuteroethylene were part of several samples [10] analyzed for B. S. Rabinovitch of the University of Washington.

As the minimum energy required to form the $C_2H_3^+$ ion in ethylene is 3.3 ev greater than that required to ionize the molecule [11], the isotopic purity of the deuteroethylenes was determined by using low-energy electrons in a manner similar to that described by Stevenson and Wagner [12] for deuteroparaffins. Corrections for deuteroethylene impurities were made by using successively corrected patterns. Traces of ethanes were observed in some of the samples, but these did not interfere in the low-voltage measurements. Corrections for the contributions of ethanes were made on the basis of patterns computed on a statistical basis, neglecting the *a* and *b* factors defined above. The measured isotopic purity of the deuteroethylenes was as follows: C_2H_3D, 95 percent; 1,1-$C_2H_2D_2$, 88 percent;

[1] University of Louvain, Belgium.
[2] Figures in brackets indicate the literature references at the end of this paper.

1,*trans*-2-$C_2H_2D_2$, 97 percent 1,*cis*-2-$C_2H_2D_2$, 99 percent; C_2HD_3, 87 percent, C_2D_4, 94 percent.

3. Results

The principal ions in the mass spectra of ethylene and five deuteroethylenes are given in table 1. The relative abundances are tabulated in the conventional manner after correcting for the contributions of ions containing C^{13} in natural abundance. The spectrum of the 1,*cis*-2-dideuteroethylene is very similar to that of the *trans* isomer and accordingly is omitted from the table. Also omitted are ions with non-integral values of *m/e*. These "metastable transition" peaks, observed in all of the ethylenes, result from a delay of the order of microseconds in the dissociation of two hydrogenic atoms from the molecule ion. The abundances relative to the molecule ion are about 0.1 percent or less, and in general increase somewhat with increased deuterium substitution.

The total ion abundances of the hydrogen group, Σi_H^+, the C_1 group, $\Sigma i_{C_1}^+$, and the C_2 group, $\Sigma i_{C_2}^+$, are given for each molecule at the bottom of the appropriate column. The measured sensitivity (ion current per unit of pressure) of the molecule ion was the same for all of the ethylenes within the estimated error in pressure measurement (about 2%).

TABLE 1. *Principal ions in the mass spectra of ethylene and deuteroethylenes for 70-v electrons*

m/e	C_2H_4	C_2H_3D	1,1-$C_2H_2D_2$	1,*trans*-2-$C_2H_2D_2$	C_2HD_3	C_2D_4
1	6.71	5.81	3.81	3.66	2.10	
2	0.88	1.17	1.70	1.67	2.47	3.78
3	.....	0.26	0.42	0.45	0.26	
4	.....	.....	.14	.09	.26	0.64
12	3.17	3.31	3.58	3.33	3.61	3.78
13	4.68	3.34	2.58	1.76	0.97	.....
13.5	0.38	0.17	0.11	0.06	.04	.....
14	7.83	5.72	6.18	4.63	4.98	6.26
14.5	.....	0.28	0.25	0.22	0.22	.....
15	0.61	4.38	1.16	8.19	4.05	0.47
15.5	.....	.....	.....	.....	0.32	.....
16	.....	0.42	4.85	0.46	5.13	10.2
17	.....	.....	0.34	.14	0.28	.....
18	.....	.....	.....	.....	.....	<0.1
24	4.62	4.15	3.75	3.70	3.35	3.04
25	13.5	7.65	4.03	4.07	1.70	.....
26	67.5	31.0	15.0	15.5	9.79	10.4
27	67.9	50.6	42.6	41.5	25.8	.....
28	100.0	55.6	39.9	41.6	38.2	63.7
29	.....	100.0	41.9	40.0	40.8	.....
30	.....	.....	100.0	100.0	22.7	60.8
31	.....	.....	.....	.....	100.0	.....
32	.....	.....	.....	.....	.....	100.0
Σi_H^+	7.89	7.24	6.07	5.87	5.09	4.42
$\Sigma i_{C_1}^+$	16.3	17.2	18.7	17.9	19.0	20.2
$\Sigma i_{C_2}^+$	253.5	249.0	247.2	246.4	242.3	237.9

3.1. C_2-Group Ions

Two different fragments containing H and D atoms contribute to some of the mass peaks in the C_2 group of the monodeutero- and the dideuteroethylenes. In order to determine the relative probabilities of dissociating two or more protium atoms and one or more deuterium atoms from these molecules, some assumption must be made concerning the relative amounts of the contributing ions. No assumption need be made in the spectrum of C_2D_3, as each of the ion peaks has only one possible configuration.

In the computation of the deuteromethane spectra, the authors assumed that the probability of removing one atom, either H or D, from the deutero compounds was equal to the probability of removing H from CH_4, and similarly for removing 2, 3, or 4 atoms. This cannot be rigorously true for the ethylenes, for it is seen in table 1 that $\Sigma i_{C_2}^+$ decreases regularly with increasing deuterium substitution. It seems reasonable to assume that each of the terms involved in this sum decreases regularly. This is seen to be the case for the loss of four atoms to give C_2^+. The ratio of relative intensities of C_2^+ of C_2H_3D to C_2^+ of C_2H_4 is 0.898; the ratio of C_2^+ of $C_2H_2D_2$ (mean of the values of columns 4 and 5 of table 1) to C_2^+ of C_2H_4 is 0.807; the ratio for C_2HD_3 is 0.725, and for C_2D_4 is 0.658. These four ratios are almost exactly equal to 0.898, $(0.898)^2$, $(0.898)^3$, and $(0.898)^4$.

TABLE 2. *Correction factors necessary to calculate the modified monoisotopic spectra of the deuteroethylenes from ordinary ethylene*

Ion	C_2H_4	C_2H_3D	$C_2H_2D_2$ (average)	C_2HD_3	C_2D_4
C_2	1	.....	0.806	0.724	0.651
	.....	(0.898)	(0.807)	(0.725)	(0.658)
ΣC_2X*	1	0.937	0.878	0.823	.....
	.....	.....	.....	(0.851)	(0.770)
ΣC_2X_2	1	0.986	0.972	0.958	.....
	.....	.....	.....	(0.948)	(0.944)
ΣC_2X_3	1	0.973	0.946	0.920	.....
	.....	.....	.....	(0.935)	(0.895)

* X represents both H and D atoms.

The first row of table 2 gives these computed ratios, and in parentheses in the second row are the observed ratios. The relative probability of losing 3 atoms from C_2D_4 as compared with C_2H_4 is observed to be 0.770, and it is assumed that the ratio will be $(0.770)^{1/4}$, $(0.770)^{2/4}$, and $(0.770)^{3/4}$ in molecules containing 1, 2, and 3 D atoms. Similarly, from the ratio of the C_2D_4 values to the C_2H_4 values one can compute ratios for the loss of 2 and 1 hydrogenic atoms. These data are presented in table 2. In C_2HD_3 the values for these ratios are observed experimentally and are in satisfactory agreement with the computed values. In C_2D_3H and $C_2H_2D_2$ the computed ratios will be used as correction terms to derive from the C_2H_4 spectrum what might be called the "modified monoisotopic spectra."

The calculations for the individual dissociation probabilities in the C_2H_3D spectrum are illustrated in table 3. In column 2 the abundance of C_2^+ and C_2H^+ are the observed values from table 1. It is assumed that $[C_2H^+ + C_2D^+]$ is equal to the C_2H^+ abundance of C_2H_4 multiplied by the correction term from table 2, namely, $13.5 \times 0.937 = 12.65$. This value minus the observed abundance of C_2H^+ from column 2 (7.65) gives the abundance of C_2D^+ as 5.00. This value subtacted from the 26 peak of C_2H_2D,

3 (table 1), gives the abundance of $C_2H_2^+$ as 26.0. Subtracting this from the corrected abundance of C[illegible] of C_2H_4, namely, $67.5 \times 0.986 = 66.5$, gives 40.5 as the abundance of C_2HD^+. Continuing in this manner, a final value of 55.9 is calculated for $C_2H_2D^+$ as compared with the observed value of 55.6. This agreement is entirely satisfactory.

Columns 3 and 4 of table 3 give the a priori probabilities and the "a priori abundances" of ions of the C_2H_3D spectrum calculated from the C_2H_4 spectrum. These values are quite different from the observed abundances in column 2, and the ratios of the values in column 2 to the values in column 4 give the "weighting factors" of column 5.

TABLE 3. *Calculation of individual dissociation probabilities and isotope weighting factors for the* C_2 *group of* C_2H_3D

Positive ion	Relative abundance	A priori probability	A priori abundance from C_2H_4	Weighting factor
C_2	4.15	1	4.62	0.90
C_2H	7.65	$\frac{3}{8}$	10.1	.76
C_2D	5.00	$\frac{1}{4}$	3.38	1.48
C_2H_2	26.0	$\frac{1}{2}$	33.7$_5$	0.77
C_2HD	40.5	$\frac{1}{2}$	33.7$_5$	1.20
C_2H_3	10.1	$\frac{3}{4}$	17.0	0.60
C_2H_2D	55.6	$\frac{3}{4}$	50.9	1.09
C_2H_3D	100.0	.....	.....	.....

Weighting factors for the other deuteroethylenes have been computed in the same manner and are summarized in table 4. As the observed abundances for the C_2 group of ions of 1,1-dideuteroethylene and *cis* and *trans* 1,2-dideuteroethylene are nearly the same, the mean values of the abundances have been used to compute the weighting factors for the $C_2H_2D_2$ molecules. The last two observed weighting factors in each column correspond, respectively, to the b and a factors as defined by Schissler, Thompson, and Turkevich [5]. This notation has been used with subscripts 1 to 4 referring to the number of deuterium atoms in the molecule. As the factors a and b give the respective probabilities of removing one H or one D atom from the deuterium substituted molecule relative to the probability of removing H from C_2H_4, it has been commonly assumed that the probability of removing two or more hydrogenic atoms will involve the appropriate powers and products of the a and b factors. These powers and products of a's and b's are included in table 4. There is in most cases approximate agreement between computed and observed values. It should be noted that experimental errors are magnified in the product terms.

It is seen from table 4 that there is a very regular sequence in the values a_1, a_2, a_3, and b_1 to b_4 of the following type: $a_2 = a_1^2$, $a_3 = a_1^3$, $b_3 = b_4^3$, $b_2 = b_4^2$, $b_1 = b_4^4$. Values $a_1 = 1.10$ and $b_4 = 0.90$ give the best fit to the observed values of a_1, a_2, a_3, b_2, b_3, and b_4. As b_4 is nearly equal to the reciprocal of a_1, it is evident that positive and negative powers of a single constant can represent all seven a's and b's, and by the relations shown in table 4 can represent all 26 weighting factors. Table 5 is similar to table 4 but with powers of a single constant $K = 1.10$ in place of a's and b's. The agreement between observed and computed values is actually better than that found in table 4 based on seven observed weighting factors. It is to be noted that this reciprocal relationship between a and b factors results in the regular sequence that is observed in the intensity of C_2^+ as deuterium

TABLE 4. *Summary of the isotope weighting factors for the* C_2 *group of the deuteroethylenes*

Positive ion	C_2H_3D		$C_2H_2D_2$*		C_2HD_3		C_2D_4	
C_2	0.90	$a_1^3b_1 = 0.78$	0.81	$a_1^2b_1^2 = 0.77$	0.73	$a_1b_1^3 = 0.69$	0.66	$b_1^4 = 0.66$
C_2H	.76	$a_1^2b_1 = .71$	.60	$a_1b_1^2 = .64$	.50	$b_1^3 = .51$	.....	.....
C_2D	1.48	$a_1^2 = 1.30$	1.16	$a_1^2b_1 = 1.06$	.97	$a_1b_1^2 = .86$	.77	$b_4^4 = .73$
C_2H_2	0.77	$a_1b_1 = 0.66$	0.66	$b_1^2 = 0.53$	.....	.....	.....	.....
C_2HD	1.20	$a_1^2 = 1.19$	.94	$a_1b_1 = .88$	.76	$b_2^2 = .64$	.....	.....
C_2D_2	.....	.....	1.43	$a_2^2 = 1.45$	1.13	$a_2b_2 = 1.07$	.95	$b_4^2 = .81$
C_2H_3	0.60	$b_3 = 0.60$	.....	.....	.....	.....	.....	.....
C_2H_2D	1.09	$a_1 = 1.09$	0.73	$b_2 = 0.73$	.....	.....	.....	.....
C_2HD_2	.....	.....	1.21	$a_2 = 1.21$	0.80	$b_3 = 0.80$	.....	.....
C_2D_3	.....	.....	.....	.....	1.34	$a_3 = 1.34$	.90	$b_4 = .90$

*Mean values of 1,1- and 1,2-$C_2H_2D_2$

TABLE 5. *Isotope weighting factors for the deuteroethylenes compared with the powers of a singe constant,* $K = 1.10$

Positive ion	C_2H_3D		$C_2H_2D_2$		C_2HD_3		C_2D_4	
C_2	0.90	$K^{-1} = 0.91$	0.81	$K^{-2} = 0.83$	0.73	$K^{-3} = 0.75$	0.66	$K^{-4} = 0.69$
C_2H	.76	$K^{-2} = .83$	.60	$K^{-4} = .69$	.50	$K^{-6} = .57$	.....	.....
C_2D	1.48	$K^1 = 1.33$	1.16	$K^0 = 1.10$	.97	$K^{-1} = .91$	.77	$K^{-2} = .75$
C_2H_2	0.77	$K^{-2} = .75$	0.66	$K^{-4} = 0.57$	.....	.....	.....	.....
C_2HD	1.20	$K^1 = 1.21$	.94	$K^{-1} = .91$	.76	$K^{-4} = .69$	.....	.....
C_2D_2	.....	.....	1.43	$K^1 = 1.47$	1.13	$K = 1.10$	.95	$K^{-2} = .83$
C_2H_3	0.60	$K^{-4} = 0.69$	.....	.....	.....	.....	.....	.....
C_2H_2D	1.09	$K = 1.10$	0.73	$K^{-2} = 0.75$	0.80	$K^{-2} = 0.83$	.....	.....
C_2HD_2	.....	.....	1.21	$K^1 = 1.21$	1.34	$K^3 = 1.33$	.....	.....
C_2D_3	.....	.....	.....	.....	.....	.....	.90	$K^{-1} = .91$

atoms are added to the molecule. This supports the assumptions used to compute the correction factors in table 2.

These relations can be expressed in terms of one equation containing only one arbitrary constant. The relative probability, $R_{l,m,n}$ of removing l H atoms and m D atoms from an ethylene molecule containing n D atoms and $(4-n)$ H atoms as compared with the probability of removing H from C_2H_4 is

$$R_{l,m,n} = A_{l,m,n} K^{[ln+m(n-5)]}$$

where $A_{l,m,n}$ is the a priori probability.

3.2. Ions in the Mass Range 1 to 18

The more abundant ions in the m/e range 12 to 18 are C^+, CH^+, and CH_2^+, or ions with one or two D atoms instead of H atoms. There are no significant differences in the spectra of *cis* and *trans* 1,2-$C_2H_2D_2$. The larger peaks in the spectra of 1,1-$C_2H_2D_2$ and 1,2-$C_2H_2D_2$ differ in a manner that is consistent with their structure. In the former compound, CH_2^+ and CD_2^+ are large, and in the latter, CHD^+ is the largest peak. However, a small peak at mass 15 in the spectrum of 1,1-$C_2H_2D_2$ must be in large part CHD^+, ($C_2H_2D_2^{++}$ accounts for only a small fraction of the observed intensity). The peak at mass 16 in the spectrum of 1,2-$C_2H_2D_2$ is not necessarily CD_2^+, for an ion CH_2D is also to be expected. Ionization processes involving rearrangements of atoms complicate the interpretation of the spectra in this mass range, and a quantitative determination of weighting factors will not be attempted.

The following ions containing three hydrogenic atoms can be identified in spectra of table 1: CH_3^+ of C_2H_4, CH_2D^+ of C_2H_3D, and CHD_2^+ from the $C_2H_2D_2$ molecules and from C_2HD_3. Other possible ions of this class are masked by other isomeric ions. A small H_2O background may mask CD_3^+ ions of C_2HD_3 and C_2D_4.

Doubly charged ions of half-integer mass number can be identified as follows: $C_2H_3^{++}$ of C_2H_4, $C_2H_3D^{++}$ of C_2H_3D, $C_2HD_2^{++}$ and C_2HD^{++} of $C_2H_2D_2$, and $C_2HD_3^{++}$, $C_2HD_2^{++}$, and C_2HD^{++} of C_2HD_3. This indicates that doubly charged ions containing 2, 3, and 4 hydrogenic atoms are present in all the spectra, with the ions of even molecular weight masked by singly charged ions.

It is apparent from table 1 that the relative abundance of the C^+ ions increases as the number of D atoms in the molecule increases, in contrast to the variation of C_2^+ ions with increasing deuterium content. If an average value of 3.45 is taken for the C^+ ions of the $C_2H_2D_2$ molecules, then the abundance of C^+ from the deuterated molecules is $(1.043)^x$ times the abundance of C^+ from C_2H_4 where x is the number of D atoms in the molecule.

The sum of the hydrogenic ions decreases progressively from C_2H_4 to C_2D_4 as the number of D atoms increases, but this decrease is not accurately represented by a power sequence. Weighting factors computed for H^+ ions (observed abundances divided by H^+ of C_2H_4 times the *a priori* probability of removing H atoms) are 1.15, 1.13, and 1.25 for C_2H_3D, $C_2H_2D_2$ (mean value), and C_2HD_3, respectively. Weighting factors for D^+ are 0.49 for C_2HD_3 and 0.56 for C_2D_4. H_2^+ makes a contribution to the mass 2 peak of C_2H_3D and $C_2H_2D_2$, and this cannot be accurately evaluated. The weighting factor for producing D^+ is somewhat less than 0.50 for $C_2H_2D_2$ and probably less than 0.5 for C_2H_3D. The data do not show any regular trend in weighting factors such as is found for the C_2 group of ions.

It is of interest that the ion HD^+ has about the same relative abundance in the different $C_2H_2D_2$ molecules. That is, the abundance is the same whether or not the two deuterium atoms are on the same carbon atom.

4. Discussion

Delfosse and Hipple [6] have previously published the mass spectrum of a *cis-trans* mixture of 1,2-$C_2H_2D_2$. The relative intensities of the $C_2H_2D_2$ and C_2H_4 spectra reported by them are entirely consistent with the results obtained in this research.

An interesting and unexpected feature of the experimental results is that in the C_2 mass range there is no appreciable difference between the mass spectra of 1,1-$C_2H_2D_2$ and *cis* and *trans* 1,2-$C_2H_2D_2$. The weighting factors remain the same whether there are two D atoms on one carbon atom or one on each carbon atom. Appearance potential measurements [11] indicate that production of $C_2H_2^+$ from C_2H_4 involves the production of H_2 rather than atoms of hydrogen, and H_2 is also formed when 3 or 4 H atoms are removed. The present results suggest that the hydrogenic molecule is formed with equal probability whether the two atoms are on the same carbon atom or not. This cannot be explained by the assumption of complete mixing of H and D atoms in the ionization process, for the fragment ions in the C_1 range reflect the molecular structures. There is some rearrangement of hydrogenic atoms, but it is relatively unimportant.

The progressive increase in C^+ and Σi_{C_1} with increasing number of D atoms in the molecule is in marked contrast to the decrease of C_2^+ and Σi_{C_2} as the number of D atoms increases. This interesting difference is not entirely unexpected, as Stevenson and Wagner [4] discuss in a general way the theoretical basis for two opposing effects of heavy isotopes on the probability of dissociation.

The analysis of the data in the C_2 range of the deuteroethylenes as given in tables 4 and 5 shows a very striking relationship between the "weighting factors" for removal of H and D and the number of D atoms in the molecule. The powers of a single constant assigned according to a definite system or pattern account for all 26 weighting factors, at least to a fairly good approximation. A relationship of this kind might be expected in other deuterated hydrocarbons. The only clear case of such a relationship among the molecules already studied is acetylene.

A previous publication [7] gives the mass spectra of C_2H_2, C_2HD, and C_2D_2, and from these data the weighting factors given in table 6 for dissociation of H and D have been computed as in table 3 for the

ethylenes. The table shows that powers of a single constant $K=1.13$ represent quite accurately the five weighting factors. The weighting factors for dissociation of H, D, HD, and D_2 from the acetylenes C_2HD and C_2D_2 are related in the same way as they are in the ethylenes $C_2H_2D_2$ and C_2D_4, except that the constant is 1.13 in the acetylenes and 1.10 in the ethylenes.

TABLE 6. *Acetylene weighting factors compared with powers of* $K=1.13$

	C_2HD		C_2D_2	
C_2	0.86	$K^{-1}=0.88$	0.79	$K^{-2}=0.78$
C^2H	.67	$K^{-2}=.69$	----	----
C^2D	1.28	$K^{2}=1.28$	.86	$K^{-1}=.88$

Schissler, Thompson, and Turkevich [5] have found that there is a roughly linear relation between the weighting factors for removing H and D from the methanes and the number of D atoms in the molecule. They report values for the *a* factor as 1.23, 1.48, and 1.80 in molecules containing 1, 2, and 3 D atoms. These *a* factors can be quite accurately represented as 1.22, $(1.22)^2=1.49$, and $(1.22)^3=1.81$, corresponding to the relation found in the ethylenes. However, the *b* factors apparently are not related to each other and to the *a* factors as they are in the ethylenes. It is to be noted that the researches of two of the authors [3] and of Schissler et al. [15] on the deuteromethanes are not in good agreement, and in the opinion of the authors the isotopic purity and the isotopic analyses leave much to be desired in both researches. The deuteromethane spectra deserve further research when compounds of better isotopic purity become available. Obviously the computation of weighting factors depends rather critically on the isotopic purity of the mass spectra.

5. References

[1] M. W. Evans, N. Bauer, and J. Y. Beach, J. Chem. Phys. **14,** 701 (1946).
[2] J. Turkevich et al., J. Am. Chem. Soc. **70,** 2638 (1948).
[3] V. H. Dibeler and F. L. Mohler, J. Research NBS **45,** 441 (1950) RP2155.
[4] D. P. Stevenson and C. D. Wagner, J. Chem. Phys. **19,** 11 (1951).
[5] D. O. Schissler, S. O. Thompson, and J. Turkevich, Discussions Faraday Soc. **10,** 46 (1951).
[6] J. Delfosse and J. A. Hipple, Phys. Rev. **54,** 1060 (1938).
[7] F. L. Mohler and V. H. Dibeler, Phys. Rev. **72,** 158 (1947); F. L. Mohler et al., J. Research NBS **48,** 188 (1952) RP2304.
[8] M. de Hemptinne, J. Jungers, and J. M. Delfosse, J. Chem. Phys. **6,** 319 (1938).
[9] M. de Hemptinne, Les isotopes, 7ième Conseil de chimie Solvay, p. 262 (1948).
[10] J. E. Douglas and B. S. Rabinovitch, J. Am. Chem. Soc. **74,** 2486 (1952).
[11] P. Kusch, A. Hustrulid, and J. T. Tate, Phys. Rev. **52,** 843 (1937).
[12] D. P. Stevenson and C. D. Wagner, J. Am. Chem. Soc. **72,** 5612 (1952).

WASHINGTON, March 16, 1954.

Journal of Research of the National Bureau of Standards Vol. 53, No. 2, August 1954 Research Paper 2523

Spectral Distribution of Energy From the Sun

Ralph Stair, Russell G. Johnston, and Thomas C. Bagg

Measurements on the spectral energy distribution of direct solar radiation, made in July 1953, at Sacramento Peak, New Mexico, altitude 9,200 feet are described. Spectral data are given for wavelengths extending from 299 to 535 millimicrons for air masses 0, 1.0, 2.0, and 3.0. A determination of atmospheric transmittance as a function of wavelength results in calculated total amounts of ozone approximating 0.21 centimeter (ntp) as a mean for 4 days during July. Preliminary measurements, employing a lead sulfide photoconducting cell, in the visible and infrared spectrum are discussed. On the basis of the spectral ultraviolet data obtained, an estimate of a value slightly exceeding 2.00 langleys per minute for the solar constant is indicated.

1. Introduction

Measurements on the spectral distribution of the ultraviolet radiant energy from the sun obtained at Climax, Colo. in September 1951 [1][1] indicated appreciable higher intensities outside the earth's atmosphere than had been reported previously. This was not only of some concern to the authors but also of interest to others. Data on the transmittance of radiant energy through the atmosphere—to which the methods and results of the measurement of solar energy contribute—are important to the work of the Air Force Cambridge Research Center.[2] It has a bearing on a more precise evaluation of the solar constant. This common interest resulted in plans to repeat the measurements under conditions that should be more favorable. Through the courtesy of John W. Evans, director, the Sacramento Peak Observatory was made available for this work during late June and early July of the summer of 1953.

Sacramento Peak is located on the east edge of the New Mexico-White Sands desert area. This station was established by Harvard University after an extensive survey had shown it to be one of the more promising locations in the southwest for use in the study of solar radiation. It is located at an altitude of 9,200 feet within a forest of Ponderosa pine and Douglas fir on a relatively level area of possibly 100 acres. Because this location is not the highest within the region, some of the summer thunderstorms and associated cloudiness miss the observing station.

2. Instruments and Procedure

The instrumental arrangement for this work was similar to that employed at Climax [1]. However, not only was no single piece of equipment employed at Climax taken to Sacramento Peak, except for the type 935 phototube, but also even a new standard of spectral radiant energy independently calibrated was employed in the calibrations of the equipment.

The spectrometer employed was a double prism mirror instrument manufactured by Carl Leiss of Berlin, Germany. This instrument uses two 30° quartz prisms, through each of which the radiant energy makes a double pass. The collimating mirrors are of simple spherical design coated with aluminum. The slits are each manually adjustable. All three slits are straight, but being only 7 mm in length, little error is introduced thereby. Each slit was set at a width of 0.30 mm throughout the course of the investigation. Changes in wavelength were accomplished through the use of a synchronous-motor drive attached to the wavelength drum. This unit permits recording at any one of three speeds, forward or reverse. A built-in clutch allows quick resetting of the wavelength drum, so that any part of the spectrum may be repeated at will. As the calibrating factors are slightly different for the two directions of operation, all measurements were made with increasing wavelength. Cams are provided to stop the instrument automatically at either end of the wavelength range and to provide, by means of an auxiliary pen, wavelength marks at suitable positions (specific wavelengths through the spectrum) on the recorder chart.

The light beam was modulated at 510 c/s and the output of the phototube fed into a tuned amplifier of design similar to that previously employed [1, 2, 3]. A strip recorder was again used to plot automatically the spectral data.

A new heliostat, designed with mirrors larger than those in the Climax instrument, was employed in this work. It is of simple design, and arranged so that an aluminized primary plane mirror reflects the beam of light along the polar axis of the instrument. Micrometer adjustments permit accurate settings for declination, latitude, and for them corrections. A second mirror set in a stationary position reflects the light beam horizontally into the spectroradiometer. Thus each of the mirrors operated at fixed angles relative to the light beam during all hours of the day, so that corrections for light polarization could be easily made.

The entire equipment, except for the heliostat, was set up in the "Large Dome" building just inside

[1] Figures in brackets indicate the literature references at the end of this paper.

[2] This work was sponsored in part by the Air Force Cambridge Research Center.

one of the south windows and arranged so that the entrance slit of the spectroradiometer faced toward the south. The solar light beam was reflected through this window onto the axis of the spectroradiometer. Reference marks on the ceiling provided a guide in making adjustments of the heliostat and auxiliary reflecting mirror as the solar declination slowly changed from day to day during the course of the measurements.

The construction of the Large Dome building was such that the temperature variations within it were small during the course of the day. Most of the time the temperature was between 65° and 70° F, and usually the daily rise in temperature was not more than 5° F.

In accordance with the procedure in previous work [1, 3], no lens or mirror was employed to produce an image of the sun on the entrance slit of the spectroradiometer because an integrated solar energy spectrum was desired. This procedure is possible because of the large amount of energy available. It is furthermore desirable because of the simplicity of the reduction of the data through comparing readings on the sun directly with similar data taken on a standard tungsten-in-quartz lamp [4]. Figure 1 gives the spectral calibration factor for the complete instrument, based upon this standard of radiant energy. Other details connected with the reduction of the data may be found in the previous report [1].

Often the polarizing characteristics of a spectroradiometer are overlooked. These, however, may produce appreciable errors if not properly accounted for in the reduction of the data. Each mirror surface produces a definite and significant amount of polarization. If all the mirrors were held to the same positions during the experiment, no difficulty would arise. However, the heliostat mirror is rotated through nearly 180° during the course of the day from soon after sunrise to before sunset. This results in an appreciable variation in spectroradiometer transmittance because of polarization of the reflected light beam. The magnitude of this effect and the correction to be applied to the data are given in figure 2.

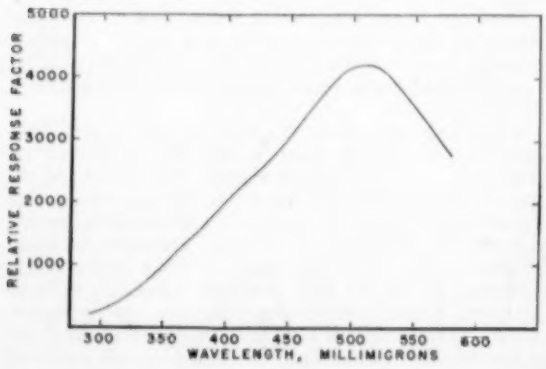

FIGURE 1. *Relative spectral-response factors for the complete spectroradiometer as employed in the Sacramento Peak measurements, by using a 935 phototube and with slit settings of 0.30 mm.*

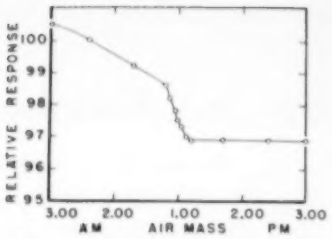

FIGURE 2. *Relative response of the complete equipment as affected by light polarization by the heliostat and spectrometer as a function of air mass during the New Mexico measurements.*

3. Ultraviolet Spectral Solar Energy Curve

Because the measurement of the solar spectral energy requires that the data be taken on the sun while it is moving to a higher or lower altitude, hence, to positions wherein the rays come through greater or lesser amounts of the atmosphere, the recorded spectra change in intensity and in spectral quality from minute to minute. Furthermore, any dust, water vapor, or other impurities within the atmosphere result in further intensity changes at the detector. Therefore, it is advantageous to make the measurements at high altitudes in a dry climate above much of the normal atmospheric contamination.

Data on the ultraviolet spectral radiant energy from the sun were taken on all clear days from the latter part of June until after July 10. Desert dust storms, together with rainy and cloudy weather, prevented measurements on part or all of many days during this period. However, on four days (July 4, 5, 9, and 10) the sky was exceptionally clear for part or most of the day. The data for these days have been reduced in a manner similar to that previously employed [1] and are tabulated in table 1 for air masses 0, 1.0, 2.0, and 3.0 at various wave lengths corresponding to minimum, maximum, or inflections in the Fraunhofer structure of the solar spectrum. Each of the values listed in columns 2 to 5, inclusive, was obtained as a mean representative of all the observations at those particular wave lengths for the days listed. The data for each of these wave lengths were extrapolated to air mass 0 in the determination of the solar-energy curve outside the earth's atmosphere. The values for the intermediate wave lengths were obtained by a method of interpolation based on the use of the best noontime observations. The spectral radiant intensities for air masses 1.00 and 0 are shown graphically in figure 3, and the integrated intensities for 5-mμ bands are tabulated in table 2. The data for air mass 1.00 represent a slight extrapolation because the lowest

TABLE I. *Spectral distribution of radiant energy from the sun for selected air masses, Sacramento Peak, N. Mex.*

Altitude 9,200 ft. Mean for 4 days in July 1953. Radiant energy in microwatts per square centimeter per 10 millimicrons.

1	2	3	4	5	6	7	8	9	10
Wavelength	July 4 Air mass 1.00	July 5 Air mass 1.00	July 9 Air mass 1.00	July 10 Air mass 1.00	Mean Air mass 1.00	M_0 factor	I_0 Air mass 0	Air mass 2.00	Air mass 3.00
mμ									
299			9.1		9.1	50	455	0.18	
299.5	24.0	21.2	19.4		21.5	45	968	48	0.01
302.5	42.8	39.0	35.0		39.0	20	780	1.95	.10
304	85.5	86.5	85.5	64.5	80.5	12	966	6.71	.56
306	120.4	115.2	121.9	108.1	116.4	7.8	908	14.9	1.91
309.2					205.6	5.5	1,131	37.4	6.80
310	176.6	187.9	178.0	174.5	179.3	5.1	914	35.2	6.89
312	310	303	325	287	306	4.3	1,316	71.2	16.5
314.9					340	3.4	1,156	100.0	29.4
315.8					372	3.2	1,190	116.3	36.3
316.5	323	334	346	330	333	3.1	1,032	107	34.7
317.9					463	2.92	1,352	159	54.3
318.5	424	424	435	401	421	2.85	1,200	148	51.8
321.1					523	2.59	1,355	202	78.0
321.7					495	2.53	1,252	196	77.3
322.8					479	2.43	1,164	197	81.1
323.5	445	451	463	431	448	2.40	1,075	187	77.8
325.5					548	2.26	1,238	242	107.3
327.5					706	2.18	1,539	324	148.6
328.5	679	703	708	679	692	2.15	1,488	322	149.7
330.3					778	2.09	1,626	372	178
331.5	684	710	736	689	705	2.05	1,445	344	168
332.9					708	2.02	1,430	351	174
333.6					696	2.00	1,392	348	174
335.3					727	1.97	1,432	369	187
337	604	607	616	592	605	1.94	1,174	312	161
340.8					745	1.87	1,393	398	213
341.7					717	1.86	1,334	385	207
343.5					730	1.84	1,343	397	216
345	612	628	660	600	625	1.82	1,138	343	189
348.6					676	1.78	1,203	380	213
351.5					759	1.75	1,328	434	248
352.6					718	1.74	1,249	413	237
355.1					798	1.72	1,373	464	270
358	616	617	636	569	609	1.70	1,035	358	211
360					751	1.68	1,262	447	266
361	723	748	723	715	727	1.67	1,214	435	261
363.8					779	1.65	1,285	472	286
367.1					907	1.62	1,469	560	346
368.6					876	1.61	1,410	544	338
371					879	1.59	1,398	553	348
375	710	717	750	701	720	1.56	1,123	462	296
379.4					989	1.53	1,513	646	422
380.7					903	1.52	1,373	594	391
385					619	1.49	922	415	279
387.7					767	1.47	1,127	522	355
391.5					985	1.45	1,428	679	468
394	660	701	691	670	680	1.44	979	472	328
396.1					914	1.43	1,307	639	447
397					878	1.42	1,247	618	435
403.3					1,456	1.39	2,024	1,047	754
406	1,381	1,423	1,452	1,381	1,409	1.38	1,944	1,021	740
410					1,441	1.36	1,960	1,060	779
416.8					1,517	1.34	2,033	1,132	845
421					1,525	1.32	2,013	1,155	875
424					1,502	1.31	1,968	1,147	875
428	1,279	1,297	1,330	1,262	1,292	1.31	1,693	986	753
432					1,463	1.30	1,902	1,125	866
436	1,560	1,578	1,627	1,545	1,578	1.29	2,036	1,223	948
441					1,724	1.275	2,198	1,352	1,061
477	1,814	1,835	1,869	1,785	1,826	1.26	2,301	1,449	1,150
455.7					1,864	1.24	2,311	1,503	1,212
468	1,668	1,676	1,727	1,657	1,682	1.23	2,069	1,367	1,112
482					1,721	1.21	2,082	1,422	1,175
487	1,529	1,543	1,556	1,526	1,539	1.21	1,862	1,272	1,051
497					1,647	1.20	1,976	1,372	1,144
500	1,605	1,601	1,631	1,598	1,609	1.195	1,923	1,346	1,127
509					1,678	1.185	1,988	1,416	1,195
520	1,613	1,635	1,636	1,594	1,620	1.18	1,912	1,373	1,163
526					1,687	1.175	1,982	1,436	1,222
530	1,723	1,731	1,701	1,702	1,714	1.17	2,005	1,465	1,252
535					1,716	1.165	1,999	1,473	1,264

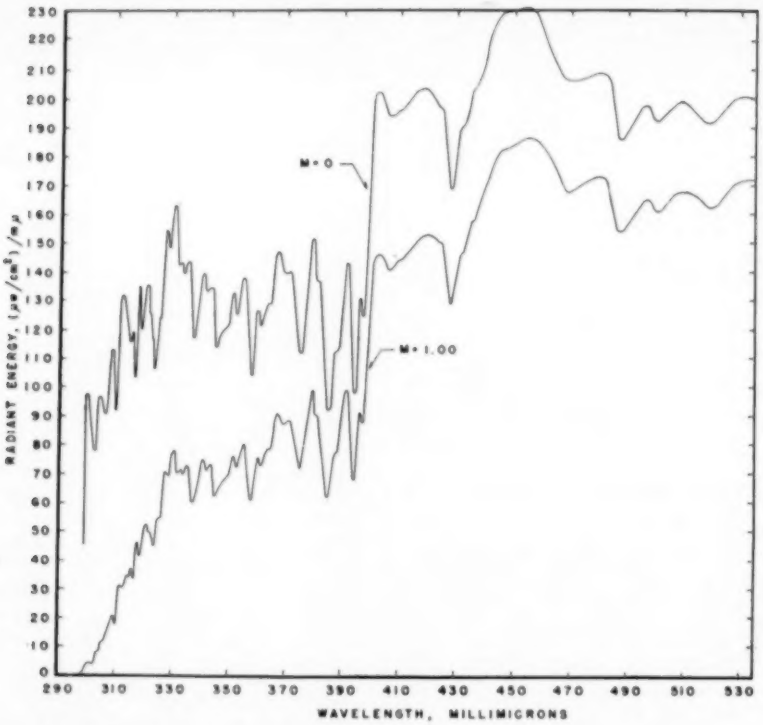

FIGURE 3. *Spectral distribution of radiant energy from the sun, based on the measurements for 4 days in July 1953, Sacramento Peak, N. Mex., altitude 9,200 feet.*

TABLE 2. *Integrated spectral distribution of radiant energy from the sun for air masses 0 and 1.00*

Evaluation made from data of table 1. Radiant energy is expressed in microwatts per square centimeter for 5 mμ bands.

1	2	3	1	2	3
Center of wavelength interval	Air mass 1.00	Air mass 0	Center of wavelength interval	Air mass 1.00	Air mass 0
mμ			mμ		
302.5	27	447	427.5	676	888
307.5	78	503	432.5	740	958
312.5	148	606	437.5	808	1,034
317.5	205	598	442.5	884	1,119
322.5	250	605	447.5	915	1,151
327.5	331	725	452.5	927	1,157
332.5	360	732	457.5	926	1,142
337.5	329	646	462.5	893	1,088
342.5	357	657	467.5	848	1,033
347.5	329	595	472.5	845	1,034
352.5	374	654	477.5	863	1,041
357.5	345	594	482.5	849	1,033
362.5	379	629	487.5	775	942
367.5	439	710	492.5	799	962
372.5	410	645	497.5	817	979
377.5	435	671	502.5	811	970
382.5	391	595	507.5	836	991
387.5	376	553	512.5	836	982
392.5	419	604	517.5	815	958
397.5	498	705	522.5	822	970
402.5	723	1,004	527.5	850	997
407.5	710	974	532.5	859	1,002
412.5	733	993			
417.5	760	1,016			
422.5	757	985			

air mass actually encountered during the course of the measurements was approximately 1.01 at apparent noon.

If a comparison is made between these data and those for Climax, Colo., in September 1951, it should be in terms of the data for air mass 0 because for larger air masses the data are not directly comparable as there is an altitude difference between the two stations. This difference in air masses results in slightly different magnitudes of Rayleigh scattering. In general, the two sets of data are in agreement within about 5 percent, the new values being slightly higher in the visible spectrum but slightly lower for wavelengths shorter than about 330 mμ. Agreement is close between about 330 and 400 mμ. As the two sets of data were obtained at different locations and at different seasons of the year with different spectroradiometric equipment independently calibrated, it is felt that the results are accurate within the limits of the experimental variations indicated in the tabulated data for the various days covered by the observations in the two cases. However, as the later data were obtained during July, a correction (3.4%) was necessarily required to reduce them to the mean solar distance. As the sun was at approximately the mean solar distance when the September 1951 data were obtained, no correction was required in that case.

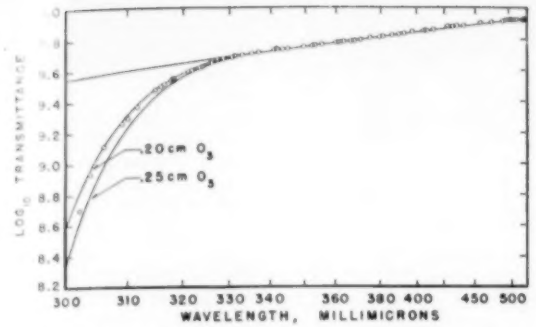

FIGURE 4. *Atmospheric transmittance at Sacramento Peak, N. Mex., altitude 9,200 feet; also determination of total ozone above the observing station.*

Upper curve, scattering; lower curves, ozone; circles, atmospheric transmittance; air mass, 1.00; wavelength scale as a function of $-(\mu-1)^2\lambda^{-4}$.

4. Atmospheric Transmittance and Ozone

Following the same procedures employed in the previous publication [1], the atmospheric transmission curve for Sacramento Peak, N. Mex., depicted in figure 4, was determined on the basis of the average of the data for the 4 days (July 4, 5, 9, and 10) given in table 1. In this illustration the logarithms of the observed transmittances of unit atmosphere for the different wavelengths are plotted as a function of the wavelength, which in turn is expanded [5] according to the funcion $-(\mu-1)^2\lambda^{-4}$ of the Rayleigh law of molecular scattering,

$$\log T_R = -\frac{32\pi^3(\mu-1)^2 H \log e}{3N\lambda^4},$$

in which λ is the wavelength of the radiant energy, and μ is the index of refraction of the atmosphere. As the atmospheric depth, H, and the molecular density, N, for the zenith position are constant, the resulting plot of the logarithm of the atmospheric transmittances becomes a straight line in those spectral regions wherein the Rayleigh law of pure scattering is applicable.

Again, the data given by Fabry and Buisson [6] were employed in the calculation of the two curves (fig. 4) representing amounts of ozone required for a similar amount of optical absorption. On the basis of these data, about 0.21 cm of ozone (ntp) was present from July 4 to July 10 at Sacramento Peak, N. Mex. This is in good agreement with previous measurements for the same season of the year for a similar latitude [7].

5. Preliminary Measurements of the Spectral Solar Radiation Between 500 and 2,500 Millimicrons

Although July weather at Sacramento Peak is not especially suitable for the study of the solar spectrum, especially in the infrared region, an opportunity was afforded on several days to make some preliminary measurements by the substitution of a lead sulfide cell for the 935 phototube. Otherwise, the spectroradiometric and recording equipment was unchanged.

Among the interesting results of this preliminary work, it was found that the PbS cell was sufficiently sensitive for use in the ultraviolet (down to about 310 mμ) and visible regions of the solar spectrum, as well as in the infrared out to about 2,500 mμ. Large changes in the water-vapor absorption bands indicated the high sensitivity of this equipment and its possible great usefulness in water-vapor studies or for the routine recording of the total water content of the atmosphere. On some days a doubling of the total atmospheric water vapor occurred within a matter of minutes. Generally, on the days on which observations were made, the water vapor increased rapidly until the sky was clouded over.

Figure 5 shows some typical recorder records extending from the ultraviolet to about 2,500 mμ in the infrared. No attempt has been made, however, to evaluate these records for spectral radiant energy. Although comparative data were taken with the tungsten-in-quartz lamp, the large variations in the over-all photoelectric sensitivity, together with a lack of precise knowledge of the spectral-energy distribution of the lamp standard, preclude the precise evaluation of these data. Also, the large variations in atmospheric water vapor during the course of the measurements rule out any extrapolation to zero air mass within those parts of the spectrum in which water-vapor absorption is pronounced. The data are given simply to illustrate what may be accomplished in this field under the proper conditions, namely, with a detector standardized for sensitivity (may be temperature controlled), in a relatively dry atmosphere (at least at nearly constant humidity), and with a suitable standard of spectral radiant energy. These requirements should exact little difficulty of fulfillment. The first can be met through a careful study and/or selection of the detector employed, the second through proper choice of the season of the year for the particular station, and the third through planned research on emissivities of a suitable lamp standard.

In connection with the study of atmospheric water vapor, changes in the optical absorption of the band located near 1,900 mμ is of especial interest. This band is broad, due to the relatively very high absorption for water vapor that occurs at this wavelength. As dispersed by a quartz-prism instrument, this band shows sufficient structure to make its use suitable over a considerable range of humidity values. However, for very high humidities one of the other water bands would be found more suitable for calibration purposes. In figure 6 the general absorption pattern of the 1,900-mμ water band is shown for a number of times during the morning of July 14. It is to be noted, that, although the air mass was decreasing during the course of these measurements, the absorption character within this band shows that the amount of water vapor in the solar beam was actually increasing between about

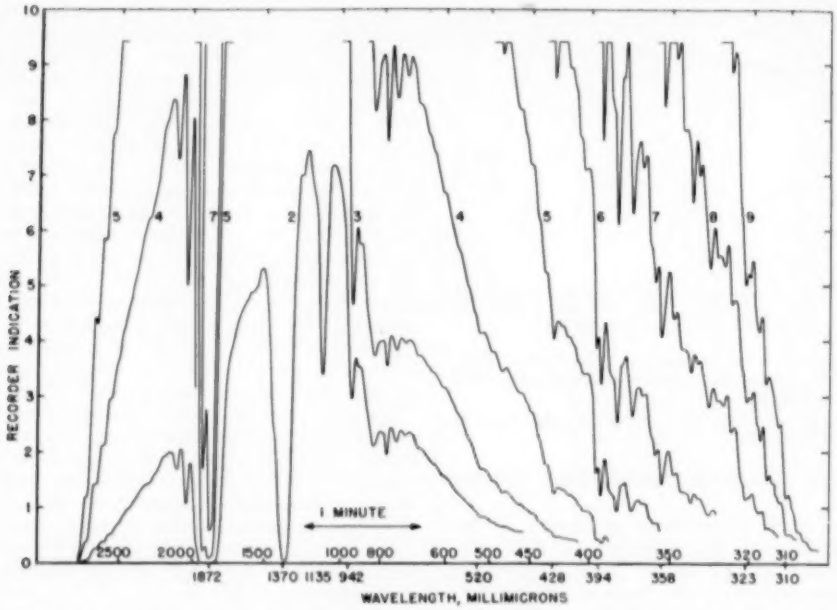

FIGURE 5. *Representative data taken from a section of the recorder chart while employing the PbS cell as detector.*

July 15, 1953, approximately 10:00 a. m. The numbers on the chart refer to amplifier sensitivity settings. The data illustrated cover a recording time of approximately 18 minutes.

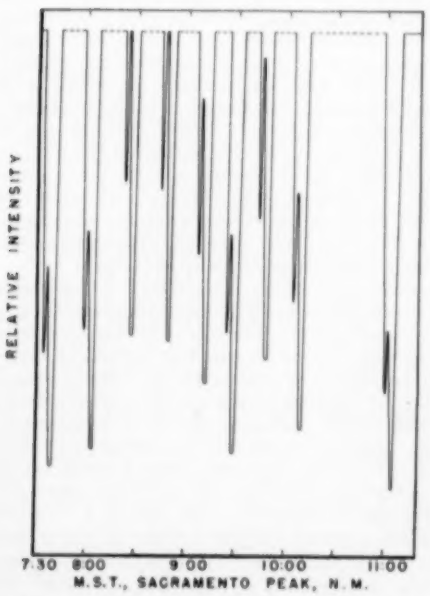

FIGURE 6. *Recorder tracings for the water-vapor absorption within the 1,900-mμ band during the morning of July 14.*

See curve 7 of figure 5 for similar data at 10:00 a. m. on July 15.

8:30 and 11:00 a. m. When correction for path-length through the atmosphere is made, the true water vapor increase is even greater than indicated by the recorded data.

6. Present Status of the Solar Constant as Indicated by the Sacramento Peak Data

The solar constant, defined as the number of gram-calories per square centimeter (langleys) per minute received from the sun at mean solar distance, is a measure of the total radiant energy emitted by the sun, and hence is one of the primary constants of astrophysics. Little work toward the establishment of the value of this constant has been done by workers outside the Smithsonian Institution of Washington. Hence the generally accepted value of 1.946 langleys per minute is based primarily upon the work of C. G. Abbot and his associates [8, 9]. Although their work was outstanding in this field at that time, the current need of certain revisions has been suggested by Schatzman [10], Allen [11], Nicolet [12], Georgi [13], Houghton [14], and others. Two points have been noted wherein the published data may be in need of revision, namely, (a) the need for the establishment of a precise spectral radiant-energy distribution for the entire solar spectrum reaching the earth's surface, and (b) careful evaluation of the solar energy in the ultraviolet and infrared regions of the spectrum, which, because of absorption within the

sphere, does not penetrate to the earth's surface. The methods employed and the use of the data by the Smithsonian Institution observers did not require precise spectral-energy determinations. They were interested primarily in variations of the solar constant with time. Hence there remains a question regarding the magnitude of any ultraviolet or infrared corrections until precise spectral radiant-energy data are available.

The spectral solar-energy distribution within the range of 346 to 2,400 mμ (containing approximately 90 percent of the total solar radiant energy), as employed by the Smithsonian Institution, is generally accepted as being approximately correct. Also, the present measurements are in close agreement with these data within the spectral range of 400 to 500 mμ. In the ultraviolet spectrum, however, the New Mexico and Colorado measurements [1] indicate a considerably higher radiant-energy emission from the sun. It is estimated that with the use of these data, supplemented by new rocket data [15, 16] for the shorter wavelengths, together with a reevaluation of the infrared above 2,400 mμ, that the value of the solar constant will be found to be slightly above 2.00 langleys per minute.

7. Summary and Conclusions

From the data obtained, the spectral distribution of the radiant energy from the sun, between 299 and 535 mμ, has been determined for various air masses at the earth's surface (altitude 9,200 feet) and for outside the earth's atmosphere. The latter is in close agreement with data obtained at Climax, Colo., in 1951. From the changes in spectral intensity as a function of air mass (solar angle), the atmosphereic transmission coefficients and the total atmospheric ozone content (0.21 cm) have been determined as a mean of the measurements for 4 days in July 1953 at Sacramento Peak, N. Mex. These data are in good agreement with the best published values.

Preliminary measurements were made on the spectral distribution of solar radiation within the visible and infrared spectrum by using a PbS photoconductive cell. Interesting possiblilites are indicated as a result of these observations for a more accurate determination of the spectral solar radiant energy (hence a more accurate establishment of the solar constant) as well as a neat method for use in the study or recording of total atmospheric water-vapor concentration.

A discussion is included relative to the possible value of the solar constant if considered in terms of the higher ultraviolet spectral intensities indicated as the result of this work. An estimated value slightly exceeding 2.00 langleys per minute is indicated.

The authors acknowledge the courtesy of members of the Geophysics Research Directorate of Air Force Cambridge Research Center in contributing to this project, in particular P. R. Gast for helpful assistance; also John W. Evans, Major James Sadler, and other members of the Upper Air Research Observatory, who placed the facilities of the observatory at their disposal and otherwise rendered valuable assistance to us while there.

8. References

[1] Ralph Stair, Ultraviolet radiant energy from the sun observed at 11,190 feet, J. Research NBS **49,** 227 (1952) RP2357.

[2] Ralph Stair, Photoelectric spectroradiometry and its application to the measurement of fluorescent lamps, J. Research NBS **46,** 437 (1951) RP2212.

[3] Ralph Stair, Ultraviolet distribution of radiant energy from the sun, J. Research NBS **46,** 353 (1951) RP2206.

[4] R. Stair and W. O. Smith, A tungsten-in-quartz lamp and its applications in photoelectric radiometry, J. Research NBS **30,** 449 (1943) RP1543.

[5] Edison Pettit, Spectral energy-curve of the sun in the ultraviolet, Astrophys. J. **91,** 159 (1940).

[6] C. Fabry and H. Buisson, Data on ozone absorption, Compt. rend. **192,** 457 (1931).

[7] Ralph Stair, Seasonal variation of ozone at Washington, D. C., J. Research NBS **43,** 209 (1949) RP2022.

[8] C. G. Abbot and others, Annals of the Astrophysical Observatory of the Smithsonian Institution, **2,** to **6,** (1908, 1913, 1922, 1932, 1942); Smithsonian Misc. Collections **74,** No. 7 (1923); **92,** No. 13 (1934); **110,** Nos. 5 and 11 (1948).

[9] L. B. Aldrich and W. M. Hoover, The solar constant, Science **116,** 3 (1952).

[10] E. Schatzman, Sur la valeur de la constante solaire, Ann. astrophys. **12,** 305 (1949).

[11] C. W. Allen, The solar constant, The Observatory **70,** 154 (1950).

[12] M. Nicolet, Sur le probleme de la constante solaire, Ann. astrophys. **14,** 249 (1951).

[13] J. Georgi, Sokarkonstante und meteorologische Strahlungmessung, Ann. Meteorol. **3–5,** 83 (1952).

[14] H. G. Houghton, The solar constant, J. Meteorol. **8,** 270 (1951).

[15] E. O. Hulburt, The upper atmosphere of the earth, J. Opt. Soc. Am. **37,** 405 (1947).

[16] E. Durand, Rocket sonde research at the Naval Research Laboratory, page 134; G. P. Kuiper, The atmospheres of the earth and planets (Univ. of Chicago Press, 1949).

Washington, March 16, 1954.

Factors Affecting the Thermal Stability of Polytetrafluoroethylene[1]

R. E. Florin, L. A. Wall, D. W. Brown, L. A. Hymo, and J. D. Michaelsen

The structure and kinetics of thermal decomposition of polytetrafluoroethylene suggested several methods for improvement of its stability: (a) polymerization in the presence of fluorocarbon catalysts or photochemically to eliminate labile centers for initiation, (b) inclusion of foreign structural units in the polymer to promote chain transfer of the free radicals active in depolymerization, (c) inclusion of foreign molecules capable of promoting chain transfer. The catalysts tried included perfluorodimethylmercury, perfluoromethyl iodide, and fluorine gas, as well as conventional catalysts. The foreign structural units and additives included sulfur, selenium, and a variety of hydrocarbon and fluorocarbon groups, mainly aromatic, added usually as dibromides to the polymerizing mixture. None of the experimental catalysts or additives brought about any change in the rate of thermal decomposition.

1. Introduction

A search for polymers for use at high temperatures may naturally begin with polytetrafluoroethylene, which is the most stable of known polymers. The commercial material, Teflon, is somewhat limited in structural applications by a physical transition occurring at 327° C, but it does not undergo rapid thermal decomposition below about 450° C. Even a moderate improvement in the thermal stability of this polymer, for example, raising the decomposition temperature range by 50° to 100° C or the creation of an induction period, would adapt it to new uses.

It is not likely that any organic or semiorganic polymer will be stable in the thermodynamic sense at 500° C. Hence, any hope for improvement in the thermal stability can arise only from kinetic or mechanistic considerations. Such an approach has decided possibilities.

The thermal decomposition of ordinary polytetrafluoroethylene has certain other peculiarities, aside from the high temperature at which it occurs. The polymer does not melt, but decomposes in a solid or extremely viscous mass. This situation could extend the lifetime of the free radicals responsible for decomposition. Also, because of the regular structure, containing only strong C—F and C—C bonds, there is no opportunity for chain-transfer reactions; as one consequence, the depolymerization of a given radical proceeds without interruption, to yield monomer almost exclusively.

To increase the thermal stability, three different mechanistic possibilities can be considered.

1. Elimination of possible impurities, i. e., nonfluorocarbon end-groups at which the depolymerization may be initiated.

2. Inclusion of structures in the chain designed to hinder or stop the depropagation reaction, by which monomer units are stripped from a free radical. These structures would produce a random type of degradation, which should result in an induction period. The effect could be enhanced if the concomitant reactions also produced cross links.

3. Inclusion of a mobile material to terminate radicals. The lifetime of the free radicals in polytetrafluoroethylene pyrolysis may be unduly long because of their immobility. If sufficiently mobile agents could reach these radicals, and terminate them wholly or in part, a more stable polymer should result.

To explore these possibilities, a number of tetrafluoroethylene polymers were prepared, using conditions and catalysts chosen to give a polymer as free as possible from thermally labile end-groups. Some conventional catalysts were also used for comparison. In addition, a number of materials were added which might either enter the polymer chain as structural units, or be intimately incorporated in the polymer mass. The degradation of the resulting polymers was studied and rates compared.

2. Polymerization of Tetrafluoroethylene

Polytetrafluoroethylene was discovered in 1946 by Plunkett [1].[2] The polymerization of tetrafluoroethylene is similar in principle to that of most vinyl monomers, and appears to proceed by a free-radical chain mechanism. A schematic summary of the principal steps in the reaction is

Initiation:

$$\underset{\text{(catalytic)}}{\text{Catalyst}\longrightarrow\text{radical}} \qquad (1a)$$

or

$$\underset{\text{(photochemical or thermal)}}{\text{Monomer}\longrightarrow\text{radical}} \qquad (1b)$$

Propagation:

$$\underset{\mathrm{R}\cdot+\mathrm{CX_2{=}CX_2}\longrightarrow\mathrm{RCX_2CX_2}.}{\text{Radical}+\text{monomer}\longrightarrow\text{larger radical}} \qquad (2)$$

[1] This work was performed as part of the research project on high-temperature-resistant polymers sponsored by the Ordnance Corps, Department of the Army.

[2] Figures in brackets indicate the literature references at the end of this paper.

Here the R· may be derived from catalyst or monomer, the X's may be like or unlike atoms or groups, depending on the monomer formula, and the step is repeated many times until a high molecular weight is reached.

Termination:

$$\text{Radical} + \text{radical} \longrightarrow \text{polymer}$$

$$R(CX_2CX_2)_r\cdot + R(CX_2CX_2)_s\cdot \longrightarrow R(CX_2CX_2)_{r+s}R \tag{3a}$$

or

$$\text{Radical} + \text{radical} \longrightarrow 2\ \text{polymer}$$

$$R(CX_2CX_2)_r\cdot + R(CX_2CX_2)_s\cdot \longrightarrow R(CX_2CX_2)_{r-1}CX_2CX_3 + R(CX_2CX_2)_{s-1}CX{=}CX_2 \tag{3b}$$

Transfer:

$$R(CX_2CX_2)_r\cdot + RCX_2R \longrightarrow RCX_2CX_3 + R\dot{C}XR. \tag{4}$$

If inhibitors are present, they may combine with the radicals to form molecules or unreactive radicals.

Some reactions are known that share most of the features given but have an over-all equation:

$$YZ + nCX_2{=}CX_2 \longrightarrow Y(CX_2CX_2)_nZ. \tag{5}$$

Such a reaction is called telomerization. The distinction is most important when n is small.

Common methods of polymerizing tetrafluoroethylene are indicated by Hanford and Joyce [2]. As catalysts, hydrogen peroxide, oxygen, persulfates, and several organic peroxides are disclosed. Conditions in the range 0 to 100° C and 15 to over 1,000 lb/in.^{2} are covered. As a typical example, monomer is introduced at 700 lb/in.^{2} into a reactor containing a large amount of water solution of catalyst. Agitation at 60° C produces a nearly complete conversion to polymer in 17 hours. To avoid explosions, it is important to remove rapidly the heat developed.

In the laboratory, Atkinson [3] studied the mercury-sensitized photochemical reactions of tetrafluoroethylene in the gas phase at room temperature and low pressures. He found large amount of hexafluorocyclopropane produced, as well as high polymer, and found that polymer once formed seemed to catalyze the formation of both products but especially of more polymer. His results led him to stress the part played by $\cdot CF_2\cdot$ radicals. The quantum yield was 0.02 to 0.2 for production of C_3F_6(C_2F_4 consumed divided by 3 times quanta absorbed) and about 0.2 for production of polymer (molecules C_2F_4 polymerized divided by quanta absorbed).

Raal and Danby [4], in gas-phase photochemical experiments at about 300° C and low pressures, found that tetrafluoroethylene was polymerized by methyl radicals derived from the photolysis of acetone and acetaldehyde; the estimated chain length was 26 units of tetrafluoroethylene polymerized per molecule of acetaldehyde decomposed. The tetrafluoroethylene accelerated the decomposition of acetaldehyde but not of acetone.

Haszeldine [5] produced telomers $CF_3(CF_2CF_2)_nI$ containing up to 10 C_2F_4 units by thermal and photochemical reaction of mixtures containing rather large amounts of iodotrifluoromethane.

Berry and Peterson [6] polymerized tetrafluoroethylene in the presence of radioactive sulfur compounds to secure an estimate of the molecular weight of the polymer. The molecular weight of polytetrafluoroethylene has never been measured directly, because no solvent for this polymer is known. The investigators sought an indirect estimate based upon radioactive measurement of sulfur incorporated in the polymer and the reasonable assumption that each polymer molecule should contain two sulfur atoms. Using redox recipes, they found that with radioactive persulfate catalyst, no radioactive sulfur appears in the polymer isolated, but that with radioactive bisulfite in a recipe containing various other components, sulfur was incorporated and was not removable by prolonged heating with water. Their calculations led to a molecular weight of 142,000 to 534,000 for their polytetrafluoroethylene. They suggest that the polymer end-groups derived from their bisulfite are sulfonic acid groups —SO_3H, and that the polymer ordinarily prepared with persulfate catalyst may contain carboxylic acid end-groups,—COOH.

Von Grosse and Cady [7] report that tetrafluoroethylene is polymerized by boron fluoride and niobium pentafluoride. The niobium pentafluoride polymerization was reported to resemble the action of aluminum chloride on ethylene, i. e., a rapid reaction leading to low molecular weights; the boron fluoride reaction was reported to proceed slowly, yielding in several days at room temperature a high polymer resembling Teflon.

It is evident that most of the catalytic methods may introduce end-groups of lower stability into the polymer molecule, for example, hydrocarbon fragments from organic peroxides, —COOH indirectly from persulfate, and possibly —O—O— from molecular oxygen. To avoid molecular oxygen and for general convenience, it was found useful to employ a vacuum-line technique, and ordinarily to polymerize the monomer in liquid phase in quartz tubes at low temperature, with activation of catalysts by ultraviolet light. Some catalysts that might avoid the introduction of thermally labile end-groups were investigated in the research described in this paper.

2.1. Materials Used in Investigation

Tetrafluoroethylene. Most of the monomer was prepared by pyrolysis of Teflon polymer at 650° to 700° C and 1 mm, using the method of Lewis and Naylor [8] with minor changes. Contrary to expectations based upon the results of these authors at moderate pressures, a small percentage of higher fluorocarbons appears to form even at pressures of

a few microns [9]. In distilling the monomer into polymerization tubes, a small tail fraction, roughly 20 percent, was rejected. Typical monomer contained traces of higher fluorocarbons and very little of hydrogen compounds.

For comparison, a small lot was also prepared by pyrolysis of pure sodium perfluoropropionate, obtained from the Minnesota Mining & Manufacturing Co. [10]. The gaseous product was scrubbed with 4 *N* sodium hydroxide to remove carbon dioxide and large head and tail fractions were rejected in subsequent distillation. Mass spectrometer analyses of the two preparations of monomer appear in table 1.

The monomer, after distillation in vacuum into the polymerization tubes, was degassed by melting in dry ice, refreezing in liquid nitrogen, and pumping in succession. Usually 4 or 5 degassing cycles were necessary to achieve a pressure of about 0.2 micron. After such degassing, a sample of monomer contained less than 1 ppm of O_2.

Special samples were also treated by distilling into 1-liter bulbs coated with sodium or potassium mirrors and having the polymerization tube sealed to a side arm; degassing as usual; sealing off and holding the gaseous monomer in contact with the mirror at room temperature for 10 days; and subsequently condensing into the polymerization tube.

Perfluoromethyl iodide, CF_3I, was prepared by heating a mixture of silver trifluoroacetate and iodine [11]. The product was used after a simple distillation.

TABLE 1. *Mass-spectrometer analyses of tetrafluoroethylene*

	Constituent	Fraction of the sample
From pyrolysis of Teflon		*Mole %*
	C_2F_4	95.0
	C_2F_6	0.1
	C_3F_6	4.5
	C_4F_8	0.3
	CO_2	.1
From pyrolysis of Teflon; degassed	O_2	0.3 ppm
	H_2O, A, N_2, CO_2, CH_4; detected, uncertain whether from sample or connecting tube.	
From $CF_3CF_2CO_2Na$; crude		*Mole %*
	C_2F_4	92.5
	C_3F_6	0.6
	CO_2	6.9
	Hydrogenated fluorocarbons: Mass 51, 1.8%, also mass 101.	
From $CF_3CF_2CO_2Na$; unreacted monomer from opened polymerization tube (expt 4) [1]		*Mole %*
	C_2F_4	97.3
	CO_2	1.1
	O_2	1.4
	N_2	1.2
	Mass 131 (possibly C_3F_3+)0.06.	

[1] The N_2, O_2, and probably CO_2 were introduced during opening of the tube.

Diperfluoromethylmercury, $(CF_3)_2Hg$, was made from iodotrifluoromethane and cadmium amalgam.[3] The resublimed product was used [12].

Fluorine was the product of Pennsylvania Salt Manufacturing Co. The manufacturer's analysis shows F_2, 96.6 percent; HF, 0.6 percent; and O_2, 2.8 percent. The mass spectrometer indicated traces of fluorocarbons.

Azo-bis (*isobutyronitrile*) was a sample furnished by Rohm & Hass Co.

1, 2, 4, 5-Tetrafluoro-3, 6-dibromobenzene was prepared at the Bureau by a syntheses reported elsewhere [13].

Other materials were, in general, commercially pure grades.

[3] Iodotrifluoromethane and diperfluoromethylmercury were prepared by A. J. Bilbo of the Bureau's Polymer Structure Section.

2.2. Apparatus and Methods

Polymerization tubes were usually of quartz, of 1-mm wall thickness, 10-mm inside diameter, and about 150-mm length. In many of the experiments with dibromide additives, thick-walled quartz tubes of 2- to 3-mm wall thickness, and otherwise similar dimensions were used. A few experiments were made in Vycor 790 tubes of about 3-mm wall thickness and 19-mm-inside diameter, and, where illumination was not desired, in thick-walled Pyrex. Tubes were filled, degassed, and sealed on the vacuum line. Monomer was weighed by difference or measured as gas. Nonvolatile materials, such as most catalysts, were weighed. Gases such as iodotrifluoromethane and boron fluoride were measured in bulbs.

Most of the polymerizations were done in a cold block, which allowed the samples to be held at a roughly controlled low temperature while exposed to ultraviolet irradiation. The block, of aluminum alloy, was partly immersed in liquid nitrogen. Cold nitrogen gas flowed upward through a central hole in which the polymerization tube and a thermocouple were supported. A slot 6 mm wide allowed irradiation from a high-pressure mercury lamp, located at a distance of 10 cm. As the equipment was designed for intensity of illumination and flexibility, rather than for reproducibility of conditions, the observations on polymerization rates should be accepted with caution. The equipment gave reasonably good constancy of temperature with time, adjustments seldom being necessary oftener than at 5-minute intervals. The variation from top to bottom of the tube was of the order of 20° C, but as the depth of monomer in the tube was usually only about 50 mm, the actual limits were considerably narrower. In some experiments a quartz plate of 2-mm thickness was fastened over the illumination slot. The plate was subject to rapid frosting, a difficulty not experienced in its absence because of the rapid outward flow of cold air.

From manufacturer's test data and dimensions of the apparatus, a very rough estimate can be made of the incident light intensity in various wavelengths; this is given in table 2. A calculation from the table shows that about 0.28 w of illumination are received per centimeter of liquid depth, and that this illumination includes about 1.4×10^{-5} einstein per minute (1.4×10^{5} quanta per second) in wavelengths 1942 and 1849 A, and 3.8×10^{-5} einstein per minute in the wavelength 2537 A.

$$4.7\times10^{-3}\,\mathrm{w\,cm^{-2}}\times0.6\,\mathrm{cm}\times\left(\frac{100\,\mathrm{cm}}{10\,\mathrm{cm}}\right)^{2}=0.28\,\mathrm{w\,cm^{-1}}.$$

It is probable that most of this light in the lower wavelengths was absorbed by tube walls and scattered by polymer, and that very little was absorbed by monomer.

Conversion was determined by weighing the polymer, except in the dibromide additive experiments, where it was determined by residual gas volume. Most of the polymer products were warmed overnight at 105° C before being submitted for pyrolysis studies.

Special equipment used in a few experiments will be described under the appropriate heading.

TABLE 2. *Characteristics of light source*

(Hanovia high-pressure mercury lamp, type L)

Total radiation at 1 m	4.7 mw cm^{-2}
Distance, lamp to sample	10 cm
Slit width	0.6 cm
Liquid depth	2 to 5 cm
Distribution, percent of total:	

Wavelength	*Percent*
Infrared and visible	71.0
2700 to 4045 A	22.2
2652	1.78
2571	0.68
2537	1.95
2482, 2400, 2360, 2300	1.82
1942, 1849	0.53

2.3. Results

The catalysts, conditions, and conversion to polymer are shown in tables 3, 4, and 5. Many of these polymerizations were found to proceed at temperatures as low as −80° C. Such temperatures are well known in Friedel-Crafts polymerizations, but are unusual in a free-radical catalyzed reaction. Schmitz and Lawton, however, have observed the polymerization of tetraethylene glycol dimethacrylate at −55° when the frozen monomer was irradiated with high-energy electrons and subsequently melted [14].

The photopolymerization of tetrafluoroethylene appears to proceed at a rather low rate, reproducible only as to order of magnitude. If we exclude experiment 5A, the rate shows a moderate irregular rise with temperature in the range −85° to −40° C. The effective wavelength for polymerization must be quite low, as is evident from the blocking effect of the quartz window (experiment 5A), as well as from the negative results of certain catalytic experiments in Vycor No. 790 (experiments 10, 17, 19), which transmits 2 to 4 percent in 2-mm thickness at 2,540 A [15]. This is reasonable in view of the absorption spectrum of the monomer, as shown in figure 1, curve 1 [16]. The values in this figure should be taken as suggestive only, since gas-phase data have been applied to liquid-phase conditions. The polymerization is probably not due to impurities, as the prolonged sodium and potassium treatment of monomer does not eliminate it. The anomalous high rate in experiments 5A and 5B is not fully understood. It may reflect an autocatalytic effect of preformed polymer, such as was found by Atkinson [3] in gas-phase work; this possibility is also implicit in warnings by the du Pont Company on handling of the monomer. Such a phenomenon would, of course, throw great uncertainty into all rates reported here.

TABLE 3. *Photopolymerization of tetrafluoroethylene*

Experiment	Temperature	Time	Conversion	Rate	Special conditions
	°C	*min*	%	*%/min*	
1	−75	45	<1	.....	aq [1]
	−75	70	≈10	.....	aq
	−75	90	≈20	.....	aq
	−75	120	19	0.16	aq
2	−40	45	17	.38	t
3	−50	50	22.3	.45	t
4	−70	90	≈1	.....	aqs
	−85	240	16	.067	aqs
5A	−80	60	<1	<.02	nqw
	−80	158	66.5	.42	anq
5B	−80	158	66.5	.42	afnq
6	+30	1 mo	0	0	d

[1] a, Time and rate are cumulative from beginning of experiment.
d, Dark; no illumination.
f, Polymer given special fluorine treatment.
n, Monomer pretreated with sodium mirror.
q, Thin-walled quartz tube.
s, Monomer from sodium perfluoropropionate, pretreated with potassium mirror.
t, Thick-walled quartz tube.
w, 2-mm quartz window.

At first sight, a comparison of experiments 4 and 1 suggests that the potassium-treated monomer derived from sodium perfluoropropionate may polymerize somewhat more slowly that the untreated monomer derived from Teflon; but the difference is hardly more than twofold, and is not established with certainty because of the difference in temperatures. Because of the occurrence of photopolymerization, and the relatively low rates of catalytic polymerization often observed, it is sometimes difficult to decide whether a given catalyst actually did have a catalytic effect.

Diperfluoromethylmercury. This catalyst is expected to dissociate into trifluoromethyl radicals and free mercury, and might be expected to lead to a completely saturated pure fluorocarbon polymer.

$$(CF_3)_2Hg \longrightarrow 2CF_3\cdot + Hg$$

$$CF_3\cdot + nC_2F_4 \longrightarrow CF_3(C_2F_4)_n\cdot$$

$$2CF_3(C_2F_4)_n\cdot \longrightarrow CF_3{-}(C_2F_4)_n{-}(C_2F_4)_n{-}CF_3$$

Actually, the absorption spectrum of the mercury compound is not very favorable for photochemical decomposition. A comparison of absorption spectra, figure 1, shows that diperfluoromethylmercury absorbs appreciably at wavelengths only a little longer than tetrafluoroethylene, both substances absorbing little light nearly down to the limit of transmission of quartz. Photopolymerization may compete with the catalyzed polymerization. The difficulty is increased by the very low solubility of this catalyst in the monomer. No polymerization occurred in Vycor, which is reasonable in view of the absorption spectrum of the catalyst and the transmission limits of Vycor. The Vycor No. 790 tube containing the sample was subsequently stored 1 month at −20° C, without further change. In experiments 7, 8, and 9

TABLE 4. *Catalytic photoactivated polymerization of tetrafluoroethylene*

Experiment	Catalyst	Catalyst concentration [1]	Monomer weight	Temperature	Time	Conversion	Rate	Special conditions [1]	Relative rate (h) [1]
		Mole %	*g*	*° C*	*min*	*%*	*%/min*		
7	$(CF_3)_2Hg$	0.05 i	5.38	−80	120	84	0.7	q	4 (1)
8	Do	.244 i	2.94	−80	40	89	2.2	q	14 (1)
9	Do	1.37 i	4.40	−80	>30	94	<3.1	q	<19 (1)
10	Do	0.29 i	5.0	−22	240	0	0	rv	0
11	Do	.124 i	4.12	−50	25	3.4	0.14	q	.3 (3)
12	Do	.163 i	3.11	−50	25	3.5	.14	q	.3 (3)
13	Do	.246 i	2.23	−50	25	5.7		qr	
14	Do	.180 i	2.96	−50	25	4.1		qr	
15	CF_3I	.387	2.61	−80	45	16	0.36	qw	>18 (5A)
16	Do	2.32	4.60	−80	80	25.5	.32	qw	>16 (5A)
17	Benzoyl peroxide	0.352 i	5.84	−25	95	Trace		bd	
	Do	.352 i	5.84	−25	215	3.8	0.02	rv	∞ (10)
18	*t*-Butyl peroxide	1.87	3.78	−50	80	31.8	.40	qw	>20 (5A)
19	Azo-bis (isobutyronitrile)	0.5 i	5.0	−80	240	0	0	rv	0 (10)
20	F_2	2.2 g	5.0	−130	25	Trace		bd	
	Do	2.2 g	5.0	−80	35	do		bd	
	Do	17	5.0	−130	50	≈10		bd	
	Do	17	5.0	−80	57	≈10	≈0.5	bd	3.2 (1)
21	BF_3	0.27	3.75	+30	>6 mo	0	0	d	0
22	Do	1.52	4.51	+30	>1 yr	0	0	d	0

[1] b, Time is cumulative from beginning of experiment, rate average of last two periods.
d, Dark; no illumination.
g, Catalyst concentration in bubbled gas.
h, Figure in parentheses shows number of photopolymerization experiment used for comparison.
i, Catalyst nearly insoluble.
q, Thin-walled quartz tube.
r, Subsequent storage appeared to give no change; see text for details.
v, Vycor tube and 2-mm quartz window.
w, 2-mm quartz window.

TABLE 5. *Additives in photoactivated polymerization of tetrafluoroethylene*

Experiment	Additive	Temperature	Time	Conversion	Rate	Special conditions or observations	Relative rate
		° C	*min*	*%*	*%/min*		
23		−70	19	64	3.4	q [1]	21 (1) [2]
24	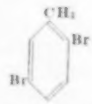	−30	35	38	1.1	t. Product tacky in benzene	3 (2)
25	$CHBr{=}CHBr$	−35	35	8	0.2	t. Product very powdery; 6% SiF_4 on pyrolysis	0.6 (2)
26	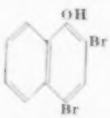	−40	175	14	.08	t. 4% SiF_4 on pyrolysis	0.2 (2)
27		−40	47	20	.43	t. Product powdery	1.1 (2)
28	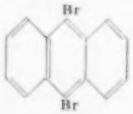	−40	27	17	.63	t	1.7 (2)
29		−40	47	9	.19	mt. Product powdery	0.5 (2)
30		−40	41	9.4	.23	mt. Product powdery	0.6 (2)
31	Se	−35	44	20	.45	mt	1.2 (2)

[1] q. Thin-walled quartz tube.
t. Thick-walled quartz tube.
m, Additive applied as mirror.
[2] Figure in parentheses shows number of photopolymerization experiment used for comparison.

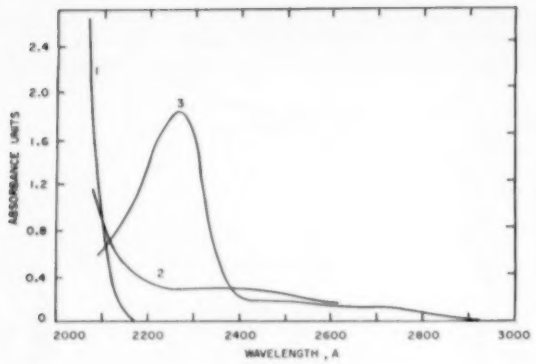

FIGURE 1. *Absorption spectra.*

Curve 1, C_2F_4, molar absorbance ϵ; curve 2, $(CF_3)_2Hg$, absorbance of qualitative dilute solution in ethanol; curve 3, $C_2F_4Br_2$, molar absorbance $\epsilon \times 10^{-3}$.

the rates seem to be much higher than photopolymerization and seem to increase with concentration of catalyst. However, the results are from samples that have proceeded to nearly 100-percent conversion and may also reflect autocatalysis by polymer. If the variation with catalyst amount is significant, it may be explicable by a process of continual replacement of catalyst in the saturated solutions.

The four experiments 11, 12, 13, and 14 were undertaken to determine whether the diperfluoromethylmercury catalyzed polymerization can continue in the dark for appreciable periods after being started photochemically. All four samples were illuminated for identical periods at −50° C. Samples 11 and 12 were opened immediately; 13 and 14 were stored in the dark for 1 month at −20° C. The stored samples seem to show a slightly higher conversion. The difference is probably not significant; the subsequent dark polymerization, if any, is certainly slight. The rates seem low for −50°, by comparison with experiments 7, 8, and 9 and the photopolymerization experiment 3.

Iodotrifluoremethane. Haszeldine [17], using large quantities of iodotrifluoromethane with tetrafluoroethylene, and activation by heat (200° C), ordinary light, and ultraviolet, obtained solid telomers containing many C_2F_4 units per CF_3I residue. Extrapolating from his results, we would expect only a very small proportion of CF_3I derived material in the present products. There was no gross appearance of iodine in the polymer, as would be necessary if large amounts of iodotrifluoromethane were consumed and pure fluorocarbon polymer formed. The pyrolysis of the polymer did not show iodine or iodine-containing fragments; the amounts may have been too small for detection in a telomer of very high molecular weight. The rates of polymerization are about alike over a sixfold variation of iodotrifluoromethane concentration, which suggests compensating increases in initiation and termination. Higher rates than these might have been expected from the strong absorption by iodotrifluoromethane, which has a maximum at 2,680 A [18].

Peroxides and azo-bis(isobutyronitrile). Benzoyl peroxide brought about a very slow polymerization in Vycor at the rather high temperature of ~25° C. This is to be compared, however, with the total lack of polymerization when diperfluoromethylmercury is used (and therefore also in a pure blank). Storage at −20° C for 1 month did not appear to increase the yield; thermal activation of the catalyst and continuation of the reaction by frozen-in free radicals were therefore negligible.

Di-*t*-butyl peroxide brought about a reasonably rapid polymerization at −50° C. The corresponding photopolymerization rate should be the very low rate experienced when a quartz window is added (experiment 5A).

Azo-bis(isobutyronitrile) did not cause any polymerization is Vycor at −80° C. The transmission of Vycor should not be responsible for this failure because the catalyst is known to be activated by light of the order of 3,600 A [19] when used with other monomers. It is possible that radicals from this catalyst are not sufficiently active to initiate polymerization of tetrafluorethylene, at least at the temperature of −80° C.

Fluorine. The action of free fluorine upon most organic compounds is known to cause complicated free-radical chain reactions, and it was found also to initiate polymerization of tetrafluoroethylene at low temperatures. Liquid fluorocarbons were also formed. The polymer product also contained some strongly held silicon tetrafluoride; its generally complicated composition created uncertainties in the subsequent pyrolysis studies. Fluorine gas diluted with helium was bubbled through monomer in Pyrex equipment, immersed in a freezing pentane slush, and subsequently in a dry-ice bath. Little solid product was formed with very dilute fluorine; a moderately rapid formation of solid polymer was observed with a higher concentration containing 17 percent of fluorine. At −80° C evaporation led to rapid losses of monomer. Impurities in the tank fluorine, which are not readily removable, such as oxygen fluoride, could have affected the reaction and the structure of the product. Refinements in equipment, higher catalyst purity, and more ideal conditions might lead to the desired type of saturated pure fluorocarbon polymer.

Boron trifluoride. Boron fluoride was reported by Von Grosse and Cady [7] to cause the slow polymerization of tetrafluoroethylene at room temperature to a solid polymer resembling Teflon. In the present study two concentrations were prepared in Pyrex tubes and left for periods of 6 to 18 months. No change was observed. Although boron fluoride is known to require a co-catalyst such as water in order to be catalytically active, the requisite traces of water are always present unless removed by a technique much more stringent than that employed here [20]; therefore, it is believed that boron fluoride is inactive, and that Von Grosse and Cady's polymerization was due to adventitious oxygen. Their polymerization with niobium pentafluoride cannot be explained in this fashion, and possibly other catalytic metal fluorides exist.

Polymerizations with added components. The technique was simplified in that approximate 0.1-g quantities of the added component were used without measurement, with about 5 g of monomer measured by pressure and volume. Most of these added components were nearly insoluble; some were applied as mirrors. Many of these materials affected the polymerization rate considerably. As little is known of high-temperature inhibition, there are few guiding principles except the obvious one that the inhibiting group should be capable of at least a short existence at about 400° to 500° C. Many dibromides were chosen, since it appeared likely that the structural group might be incorporated into a fluorocarbon polymer by removal of bromine, either photochemically or by free radicals. It is still uncertain to what extent the added groups were incorporated in the polymer structure; that this extent was probably small is likely from their failure to appear among pyrolysis products.

For dibromotetrafluorobenzene the absorption spectrum (fig. 1) shows considerable absorption in the range 2,900 to below 2,100 A, with a molar absorbance $\epsilon = 18{,}400$ at the maximum of 2,275 A.

Under exposure to ultraviolet light the dibromo compound alone and in perfluorotriethylamine solution appears to react very slowly; in 12 hours a slight brown color and an odor of bromine were noted, and nearly all the material was recovered unchanged. The mass-spectrometer pattern does not indicate that the bromine atoms or any others are especially labile; however, the compound will undergo Wurtz-type condensations at about 300° C [21]. The polymerization of tetrafluoroethylene with added dibromotetrafluorobenzene was more rapid at −80° C than any of the other catalytic polymerizations at any temperature. Unpolymerized volatile material contained 95.(6) percent of C_2F_4, 3.9 percent of C_3F_6, and 0.5 percent of SiF_4, as well as traces of fluorocarbons up to C_4. Because the dibromotetrafluorobenzene decomposes quite slowly alone and its presence in the polymer in substantial amount was not proved, the material may possibly act merely by efficient transfer of energy to the monomer, by a process loosely analogous to that occurring in mercury-sensitized photodecompositions.

The other dibromides were less-spectacular promoters. Dibromotoluene showed a smaller acceleration; dibromoethylene, dibromodiphenyl ether, and dibromoanthracene had little or no effect, the first of these being perhaps a mild retarder; and dibromo-alpha-naphthol was a powerful retarder. The nonpolymeric residue from the latter material contained perfluoro-olefins up to C_8, with no volatile bromine compounds or partially fluorinated compounds. Of the others, anthracene and sulfur were probably mild retarders, and selenium did not appreciably affect the rate. Possibly with dibromides of the hydrocarbon type, photochemical dissociation of the C—Br bond brings about a more rapid initiation, which accounts for observed promoter action; but parallel with this, there may be a transfer reaction of the fluorocarbon polymer radical to abstract hydrogen from C—H bonds. If the resulting hydrocarbon radical is reactive, ordinary transfer results; if unreactive, an effective retardation.

If the retardation by sulfur is real here, it may be due to addition of a fluorocarbon free radical to sulfur to form a stable radical of similar formula to those postulated in the explanation of mercaptan retardation.

3. Discussion of Pyrolyses

3.1. General Considerations

A few important points concerning the thermal decomposition of tetrafluoroethylene polymers were mentioned in the introduction. One of the prime considerations governing thermal stability is the strength of the bonds in the molecule. In this respect tetrafluoroethylene should be outstanding. The C—C bond, which forms the backbone of the chain, is one of the strongest single bonds capable of forming large molecules, and the C—F bond is much stronger [22]. There is some evidence that the C—C bond in fluorocarbons may have a higher strength than the value given. Exact thermochemical data from which to compute bond energies are lacking for fluorocarbons, but electron-impact data indicate a value of 124 kcal for the dissociation energy of the C—C bond in fluorocarbons, as against only 79 to 83 kcal for this bond in paraffin hydrocarbons [23, 241]. (Although these bond dissociation energies are not equivalent to the bond energies derived thermochemically, they are perhaps more pertinent to the question of thermal decomposition.)

From the standpoint of the bond energies in analogous low-molecular-weight compounds, the actual thermal behavior of polytetrafluoroethylene is disappointing. Polyethylene decomposes appreciably, 0.16 percent per minute at 385° C; polytetrafluoroethylene decomposes at the same rate at 489° C, only 104 deg higher [9, 25]. For comparison, bond-dissociation energies in related simple molecules are: for C_2H_6 and other lower paraffins, C—C = 80 kcal, C—H = 101 kcal; for C_2F_6, C—C = 124 kcal, C—F = 107 kcal. All figures except C—F are derived from electron-impact data.

It is evident that the correlation between bond energies and thermal stability is only rough and imperfect; a more direct insight is to be found in the detailed kinetics of pyrolysis. A large number of vinyl polymers, including polytetrafluoroethylene, decompose thermally by a depolymerization with splitting of the polymer chain. Others, with which we are not concerned here, decomposed by stripping off side groups from the carbon chain. A comprehensive theory of thermal depolymerization has been developed by Wall, Simha, and others [26, 27] and special cases in partially equivalent forms by Jellinek [28] and by Grassie and Melville [29], and it has been the subject of extensive experimental investigation. The elementary processes, according to this theory, are: (1) initiation, by which free radicals are formed, (2) depropagation or "unzipping," in which successive monomer units are broken off from these free

radicals, (3) transfer, in which one radical is stabilized and a new one formed, and (4) termination, destroying two radicals.

Initiation:

$$\sim CX_2CX_2CX_2CX_2 \sim \longrightarrow \sim CX_2CX_2\cdot + \sim CX_2CX_2\cdot \quad (1a)$$

or

$$Y{-}CX_2CX_2 \sim \longrightarrow Y\cdot + \sim CX_2CX_2. \quad (1b)$$

(De)propagation:

$$\sim CX_2CX_2CX_2CX_2\cdot \longrightarrow \sim CX_2CX_2\cdot + CX_2{=}CX_2 \quad (2)$$

Transfer:

$$\sim CX_2CX_2\cdot + \sim \underset{\displaystyle X}{\overset{\displaystyle H}{\overset{|}{\underset{|}{C}}}}{-}CX_2CX_2CX_2 \sim$$

$$\longrightarrow \sim CX_2CX_2H + \sim CX{=}CX_2 + \cdot CX_2CX_2 \sim \quad (3)$$

Termination:

$$2 \sim CX_2CX_2\cdot \longrightarrow \sim CX{=}CX_2 + \sim CX_2CX_2. \quad (4)$$

The resulting rate equations are tractable for certain cases, though not simple, and for chosen values of the rate constants or their ratios, curves can be constructed to show the course of monomer yield, total volatile products, and molecular weight of residue during depolymerization.

It may be noted that the initiation step can occur either at an ordinary C—C bond (eq 1a) or at a much weaker bond (eq 1b), which can be present in a catalyst fragment, a foreign group present in the chain, or even in a separate molecule of some contaminant, such as unreacted catalyst. If many of these labile centers of initiation are present, the stability of the polymer may be greatly reduced. A spectacular example is the case of polymethylmethacrylate; this polymer when prepared photochemically with diphenylcyanomethyl end- groups, decomposes slowly at 280° C, but when prepared with large amounts of benzoyl peroxide catalyst, will decompose more rapidly at a temperature 40 deg lower [29].

It may also be noted that, depending upon circumstances and the character of the polymer, the depropagation reaction may proceed through few or many stages before being interrupted by transfer or termination. In impure mixtures, still other types of interruption are conceivable. The free radical may lose monomer units until a structural irregularity in the chain is reached, from which further loss is difficult; or it may react with foreign molecules to produce stable products. The latter type of interruption of free-radical reactions is well known in the allied fields of polymerization and oxidation, but does not seem to have been found thus far in high-temperature depolymerization, although inhibition with nitric oxide is well known in gas-phase systems at these temperatures [29].

In the case of polytetrafluoroethylene the structure offers no opportunity for transfer reactions, and the product of pyrolysis is nearly pure monomer. Initiation may be difficult, except at thermally labile end-groups derived from the catalyst. The solid or highly viscous state of the material undergoing pyrolysis may render the free radicals immobile and inaccessible to most reactions except depropagation. This circumstance may greatly extend the lifetime of the radicals, and thus increase the rate of decomposition.

Such considerations made it plausible (a) that available preparations of polytetrafluoroethylene might not be the most stable possible, and (b) that even the purest polytetrafluoroethylene might be less stable than preparations containing suitable structural irregularities or foreign additives.

3.2. Results of Pyrolyses

The pyrolysis data given in table 6 are from the work of Madorsky, Hart, Straus, and Sedlak, full details of which are included in their report [9]. The product of pyrolysis was nearly pure tetrafluorochylene. Catalyst and additive fragments were not found, except for occasional hydrocarbon peaks (in the mass spectrometer), which may have been background, and occasional percentages of silicon tetrafluoride above the normal trace, which may or may not have been due to liberation of hydrogen fluoride from hydrogen-containing fragments. Extrapolated initial rates are quoted, but any other basis would have served as well, since the data of any individual experiment fitted a first-order rate curve closely over practically the whole course of the decomposition, an unusual occurrence in the pyrolysis of high polymers.

TABLE 6. *Pyrolysis of tetrafluoroethylene polymers*

Sample [1]	Temperature	Initial rate	Rate for Teflon at temperature shown	Ratio, or relative rate
	°C	%/min	%/min	
1	497	0.400	0.305	1.31
5B	501	.428	.403	1.06
3	513	1.074	1.059	1.015
8	490	0.219	0.185	1.083
9	460	.026	.019	1.37
9	470	.054	.042	1.28
9	480	.111	.089	1.25
9	490	.225	.185	1.22
9	500	.444	.375	1.18
9	510	.840	.755	1.11
15	502	.356	.436	0.82
16	496	.235	.284	.79
17	498	.442	.328	1.35
18	494	.245	.245	1.00
20	470	.0469	.0419	1.12
20	450	.0158	.0132	1.20
23	513	1.109	1.059	1.05
24	513	0.716	1.059	0.68
24	450	.0171	0.0146	1.17
25	513	.961	1.059	0.91
26	513	1.244	1.059	1.17
27	513	0.964	1.059	0.91
28	513	.929	1.059	.88
29	513	1.032	1.059	.97
31	513	0.902	1.059	.85

[1] Sample numbers refer to polymers obtained in the corresponding numbered experiments in tables 3, 4, and 5.

The first few minutes of pyrolysis, representing from a fraction of a percent to a few percent decomposition, are obscured because of the heating-up period before constant temperature is reached. This uncertain period is about 5 minutes in most experiments, but probably only 2 minutes in the experiments on samples 23 to 31. Experimental considerations made it most convenient to compared the rates of given samples with those of commercial Teflon at corresponding temperatures; this reference material showed highly consistent and reproducible behavior. In figure 2 the relation of initial rate and temperature for Teflon is shown as a solid line, and the rates for the special tetrafluoroethylene polymers are indicated by numbered points, the numbers referring to polymers in tables 3, 4, and 5. These data are also given in table 6.

It will be recalled from discussion of the mechanism of pyrolysis that the decomposition rate should be lowered by (a) replacing more labile end-groups by completely fluorinated saturated end-groups, which would decrease the formation of free radicals; (b) incorporating inhibitors, which would react with the radicals as soon as formed, for a limited period; or (c) incorporating hydrogen-containing groups, which would give rise to cross linking as a competing reaction besides depropagation. In the third case, a drop in molecular weight could occur, but the material would still remain polymeric.

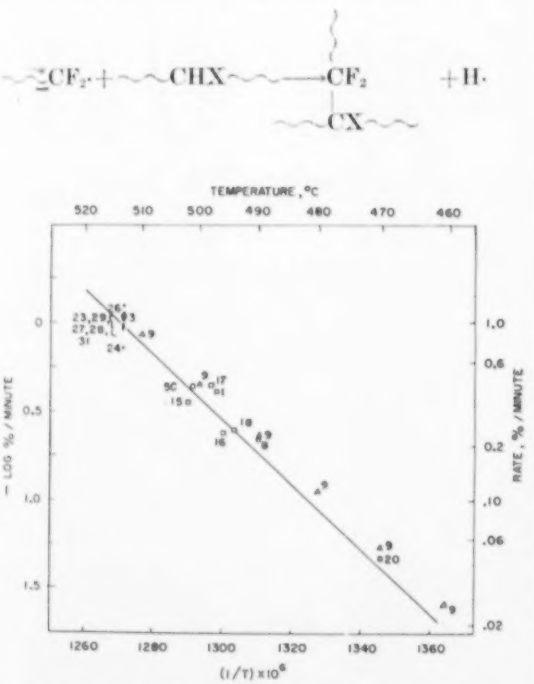

FIGURE 2. *Pyrolysis of various tetrafluoroethylene polymers.*

———, reference curve, commercial Teflon; ○ photopolymers; △, □, catalytic polymers; ·, polymers with additives. Numbers refer to samples in tables 3, 4, and 5.

The most striking experimental generalization is that none of the products differed greatly from ordinary Teflon in pyrolysis rate. The small differences that did occur are probably less than the experimental error. Possibly in all products, including Teflon, most of the labile groups were removed long before the pyrolysis temperature was reached, to form fairly stable olefinic end-groups. For example,

$$\sim\sim CF_2CF_2CO_2H \longrightarrow \sim\sim CF{=}CF_2 + HF + CO_2.$$

The photopolymers should be free from nonfluorocarbon groups but not necessarily saturated. Sample 5B, exposed to fluorine gas after polymerization, should be the most completely saturated photopolymer. Although one of the photopolymers listed in table 6, No. 1, decomposed with a relative rate of 1.3, the other two were indistinguishable from Teflon in their behavior.

Samples 8 and 9 should have perfluoromethyl end-groups derived from diperfluoromethylmercury. They appeared to decompose at slightly higher rates than Teflon. The difference may be within experimental error; no explanation can be given for the lower stability, if real.

Samples made with iodotrifluoromethane appeared slightly more stable than Teflon; the stability did not depend upon the amount of iodotrifluoromethane used. If the polymer molecules contain C—I linkages (as Haszeldine's low telomers do), a lower rather than higher stability might have been expected because of the weaker C—I bond. Perhaps the C—I bonds, or iodine atoms derived from them, encourage chain transfer.

The peroxide polymers, 17 and 18, might have been expected to be the least stable; actually, the *t*-butyl peroxide polymer was about normal, and the benzoyl peroxide polymer decomposed at a rate 1.35 times normal.

The polymer made with gaseous fluorine might be expected to have saturated fluorocarbon end-groups:

$$F_2 \longrightarrow 2F\cdot$$

$$F\cdot + CF_2{=}CF_2 \longrightarrow CF_3CF_2\cdot$$

With the very active fluorine atoms, side reactions such as C—C bond splitting might also have been possible during polymerization, leading to lower molecular weight. The fluorine catalyzed polymer actually decomposed at about the normal rate. The experimental determination of rate was open to some objection, as large quantities of low-molecular-weight material and silicon tetrafluoride were evolved in early stages before a steady rate was observed.

The additives (23 to 31) might have served conceivably either as structural elements in the polymer chain, capable of acting as internal inhibitors or as cross-linking agents, or an inhibitors mechanically admixed with the polymer. Because of negative mass-spectrometer results, there is not much direct evidence that any of the additives were incorporated in the polymer chain in large amounts, except that the increased production of silicon tetrafluoride from

the dibromoethylene sample 25 and the dibromo-α-naphthol sample 26 may reflect evolution of hydrogen fluoride from adjacent C—H bonds of the additive and C—F bonds of the regular monomer sequence. The polymerization rate-results mentioned earlier do indeed suggest that the additives are involved in some fashion in the polymerization. Probably most of the dibromide additives, if not incorporated in the polymer chain, were sufficiently volatile to be eliminated from thin layers of polymer during the evacuation period preceding pyrolysis. The hydrocarbon groups derived from dibromides were expected to act as chain-transfer agents, the tetrafluorobenzene group from dibromotetrafluorobenzene merely as a structural irregularity, with some likelihood of extra resonance stabilization. Of these materials 1, 2-dibromoethylene increased the pyrolysis rate somewhat, and the others were practically neutral.

It is evident that eliminating thermally labile end-groups and replacing with fluorocarbon end-groups did not greatly lessen the rate of pyrolysis of polytetrafluoroethylene. This result makes it plausible that in tetrafluoroethylene polymers generally, the initiation step occurs by breaking of fluorocarbon C—C bonds rather than through some weaker bond derived from catalyst or impurity.

None of the chain-transfer agents seem to have produced observable reductions in pyrolysis rate. It may be possible to get observable effects by the use of aromatic rings containing many methyl groups. If we consider the unusual maintenance of a solid state during decomposition, it seems probable that, to be highly effective, a chain transfer agent or inhibitor should be capable of rapid diffusion in order to reach immobile free radicals in the polymer. The problem of maintaining such agents in a polymer at high temperatures might be solved by (a) a compromise between volatility and diffusion rates, or (b) the slow generation of such active agents within the polymer mass. Further work in these unexplored fields seems desirable.

WASHINGTON, December 18, 1953.

4. References

[1] R. J. Plunkett, U. S. Pat. 2,230,654.
[2] W. E. Hanford and R. M. Joyce, J. Am. Chem. Soc. **68,** 2082 (1946).
[3] B. Atkinson, J. Chem. Soc. **1952,** 2684.
[4] F. A. Raal and C. J. Danby, J. Chem. Soc. **1950,** 1556.
[5] R. N. Haszeldine, J. Chem. Soc. **1950,** 3041.
[6] K. L. Berry and J. H. Peterson, J. Am. Chem. Soc. **73,** 5195 (1951).
[7] A. V. Grosse and G. H. Cady, Ind. Eng. Chem. **39,** 367 (1947).
[8] E. E. Lewis and M. A. Naylor, J. Am. Chem. Soc. **69,** 1968 (1947).
[9] S. L. Madorsky, V. E. Hart, S. Straus, and V. A. Sedlak, J. Research NBS **51,** 327 (1953) RP2461.
[10] L. J. Hals, T. S. Reid, and G. H. Smith, J. Am. Chem. Soc. **73,** 4054 (1951).
[11] R. N. Haszeldine, J. Chem. Soc. **1951,** 584; A. L. Henne and W. G. Finnegan, J. Am. Chem. Soc. **72,** 3806 (1950).
[12] H. J. Emeleus and R. N. Haszeldine, J. Chem. Soc. **1948,** 2953.
[13] Max Hellmann and A. J. Bilbo, J. Am. Chem. Soc. **75,** 4590 (1953).
[14] J. V. Schmitz and E. J. Lawton, Science **114,** 718 (1951).
[15] Corning Glass Works Catalog LP24, p. 131.
[16] J. R. Lacher, L. E. Hummel, E. F. Bohmfalk, and J. D. Park, J. Am. Chem. Soc. **72,** 5486 (1950).
[17] R. N. Haszeldine, J. Chem. Soc. **1949,** 2856.
[18] J. Banus, H. J. Emeleus, and R. N. Haszeldine, J. Chem. Soc. **1950,** 3041.
[19] M. S. Matheson, E. E. Auer, E. B. Bevilacqua, and E. J. Hart, J. Am. Chem. Soc. **71,** 2610 (1949).
[20] A. G. Evans and G. W. Meadows, Trans. Faraday Soc. **46,** 327 (1950); A. G. Evans, G. W. Meadows, and M. Polanyi, Nature **158,** 94 (1946).
[21] M. Hellmann (unpublished work).
[22] L. Pauling, The nature of the chemical bond, 2d ed., p. 52 (Cornell University Press, Ithaca, N. Y., 1945).
[23] V. H. Dibeler, R. M. Reese, and F. L. Mohler, J. Chem. Phys. **20,** 761 (1952).
[24] J. A. Hipple and D. P. Stevenson, Phys. Rev. **63,** 121 (1943) and earlier papers; discussed in E. W. R. Steacie, Free radical mechanisms, p. 61 (Reinhold Publishing Co., New York, N. Y., 1946).
[25] S. L. Madorsky, J. Polymer Sci. **9,** 133 (1952).
[26] Robert Simha, L. A. Wall, and P. J. Blatz, J. Polymer Sci. **5,** 615 (1950).
[27] Robert Simha and L. A. Wall, J. Polymer Sci. **6,** 39 (1951).
[28] H. H. G. Jellinek, J. Polymer Sci. **3,** 850 (1945); **4,** 113 (1949).
[29] N. Grassie and H. W. Melville, Proc. Roy. Soc. **A199,** 1, 14, 24 (1949).